www.czasopisma.pan.pl PAN POLSKA AKADEMIA NAUK www.journals.pan.pl

POLISH ACADEMY OF SCIENCES

COMMITTEE OF AUTOMATIC CONTROL AND ROBOTICS

ARCHIVES OF CONTROL SCIENCES

VOLUME 27 (LXIII), No. 1

QUARTERLY

Institute of Automatic Control
Silesian University of Technology
Gliwice 2017

Archives of Control Sciences welcomes for consideration papers on topics of significance in broadly understood control science and related areas, including: basic control theory, optimal control, optimization methods, control of complex systems, mathematical modeling of dynamic and control systems, expert and decision support systems and diverse methods of knowledge modeling and representing uncertainty (by stochastic, set-valued, fuzzy or rough set methods, etc.), robotics and flexible manufacturing systems. Related areas that are covered include information technology, parallel and distributed computations, neural networks and mathematical biomedicine, mathematical economics, applied game theory, financial engineering, business informatics and other similar fields.

Warunki prenumeraty: Roczna prenumerata *Archives of Control Sciences* może być rozpoczęta w dowolnym momencie. Opłata za prenumeratę krajową w roku 2017 wynosi 120 zł, a zagraniczna 160 $. Głównym dystrybutorem jest Warszawska Drukarnia Naukowa PAN. Zamówienia należy składać przez e-mail, fax lub pocztą na adres: Warszawska Drukarnia Naukowa Polskiej Akademii Nauk 00-656 Warszawa, ul. Śniadeckich 8 tel./fax (0-22) 628-76-14, (0-22) 628-87-77, e-mail: wdnpan@home.pl lub dystrybucja@wdnpan.home.pl
Zamówienia z zagranicy można kierować: Ars Polona JSC, Foreign Trade Enterprise, Obrońców 25, 03-933 Warszawa, Fax: 022 509-86-48.

Subscription information: The promotional subscription price in 2017 is EUR 122,- plus surface postage EUR 12,- At subscriber's request this journal will be air mailed at additional fee. Subscription for foreign customers is available through: Ars Polona JSC Foreign Trade Enterprise 25, Obrońców Street 03-933 Warsaw, Poland Fax: 004822/5098648

The publication of this Journal is supported by funds from
the Polish Ministry of Science and Higher Education.

Address of the Editor: Institute of Automatic Control, Silesian University of Technology
Akademicka 16, 44–100 Gliwice, Poland. Tel: +(48–32) 237–23–98, fax +(48–32) 237–21–27

`http://acs.polsl.pl`

Typeset in TEX at the Institute of Automatic Control, Silesian University of Technology

Printing: Centrum Poligrafii Sp. z o.o., ul. Łopuszańska 53,
02-232 Poland

CONTENTS

Archives of Control Sciences
Volume 27(LXIII), 2017
No. 1*, pages 5–27*

Rational taxation in an open access fishery model

DMITRY B. ROKHLIN and ANATOLY USOV

We consider a model of fishery management, where n agents exploit a single population with strictly concave continuously differentiable growth function of Verhulst type. If the agent actions are coordinated and directed towards the maximization of the discounted cooperative revenue, then the biomass stabilizes at the level, defined by the well known "golden rule". We show that for independent myopic harvesting agents such optimal (or ε-optimal) cooperative behavior can be stimulated by the proportional tax, depending on the resource stock, and equal to the marginal value function of the cooperative problem. To implement this taxation scheme we prove that the mentioned value function is strictly concave and continuously differentiable, although the instantaneous individual revenues may be neither concave nor differentiable.

Key words: marginal value function, stimulating taxes, myopic agents, optimal control.

1. Introduction

An unregulated open access to marine resources, where many individual users are involved in the fishery, may easily lead to the over-exploitation or even extinction of fish populations. Moreover, it results in zero rent. These negative consequences of the unregulated open access (the "tragedy of commons": [13]) were widely discussed in the literature: see [11, 6, 8, 2]. Maybe the most evident reason for the occurrence of these phenomena is the myopic behavior of competing harvesting agents, who are interested in the maximization of instantaneous profit flows, and not in the conservation of the population in the long run. In the present paper we consider the problem of rational regulation of an open access fishery, using taxes as the only economical instrument. Other known instruments include fishing quotas of different nature, total allowable catch, limited entry, sole ownership, community rights, various economic restrictions, etc: see, e.g, [8, 2].

We should also mention that there is a natural and popular approach to modeling resource exploitation via the dynamic games. This approach is not touched in the present paper, we only refer to [19] for a survey.

The Authors are with Institute of Mathematics, Mechanics and Computer Sciences, Southern Federal University, Mil'chakova str., 8a, 344090, Rostov-on-Don, Russia. E-mails: rokhlin@math.rsu.ru, usov@math.rsu.ru.

The research is supported by Southern Federal University, project 213.01-07-2014/07.
Received 24.10.2016.

Assume for a moment that n agents coordinate their efforts to maximize the aggregated long-run discounted profit. The related aggregated agent, which can be considered as a sole owner of marine fishery resources, conserves the resource under optimal strategy, unless the discounting rate is very large. How such an acceptable cooperative behavior can be realized in practice?

We consider the following scheme. Suppose that some regulator (e.g., the coastal states), being aware of the revenue function and maximal productivity of each agent, declares the amount of proportional tax on catch. Roughly speaking, it turns out that if this tax is equal to the marginal indirect utility (marginal value function) of the cooperative optimization problem, then the myopic profit maximizing agents will follow an optimal cooperative strategy, maximizing the aggregated long-run discounted profit. The idea of using such taxes in harvesting management was often expressed in the bioeconomic literature: see [7], [20], [12, Chapter 10], [15, Chapter 7]. Our goal is to study this idea more closely from the mathematical point of view.

The first theoretical question we encounter, trying to implement the mentioned taxation scheme, concerns the differentiability of the value function v of the cooperative problem. Assuming that the population growth function is strictly concave and continuously differentiable, in Sections 2 and 3 we prove v inherits these properties, although the instantaneous revenue functions may be non-concave.

The differentiability of v is proved by the tools from optimal control and convex analysis. Our approach relies on the characterization of v as the unique solution of the related Hamilton-Jacobi-Bellman equation. We neither use the general results like [22], nor the related technique. At the same time, our results are not covered by [22]. Simultaneously we construct optimal strategies and prove that optimal trajectories are attracted to the biomass level $\widehat{x}$, defined by the well known “golden rule”. This level depends on the discounting rate, which is at regulator’s disposal.

If the agent revenue function are non-concave, then an optimal solution of the infinite horizon cooperative problem may exist only in the class of relaxed (or randomized) harvesting strategies. Such strategies can hardly be realized in practice, and certainly cannot be stimulated by taxes. Nevertheless, in Section 4 we show that piecewise constant strategies (known as the “pulse fishing”) of myopic agents, stimulated by the proportional tax $v'\alpha$ on the fishing intensity α, are ε-optimal for the cooperative problem. Moreover, the related trajectory is retained in any desired neighbourhood of $\widehat{x}$ for large values of time. Finally, we introduce the notion of the critical tax $v'(\widehat{x})$ and prove that it can only increase, when the agent community widens.

2. Cooperative harvesting problem: the case of concave revenues

Let a population biomass X satisfy the differential equation

$$X_t = x + \int_0^t b(X_s)\,ds - \sum_{i=1}^n \int_0^t \alpha_s^i\,ds, \tag{1}$$

where b is the growth rate of the population, and α^i is the harvesting rate of i-th agent. We assume that b is a *differentiable strictly concave* function defined on an open neighbourhood of $[0,1]$, and

$$b(x) > 0, \quad x \in (0,1), \quad b(0) = b(1) = 0.$$

The widely used Verhulst growth function $b(x) = x(1-x)$ is a typical example. Agent harvesting strategies α^i are (Borel) measurable functions with values in the intervals $[0,\overline{\alpha}^i]$, $\overline{\alpha}^i > 0$. A harvesting strategy $\alpha = (\alpha^1,\dots,\alpha^n)$ is called *admissible* if the solution $X^{x,\alpha}$ of (1) stays in $[0,1]$ forever: $X_t^{x,\alpha} \in [0,1]$, $t \geqslant 0$. Note that for given α the solution $X^{x,\alpha}$ is unique, since b, being concave, is Lipschitz continuous. The set of admissible strategies, corresponding to an initial condition x, is denoted by $\mathscr{A}_n(x)$.

Consider the cooperative objective functional

$$J_n(x,\alpha) = \sum_{i=1}^n \int_0^\infty e^{-\beta t} f_i(\alpha_t^i)\,dt, \quad \beta > 0$$

of the agent community. *We always assume* that the instantaneous revenue function $f_i : [0,\overline{\alpha}^i] \mapsto \mathbb{R}_+$ of i-th agent is at least *continuous*, and $f_i(0) = 0$. Let

$$v(x) = \sup_{\alpha \in \mathscr{A}_n(x)} J_n(x,\alpha), \quad x \in [0,1] \tag{2}$$

be the value function of the cooperative optimization problem.

When studying the properties of the value function it is convenient to reduce the dimension of the control vector to 1. Recall that the function

$$(g_1 \oplus \dots \oplus g_n)(x) = \inf\{g_1(x_1) + \dots + g_n(x_n) : x_1 + \dots + x_n = x\}$$

is called the *infimal convolution* of $g_1,\dots,g_n$. Let us extend the functions f_i to $\mathbb{R}$ by the values $f_i(u) = -\infty$, $u \notin [0,\overline{\alpha}^i]$ and put

$$\begin{aligned} F(q) &= \sup\{f_1(\alpha_1) + \dots + f_n(\alpha_n) : \alpha_1 + \dots + \alpha_n = q\} \\ &= -((-f_1) \oplus \dots \oplus (-f_n))(q). \end{aligned} \tag{3}$$

The function F is finite on $[0,\overline{q}]$, $\overline{q} = \sum_{i=1}^n \overline{\alpha}^i$, and takes the value $-\infty$ otherwise. From the properties of an infimal convolution it follows that if f_i are continuous (resp., concave), then F is also continuous (resp., concave): see, e.g., [28] (Corollary 2.1 and Theorem 3.1).

Let $q : \mathbb{R}_+ \mapsto [0, \overline{q}]$ be a measurable function. Consider the equation

$$X_t^{x,q} = x + \int_0^t b(X_s^{x,q})\,ds - \int_0^t q_s\,ds \tag{4}$$

instead of (1). If $X_t^{x,q} \geqslant 0$, then the strategy q is called admissible. The set of such strategies is denoted by $\mathscr{A}(x)$. Using an appropriate measurable selection theorem (see [27, Theorem 5.3.1]), we conclude that for any $q \in \mathscr{A}(x)$ there exists $\alpha \in \mathscr{A}_n(x)$ such that $F(q_t) = \sum_{i=1}^n f_i(\alpha_t^i)$. It follows that the value function (2) admits the representation

$$v(x) = \sup_{q \in \mathscr{A}(x)} J(x,q), \quad J(x,q) = \int_0^\infty e^{-\beta t} F(q_t)\,dt.$$

Clearly, for any measurable control $q : \mathbb{R}_+ \mapsto [0, \overline{q}]$ the trajectory $X^{x,q}$ cannot leave the interval $[0,1]$ through the right boundary. Denote by

$$\tau^{x,q} = \inf\{t \geqslant 0 : X_t^{x,q} = 0\}$$

the time of population extinction. As usual, we put $\tau^{x,\alpha} = +\infty$ if $X^{x,\alpha} > 0$. Note that $q_t = 0$, $t \geqslant \tau^{x,q}$ for any admissible control q.

First, we prove directly that v inherits the concavity property of f_i (see Lemma 2 below).

Lemma 1 *Let Y be a continuous solution of the inequality*

$$Y_t \leqslant x + \int_0^t b(Y_s)\,ds - \int_0^t q_s\,ds.$$

Then $Y_t \leqslant X_t^{x,q}$, $t \leqslant \tau := \inf\{s \geqslant 0 : Y_s = 0\}$.

Proof We follow [5] (Chapter 1, Theorem 7). Assume that $Y_{t_1} > X_{t_1}^{x,q}$, $t_1 \leqslant \tau$. Let $t_0 = \max\{t \in [0,t_1] : Y_t \leqslant X_t^{x,q}\}$. We have

$$Y_{t_0} = X_{t_0}^{x,q}, \quad Y_t > X_t^{x,q}, \quad t \in (t_0, t_1]. \tag{5}$$

The function $Z = Y - X^{x,q}$ satisfies the inequality

$$0 \leqslant Z_t \leqslant \int_{t_0}^t (b(Y_s) - b(X_s^{x,q}))\,ds \leqslant K \int_{t_0}^t Z_s\,ds, \quad t \in [t_0, t_1],$$

where K is the Lipschitz constant of b. By the Gronwall inequality (see, e.g., [21, Theorem 1.2.1]) we get a contradiction with (5): $Z_t = 0$, $t \in [t_0, t_1]$. □

Lemma 2 *The function v is non-decreasing. If f_i are concave, then v is concave.*

Proof Let $q \in \mathscr{A}(x)$ and $y > x$. Then

$$X_t^{x,q} \leqslant y + \int_0^t b(X_s^{x,q})\, ds - \int_{t_0}^t q_s\, ds.$$

By Lemma 1 we have $X_t^{x,q} \leqslant X_t^{y,q}$ for $t \leqslant \tau^{x,q}$, and hence for all $t \geqslant 0$. It follows that $\mathscr{A}(x) \subset \mathscr{A}(y)$ and $v(x) \leqslant v(y)$.

Let $0 \leqslant x^1 < x^2 \leqslant 1$, $x = \gamma_1 x^1 + \gamma_2 x^2$, $\gamma_1, \gamma_2 > 0$, $\gamma_1 + \gamma_2 = 1$. For $q^i \in \mathscr{A}(x^i)$ by the concavity of b we have

$$\gamma_1 X_t^{x^1,q^1} + \gamma_2 X_t^{x^2,q^2} \leqslant x + \int_0^t b(\gamma_1 X_t^{x^1,q^1} + \gamma_2 X_t^{x^2,q^2})\, dt - \int_0^t (\gamma_1 q_t^1 + \gamma_2 q_t^2)\, dt.$$

Put $q = \gamma_1 q^1 + \gamma_2 q^2$. Applying Lemma 1 to $Y = \gamma_1 X^{x^1,q^1} + \gamma_2 X^{x^2,q^2}$ and $X^{x,q}$ we get the inequality $Y \leqslant X^{x,q}$. It follows that $q \in \mathscr{A}(x)$. By the concavity of F we obtain:

$$J(x,q) \geqslant \int_0^\infty e^{-\beta t} \left(\gamma_1 F(q_t^1) + \gamma_2 F(q_t^2)\right)\, dt = \gamma_1 J(x^1, q^1) + \gamma_2 J(x^2, q^2).$$

It follows that v is concave: $v(x) \geqslant \gamma_1 v(x^1) + \gamma_2 v(x^2)$. □

Let us introduce the Hamiltonian

$$\begin{aligned} H(x,z) &= b(x)z + \widehat{F}(z), \\ \widehat{F}(z) &= \sup_{q \in [0,\overline{q}]} (F(q) - qz) = \max_{q \in [0, \overline{\alpha}_1 + \cdots + \overline{\alpha}_n]} \max \left\{ \sum_{i=1}^n f_i(\alpha_i) - zq : \sum_{j=1}^n \alpha_j = q \right\} \\ &= \sum_{i=1}^n \max_{\alpha_i \in [0, \overline{\alpha}^i]} (f_i(\alpha_i) - z\alpha_i). \end{aligned} \tag{6}$$

Recall that a continuous function $w : [0,1] \mapsto \mathbb{R}$ is called a *viscosity subsolution* (resp., a *viscosity supersolution*) of the Hamilton-Jacobi-Bellman (HJB) equation

$$\beta w(x) - H(x, w'(x)) = 0 \tag{7}$$

on a set $K \subset [0,1]$, if for any $x \in K$ and any test function $\varphi \in C^1(\mathbb{R})$ such that x is a local maximum (resp., minimum) point of $w - \varphi$, relative to K, the inequality

$$\beta w(x) - H(x, \varphi'(x)) \leqslant 0 \quad \text{(resp., } \geqslant 0)$$

holds true. A function $w \in C([0,1])$ is called a *constrained viscosity solution* (see [26]) of (7) if u is a viscosity subsolution on $[0,1]$ and a viscosity supersolution on $(0,1)$.

By Lemma 2 the value function is continuous. Hence, by Theorem 2.1 of [26], we conclude that v is the unique constrained viscosity solution of (7). However, in our case it is possible to give a more simple characterization of v.

Lemma 3 *Assume that f_i are concave. Then v is the unique continuous function on $[0,1]$, with $v(0) = 0$, satisfying the HJB equation (7) on $(0,1)$ in the viscosity sense.*

Proof Since the equality $v(0) = 0$ follows from the definition of v, we need only to prove that a continuous function w with $w(0) = 0$, satisfying the equation (7) on $(0,1)$ in the viscosity sense, is uniquely defined. To do this we simply show that w is a viscosity subsolution of (7) on $[0,1]$ and refer to the cited result of [26].

The inequality

$$0 = \beta w(0) \leqslant H(0, \varphi'(0)) = \widehat{F}(\varphi'(0))$$

is evident (for any $\varphi \in C^1(\mathbb{R})$). Furthermore, in the terminology of [9, Definitions 2 and 4], the point $x = 1$ is *irrelevant* and *regular* for the left-hand side of the HJB equation. These properties follow from the fact that $z \mapsto \widehat{F}(z)$ is non-increasing and $b(1) = 0$. By the result of [9] (Theorem 2), w automatically satisfies the equation (7) in the viscosity sense on $(0,1]$. □

The subsequent study of the value function strongly relies on its characterization given in Lemma 3. Let

$$\partial w(x) = \{\gamma \in \mathbb{R} : w(y) - w(x) \geqslant \gamma(y - x)\},$$
$$\partial^+ w(x) = \{\gamma \in \mathbb{R} : w(y) - w(x) \leqslant \gamma(y - x)\}$$

be the sub- and superdifferential of a function w. Since $H(x,p)$ is convex in p and satisfies the inequality

$$|H(x,p) - H(y,p)| = |(b(x) - b(y))p| \leqslant K|p||x - y|,$$

by [4, Chapter II, Theorem 5.6] we infer that

$$\beta v(x) - H(x,\gamma) = 0, \quad \gamma \in \partial^+ v(x), \quad x \in (0,1). \tag{8}$$

As a concave function, v is differentiable on a set $G \subset (0,1)$ with a countable complement $(0,1)\backslash G$. Moreover, v' is continuous and non-increasing on G (see [23, Theorem 25.2]). Thus,

$$\beta v(x) - H(x, v'(x)) = 0, \quad x \in G. \tag{9}$$

Denote by δ^i_* the least maximum point of f_i:

$$\delta^i_* = \min\left(\arg \max_{u \in [0,\overline{\alpha}^i]} f_i(u)\right).$$

Let us call a strategy α *static* if it does not depend on t.

Assumption 1 *The static strategy $\delta_* = (\delta_*^1, \dots, \delta_*^n)$ is not admissible for any $x \in [0,1]$. Equivalently, one can assume that $\tau^{x,\delta_*} < \infty$, or*

$$\max_{x\in[0,1]} b(x) < \sum_{i=1}^n \delta_*^i.$$

In what follows *we suppose that the Assumption 1 is satisfied* without further stipulation.

Denote by

$$v'_+(x) = \lim_{y\downarrow x} \frac{v(y)-v(x)}{y-x}, \quad v'_-(x) = \lim_{y\uparrow x} \frac{v(y)-v(x)}{y-x}$$

the right and left derivatives of v. It is well known that $\partial^+ v(x) = [v'_+(x), v'_-(x)]$, $x \in (0,1)$ and the set-valued mapping $x \mapsto \partial^+ v(x)$ is non-increasing:

$$\partial^+ v(x) \geqslant \partial^+ v(y), \quad x < y. \tag{10}$$

For $A, B \subset \mathbb{R}$ we write $A \leqslant B$ if $\xi \leqslant \eta$ for all $\xi \in A$, $\eta \in B$.

Lemma 4 *Assume that f_i are concave. Then the function v' is strictly decreasing on G, and v is strictly concave and strictly increasing.*

Proof To prove that v is strictly concave it is enough to show that $x \mapsto \partial^+ v(x)$ is strictly decreasing:

$$\partial^+ v(x) > \partial^+ v(y), \quad x < y$$

(see [14, Chapter D, Proposition 6.1.3]). Assume that $\partial^+ v(x) \cap \partial^+ v(y) \neq \varnothing$, $x < y$. Then the interval (x,y) contains some points $x_1 < y_1$, $x_1, y_1 \in G$ such that $v'(x_1) = v'(y_1)$. From (10) it follows that v' is differentiable on (x_1,y_1) and equals to a constant. Differentiating the HJB equation (9), we get

$$\beta v'(x) = b'(x)v'(x), \quad x \in (x_1, y_1).$$

Since b is strictly concave, the equality $b'(x) = \beta$, $x \in (x_1,y_1)$ is impossible. Thus, $v'(x) = 0$, $x \in (x_1,y_1)$ and

$$\beta v(x) = \widehat{F}(0) = \sum_{i=1}^n f(\delta_*^i), \quad x \in (x_1, y_1).$$

An optimal solution $\alpha^* \in \mathscr{A}_n(x)$ of the problem (2) exists (see, e.g., [10, Theorem 1]). If $f_i(\alpha_t^{i,*}) < f_i(\delta_*^i) = \max_{u\in[0,\overline{q}^i]} f_i(u)$ on a set of positive measure for at least one index i, then

$$v(x) = J_n(x,\alpha^*) < \sum_{i=1}^n \int_0^\infty e^{-\beta t} f_i(\delta_*^i)\,dt = \frac{1}{\beta}\sum_{i=1}^n f_i(\delta_*^i).$$

If $f_i(\alpha_t^{i,*}) = f_i(\delta_*^i)$ a.e., $i = 1,\dots,n$, then $\alpha_t^{i,*} \geqslant \delta_*^i$ a.e. by the definition of δ_*. But this is impossible since the strategy δ_* is not admissible for x and a fortiori so is α^* (see Lemma 1).

The obtained contradiction implies that $\partial^+ v$ is strictly decreasing. Hence, v is strictly concave. In view of Lemma 2 this property implies that v is strictly increasing. □

Denote by $g^*(x) = \sup_{y\in\mathbb{R}}(xy - g(y))$ the Young-Fenchel transform of a function $g : \mathbb{R} \mapsto (-\infty,\infty]$. Recall (see [24, Proposition 11.3]) that for a continuous convex function $g : [a,b] \mapsto \mathbb{R}$ we have

$$\partial g^*(x) = \arg\max_{y\in[a,b]}(xy - g(y)). \tag{11}$$

The next result establishes a connection between the differentiability of the value function and the optimality of static strategies.

Lemma 5 *Let f_i be concave. If the value function v is not differentiable at $x_0 \in (0,1)$, then the static strategy $q_t = b(x_0) \in \mathscr{A}(x_0)$ is optimal, and x_0 is uniquely defined by the "golden rule": $b'(x_0) = \beta$.*

Proof Assume that $v'_-(x_0) > v'_+(x_0)$, $x_0 \in (0,1)$. By (8) we have

$$\beta v(x_0) = b(x_0)\gamma + \widehat{F}(\gamma), \quad \gamma \in (v'_+(x_0), v'_-(x_0)). \tag{12}$$

Since

$$\widehat{F}(z) = \sup_q\{-zq - (-F(q)\} = (-F)^*(-z), \tag{13}$$

by (11), (12) we obtain

$$\{\widehat{F}'(\gamma)\} = \{-b(x_0)\} = -\arg\max_{q\in[0,\overline{q}]}(F(q) - \gamma q), \quad \gamma \in (v'_+(x_0), v'_-(x_0)). \tag{14}$$

Hence, $\widehat{F}(\gamma) = F(b(x_0)) - b(x_0)\gamma$, $\gamma \in (v'_+(x_0), v'_-(x_0))$ and $b(x_0) \in \mathscr{A}(x_0)$ is optimal:

$$\beta v(x_0) = F(b(x_0)) = \beta J(x_0, b(x_0)).$$

Now assume that the static strategy $b(x_0)$ is optimal. Let us apply the relations Pontryagin's maximum principle to the stationary solution $(X_t, q_t) = (x_0, b(x_0))$ of (4). Consider the adjoint equation

$$\dot\psi(t) = -b'(x_0)\psi(t) \tag{15}$$

and the basic relation of the Pontryagin maximum principle:

$$\psi^0 e^{-\beta t} F(b(x_0)) = \max_{q\in[0,\overline{q}]}\left(\psi^0 e^{-\beta t} F(q) + (b(x_0) - q)\psi(t)\right). \tag{16}$$

We have $\psi(t) = Ae^{-b'(x_0)t}$ for some $A \in \mathbb{R}$. If $(x_0, b(x_0))$ is an optimal solution, then there exist $\psi^0 \in \mathbb{R}_+$, $A \in \mathbb{R}$ such that $(\psi^0, A) \neq 0$ and the relations (15), (16) hold true: see [3, Theorem 1].

Let us rewrite (15), (16) as follows

$$\psi^0 F(b(x_0)) = \max_{q\in[0,\overline{q}]} \left(\psi^0 F(q) + A(b(x_0)-q)e^{(\beta-b'(x_0))t}\right).$$

Assume that $b'(x_0)\neq\beta$. If $\psi^0=0$, then we get a contradiction since $b(x_0)-q$ changes sign on $[0,\overline{q}]$. Thus, we may assume that $\psi^0=1$:

$$\begin{aligned} F(b(x_0)) &= Ab(x_0)e^{(\beta-b'(x_0))t} + \max_{q\in[0,\overline{q}]} \left(F(q) - Ae^{(\beta-b'(x_0))t}q\right) \\ &= H(x_0,z_t), \quad z_t = Ae^{(\beta-b'(x_0))t}. \end{aligned} \tag{17}$$

But the equality (17) is impossible, since either $|z_t|\to\infty$ and $H(x_0,z_t)\to+\infty$, $t\to\infty$, or $|z_t|\to 0$ and

$$H(x_0,z_t)\to H(x_0,0)=\widehat{F}(0)=\sum_{i=1}^n f_i(\delta_*^i), \quad t\to\infty.$$

In the latter case by (3) and (17) we have

$$F(b(x_0))=\sum_{i=1}^n f_i(\nu_i)=\sum_{i=1}^n f_i(\delta_*^i)$$

for some $\nu_i\in[0,\overline{\alpha}^i]$ with $\nu_1+\dots+\nu_n=b(x_0)$. From the definition of δ_*^i it then follows that $\nu_i\geqslant\delta_*^i$, $i=1,\dots,n$. This is a contradiction, since $\sum_{i=1}^n\delta_*^i\notin\mathscr{A}(x_0)$, and $\sum_{i=1}^n\nu^i=b(x_0)$ should retain this property. □

From the properties of b it follows that either $b'(x)<\beta$, $x\in(0,1)$, or the equation

$$b'(x)=\beta, \quad x\in(0,1) \tag{18}$$

has a unique solution $\widehat{x}\in(0,1)$.

Theorem 1 *Suppose that f_i are concave. Then the value function v is strictly increasing, strictly concave and continuously differentiable on $(0,1)$, except maybe the point $\widehat{x}$. If F is differentiable at $b(\widehat{x})$, then v is continuously differentiable.*

Proof From Lemma 5 it follows that $\widehat{x}$ is the only possible discontinuity point of v. If v is not differentiable at $\widehat{x}$, then the interval $(v'_+(\widehat{x}),v'_-(\widehat{x}))$ is non-empty. But if F is differentiable at $b(\widehat{x})$, then (14) gives a contradiction: $F'(b(\widehat{x}))=\gamma$ for all $\gamma\in(v'_+(x_0),v'_-(x_0))$.
□

Note that the assumption, concerning the existence of $F'(b(\widehat{x}))$ is not restrictive. Firstly, F' can have only countably many discontinuity points. Thus, $\widehat{x}$ is not one of these points for all $\beta\in D$, where $(0,\infty)\setminus D$ is countable. Secondly, the formula

$$\partial^+F(q)=\bigcap_{i=1}^n\partial^+f_i(\alpha^i), \quad \sum_{i=1}^n\alpha^i=q, \quad \sum_{i=1}^n f_i(\alpha^i)=F(q) \tag{19}$$

(see [14, Chapter D, Corollary 4.5.5]) shows that $F'(b(\widehat{x}))$ exists if any of the functions f_i is differentiable at α^i, satisfying (19).

The next result shows that the static strategy $q = b(\widehat{x})$ is indeed optimal.

Theorem 2 *Assume that f_i are concave. A static strategy $b(x_0) \in \mathscr{A}(x_0)$, $x_0 \in (0,1)$ is optimal if and only if x_0 coincides with the solution $\widehat{x}$ of* (18).

Proof The necessity is proved in Lemma 5. It remains to prove that $b(\widehat{x}) \in \mathscr{A}(\widehat{x})$ is optimal. If v is not differentiable at $\widehat{x}$, the result follows from Lemma 4. Assume that v is continuously differentiable.

The convex function $\widehat{F}$ is continuously differentiable on a co-countable set $U \subset \mathbb{R}$. Furthermore, v is twice differentiable a.e., and $v'' \leqslant 0$ a.e., since v' is decreasing. Hence, $\widehat{F}(v'(x))$ is differentiable on the co-countable set $(v')^{-1}(U) = \{x \in (0,1) : v'(x) \in U\}$. Differentiating the HJB equation (9), by the chain rule we obtain

$$(\beta - b'(x))v'(x) = v''(x)\left(b(x) + \widehat{F}'(v'(x))\right) \quad a.e.$$

The inequalities

$$\beta - b'(x) < 0, \quad x \in (0,\widehat{x}); \quad \beta - b'(x) > 0, \quad x \in (\widehat{x},1)$$

imply that $v''(x) < 0$ a.e. and

$$b(x) + \widehat{F}'(v'(x)) > 0, \quad \text{a.e. on } (0,\widehat{x}), \quad b(x) + \widehat{F}'(v'(x)) < 0, \quad \text{a.e. on } (\widehat{x},1). \tag{20}$$

Since v' is continuous and strictly decreasing we get the inequalities

$$b(\widehat{x}) + \widehat{F}'_+(v'(\widehat{x})) \geqslant 0 \geqslant b(\widehat{x}) + \widehat{F}'_-(v'(\widehat{x})).$$

Using (11), (13), we obtain

$$b(\widehat{x}) \in -\partial\widehat{F}(v'(\widehat{x})) = \arg\max_{q\in[0,\overline{q}]}\{F(q) - v'(\widehat{x})q\}. \tag{21}$$

It follows that the static strategy $q_t = b(\widehat{x}) \in \mathscr{A}(\widehat{x})$ is optimal:

$$\beta v(\widehat{x}) = b(\widehat{x})v'(\widehat{x}) + \widehat{F}(v'(\widehat{x})) = F(b(\widehat{x})), \quad v(\widehat{x}) = J(\widehat{x}, b(\widehat{x})).$$

□

We turn to the analysis of optimal strategies $q \in \mathscr{A}(x)$ for $x \neq \widehat{x}$. Put

$$\widehat{q}(z) = -\partial\widehat{F}(z). \tag{22}$$

On the co-countable set U, where $\widehat{F}$ is differentiable, the mapping (22) is single-valued. By (21) we have

$$\widehat{q}(v'(x)) = \arg\max_{q\in[0,\overline{q}]}(F(q) - qv'(x)), \quad v'(x) \in U.$$

Note, that $H_z(x,z) = b(x) - \widehat{q}(z)$, $z \in U$. From (20) we know that

$$H_z(x, v'(x)) > 0, \quad \text{a.e. on } (0, \widehat{x}), \qquad H_z(x, v'(x)) < 0, \quad \text{a.e. on } (\widehat{x}, 1).$$

We want to use $\widehat{q}(v'(x))$ as a *feedback control*, formally considering the equation

$$\dot{X} = b(X) - \widehat{q}(v'(X)) = H_z(X, v'(X)), \quad X_0 = x.$$

To do it in a rigorous way let us first introduce

$$\tau^x = \int_x^{\widehat{x}} \frac{du}{H_z(u, v'(u))}.$$

This definition allows τ^x to be infinite. Let $x < \widehat{x}$ (resp., $x > \widehat{x}$). Then the mapping

$$\Psi(y) = \int_x^y \frac{du}{H_z(u, v'(u))}, \quad \Psi : (x, \widehat{x}) \mapsto (0, \tau^x) \quad (\text{resp.}, \Psi : (\widehat{x}, x) \mapsto (0, \tau^x))$$

is a bijection.

Lemma 6 *Let $\psi : [a,b] \mapsto \mathbb{R}$ be continuous and strictly monotonic. Then ψ^{-1} is absolutely continuous if and only if $\psi' \neq 0$ a.e. on (a,b).*

By Lemma 6, which proof can be found in [29] (Theorem 2), the equation

$$t = \int_x^{Y_t} \frac{du}{H_z(u, v'(u))} \tag{23}$$

uniquely defines a locally absolutely continuous function Y_t, $t \in (0, \tau^x)$. Moreover, Y is strictly increasing if $x < \widehat{x}$ and strictly decreasing if $x > \widehat{x}$. From (23) we get

$$\dot{Y}_t = H_z(Y_t, v'(Y_t)) = b(Y_t) - \widehat{q}(v'(Y_t)) \quad \text{a.e. on } (0, \tau^x), \quad Y_0 = x. \tag{24}$$

Theorem 3 *Let f_i be concave and $x \neq \widehat{x}$. Put $\mathscr{T} = \{t \in (0, \tau^x) : v'(Y_t) \in U\}$, where Y is defined by* (23). *Define the strategy*

$$q_t^* = \widehat{q}(v'(Y_t)), \quad t \in \mathscr{T}.$$

On the countable set $(0, \tau^x) \setminus \mathscr{T}$ the values q_t^* can be defined in an arbitrary way. If τ^x is finite put

$$q_t^* = b(\widehat{x}), \quad t \geqslant \tau^x.$$

The strategy $q^* \in \mathscr{A}(x)$ is optimal.

Proof The equality (24) means that $Y_t = X^{x,q^*}$ on $(0,\tau^x)$. Furthermore, $X^{x,q^*} = \widehat{x}$ on $[\tau^x,\infty)$ by the definition of q^*. Clearly, q^* is admissible. To prove that q^* is optimal it is enough to show that

$$W_t = \int_0^t e^{-\beta s} F(q_s^*)\, ds + e^{-\beta t} v(X_t^{x,q^*})$$

is constant, since then

$$W_0 = v(x) = \lim_{t\to\infty} W_t = \int_0^\infty e^{-\beta s} F(q_s^*)\, ds.$$

We have

$$\begin{aligned} \dot W_t &= e^{-\beta t} F(q_t^*) + e^{-\beta t}\left(-\beta v(X_t^{x,q^*}) + v'(X_t^{x,q^*})(b(X_t^{x,q^*}) - q_t^*)\right) \\ &= e^{-\beta t}(-\beta v(X_t^{x,q^*}) + H(X_t^{x,q^*}, v'(X_t^{x,q^*}))) = 0 \quad \text{a.e. on } (0,\tau^x). \end{aligned}$$

For $t > \tau^x$ we have

$$\begin{aligned} W_t &= \int_0^\tau e^{-\beta s} F(q_s^*)\, ds + \frac{F(b(\widehat{x}))}{\beta}(e^{-\beta\tau} - e^{-\beta t}) + e^{-\beta t} v(\widehat{x}) \\ &= \int_0^\tau e^{-\beta s} F(q_s^*)\, ds + \frac{F(b(\widehat{x}))}{\beta} e^{-\beta\tau}, \end{aligned}$$

since $v(\widehat{x}) = F(b(\widehat{x}))/\beta$ by the optimality of the static strategy $b(\widehat{x})$. □

From Theorem 3 we see that if the solution $\widehat{x}$ of (18) exists, then it attracts any optimal trajectory. Moreover, X^{x,q^*} is strictly increasing (resp., decreasing) on $(0,\tau^x)$, if $x < \widehat{x}$ (resp. $x > \widehat{x}$).

We also mention that the multivalued feedback control $\widehat{q}(v'(x))$ satisfies the inequalities

$$b(x) > \widehat{q}(v'(x)), \quad x \in (0,\widehat{x}); \quad b(x) < \widehat{q}(v'(x)), \quad x \in (\widehat{x},1). \tag{25}$$

Indeed, $\widehat{q}(z) = -\partial F(z)$ is a non-increasing multivalued mapping. On a co-countable set U the mappings $\widehat{q}(v'(x))$ are single-valued, non-decreasing and satisfy the inequalities (20). Thus, in any neighbourhood of a point $x \neq \widehat{x}$ there exist $x_1 < x$, $x_2 > x$ such that

$$\widehat{q}(v'(x_1)) \leqslant \widehat{q}(v'(x)) \leqslant \widehat{q}(v'(x_2)),$$

where $\widehat{q}(v'(x_i))$ are single-valued and satisfy (20). It easily follows that

$$b(x) \geqslant \widehat{q}(v'(x)), \quad x \in (0,\widehat{x}); \quad b(x) \leqslant \widehat{q}(v'(x)), \quad x \in (\widehat{x},1). \tag{26}$$

Assume that $b(x_0) \in \widehat{q}(v'(x_0))$, $x_0 \neq \widehat{x}$. Then from the HJB equation (9) it follows that $q = b(x_0) \in \mathscr{A}(x_0)$ is an optimal strategy: $\beta v(x_0) = F(b(x_0))$, in contradiction with Lemma 5. Thus, the inequalities (26) are strict.

3. Cooperative harvesting problem: the case of non-concave revenues

Now we drop the assumption that f_i are concave. Let us extend the class of harvesting strategies. A family $(\mu_t(dx))_{t\geqslant 0}$ of probability measures on $[0,\overline{q}]$ is called a *relaxed control* if the function

$$t \mapsto \int_0^{\overline{q}} \varphi(y)\,\mu_t(dy)$$

is measurable for any continuous function φ. A relaxed control μ induces the dynamics

$$X_t = x + \int_0^t b(X_s)\,ds - \int_0^t \int_0^{\overline{q}} y\mu_s(dy)\,ds.$$

The related value function is defined as follows

$$v_r(x) = \sup_{\mu\in\mathscr{A}^r(x)} J^r(x,\mu), \quad J^r(x,\mu) = \int_0^\infty e^{-\beta t} \int_0^{\overline{q}} F(y)\mu_t(dy)\,dt, \quad x\in[0,1], \tag{27}$$

where $\mathscr{A}^r = \{\mu : X^{x,\mu} \geqslant 0\}$ is the class of admissible relaxed controls.

Denote by $\widetilde{F}$ the concave hull of F: $\widetilde{F} = -(-F)^{**}$. Let

$$\widetilde{v}(x) = \sup_{q\in\mathscr{A}(x)} \widetilde{J}(x,q), \quad \widetilde{J}(x,q) = \int_0^\infty e^{-\beta t}\widetilde{F}(q_t)\,dt \tag{28}$$

be the related value function. Note that by (3) and the properties of infimal convolution ([16], Chapter 3, § 3.4, Theorem 1) we have

$$-\widetilde{F} = (-F)^{**} = (-f_1)^{**}\oplus\cdots\oplus(-f_n)^{**} = (-\widetilde{f}_1)\oplus\cdots\oplus(-\widetilde{f}_n),$$

where $\widetilde{f}_i$ and f^{**} are the convex hull and the double Young-Fenchel transformation of f respectively. Hence,

$$\widetilde{F}(q) = \sup\{\widetilde{f}_1(\alpha_1)+\cdots+\widetilde{f}_n(\alpha_n) : \alpha_1+\cdots+\alpha_n = q\}. \tag{29}$$

Since $\widetilde{F} \geqslant F$ it follows that $\widetilde{v} \geqslant v$. By the Jensen inequality we have

$$J^r(x,\mu) \leqslant \int_0^\infty e^{-\beta t} \int_0^{\overline{q}} \widetilde{F}(y)\mu_t(dy)\,dt \leqslant \int_0^\infty e^{-\beta t}\widetilde{F}(\widetilde{q}_t)\,dt,$$

where $q_t = \int_0^{\overline{q}} y\mu_t(dy)$ is an admissible control for the problem (4). Thus,

$$v(x) \leqslant v_r(x) \leqslant \widetilde{v}(x).$$

Lemma 7 *For any* $p \in [0,\overline{q}]$ *there exists* $p_1, p_2 \in [0,\overline{q}]$, $\varkappa \in (0,1)$ *such that*

$$p = \varkappa p_1 + (1-\varkappa)p_2, \quad \widetilde{F}(p) = \varkappa F(p_1) + (1-\varkappa)F(p_2).$$

The proof of a more general result can be found in [14] (Chapter E, Proposition 1.3.9(ii)).

Denote by $\widetilde{q}_t$ the strategy, constructed in Theorem 3, where F is replaced by $\widetilde{F}$. We claim that

$$\widetilde{F}(\widetilde{q}_t) = F(\widetilde{q}_t), \quad \text{a.e. on } (0,\tau^x). \tag{30}$$

By construction, $\widetilde{q}_t$ is the unique maximum point of $q \mapsto \widetilde{F}(q) - qv'(Y_t)$ on $[0,\overline{q}]$ for all $t \in \widetilde{\mathscr{T}}$, where $(0,\tau^x)\backslash\widetilde{\mathscr{T}}$ is countable. If $\widetilde{F}(\widetilde{q}_t) \neq F(\widetilde{q}_t)$, $t \in \widetilde{\mathscr{T}}$ then, by Lemma 7, $\widetilde{F}$ is affine in an open neighbourhood of $\widetilde{q}_t$, and

$$\arg\max_{q\in[0,\overline{q}]} (\widetilde{F}(q) - v'(Y_t)q\}$$

contains this neighbourhood: a contradiction.

Furthermore, by Lemma 7 there exist $p_1, p_2 \in [0,1]$, $\varkappa \in (0,1)$ such that

$$b(\widehat{x}) = \varkappa p_1 + (1-\varkappa)p_2, \qquad \widetilde{F}(b(\widehat{x})) = \varkappa F(p_1) + (1-\varkappa)F(p_2). \tag{31}$$

Consider the static relaxed control

$$\mu_s = \begin{cases} \widetilde{q}_s, & s < \tau^x, \\ \varkappa\delta_{p_1} + (1-\varkappa)\delta_{p_2}, & s \geqslant \tau^x, \end{cases} \tag{32}$$

where δ_a is the Dirac measure, concentrated at a. By (30), (31) we have

$$J^r(x,\mu) = \int_0^{\tau^x} e^{-\beta t}F(\widetilde{q}_t)\,dt + \int_{\tau^x}^{\infty} e^{-\beta t}(\varkappa F(p_1) + (1-\varkappa)F(p_2))\,dt = \widetilde{J}(x,\widetilde{q}).$$

Thus, $v_r(x) = \widetilde{v}(x)$ and the strategy (32) is optimal for the relaxed problem (27).

To prove that $v_r(x) = v(x)$ let us construct an approximately optimal strategy

$$q^\varepsilon \in \mathscr{A}(x) : J(x,q^\varepsilon) \to v_r(x), \quad \varepsilon \to 0. \tag{33}$$

We may assume that $p_1 \neq p_2$ and $p_1 < b(\widehat{x}) < p_2$. Otherwise, the strategy (32) reduces to an ordinary control $\mu_s = \widetilde{q}_s I_{\{s<\tau^x\}} + b(\widehat{x})I_{\{s\geqslant\tau^x\}}$ and we conclude that $v(x) = v_r(x) = \widetilde{v}(x)$.

Define g by the equation

$$\int_{\widehat{x}-\varepsilon}^{\widehat{x}} (b(\widehat{x}) - b(x))\rho(x)\,dx = \int_{\widehat{x}}^{\widehat{x}+g(\varepsilon)} (b(x) - b(\widehat{x}))\rho(x)\,dx, \tag{34}$$

$$\rho(x) = \frac{1}{(b(x)-p_1)(p_2-b(x))}.$$

Note, that for sufficiently small $\varepsilon > 0$ we have $\rho(x) > 0$ on $(\widehat{x} - \varepsilon, g(\varepsilon))$ and integrands in (34) are positive. Clearly, $g(\varepsilon) \downarrow 0$, $\varepsilon \to 0$. Put

$$\tau_1 = \int\limits_{\widehat{x}}^{\widehat{x}+g(\varepsilon)} \frac{dx}{b(x) - p_1}, \quad \tau_2 = \int\limits_{\widehat{x}-\varepsilon}^{\widehat{x}+g(\varepsilon)} \frac{dx}{p_2 - b(x)},$$

$$\tau_3 = \int\limits_{\widehat{x}-\varepsilon}^{\widehat{x}} \frac{dx}{b(x) - p_1}, \quad \tau = \tau_1 + \tau_2 + \tau_3.$$

For brevity, we omit the dependence of τ_i on ε. Put

$$q_t^\varepsilon = \sum_{j=0}^{\infty} \left(p_1 I_{[j\tau, j\tau+\tau_1)}(t) + p_2 I_{[j\tau+\tau_1, j\tau+\tau_1+\tau_2)}(t) + p_1 I_{[j\tau+\tau_1+\tau_2,(j+1)\tau)}(t) \right). \tag{35}$$

The trajectory $X^{\widehat{x},q^\varepsilon}$ is periodic:

$$\begin{aligned}
&\dot{X}_t^{\widehat{x},q^\varepsilon} = b(X_t^{\widehat{x},q^\varepsilon}) - p_1, \quad (j\tau, j\tau + \tau_1), \quad X_{j\tau}^{\widehat{x},q^\varepsilon} = \widehat{x},\\
&\dot{X}_t^{\widehat{x},q^\varepsilon} = b(X_t^{\widehat{x},q^\varepsilon}) - p_2, \quad (j\tau + \tau_1, j\tau + \tau_1 + \tau_2), \quad X_{j\tau+\tau_1}^{\widehat{x},q^\varepsilon} = \widehat{x} + g^\varepsilon,\\
&\dot{X}_t^{\widehat{x},q^\varepsilon} = b(X_t^{\widehat{x},q^\varepsilon}) - p_1, \quad (j\tau + \tau_1 + \tau_2, (j+1)\tau)), \quad X_{j\tau+\tau_1+\tau_2}^{\widehat{x},q^\varepsilon} = \widehat{x} - \varepsilon.
\end{aligned}$$

It sequentially visits the points $\widehat{x}, \widehat{x} + g^\varepsilon, \widehat{x} - \varepsilon, \widehat{x}$ and moves monotonically between them. Furthermore,

$$\int\limits_{j\tau}^{(j+1)\tau} e^{-\beta t} F(q_t^\varepsilon)\, dt = \frac{e^{-\beta j\tau}}{\beta} \Big((1 - e^{-\beta\tau_1}) F(p_1) + (e^{-\beta\tau_1} - e^{-\beta(\tau_1+\tau_2)}) F(p_2)$$
$$+ (e^{-\beta(\tau_1+\tau_2)} - e^{-\beta\tau}) F(p_1) \Big)$$

Thus,

$$J(\widehat{x}, q^\varepsilon) = \frac{1}{\beta(1 - e^{-\beta\tau})} \Big((1 - e^{-\beta\tau_1}) F(p_1) + (e^{-\beta\tau_1} - e^{-\beta(\tau_1+\tau_2)}) F(p_2)$$
$$+ (e^{-\beta(\tau_1+\tau_2)} - e^{-\beta\tau}) F(p_1) \Big) = \frac{1}{\beta} \left(\frac{\tau_1 + \tau_3}{\tau} F(p_1) + \frac{\tau_2}{\tau} F(p_2) \right) + o(1), \quad \varepsilon \to 0.$$

Since

$$\tau_1 = \frac{g(\varepsilon)}{b(\widehat{x}) - p_1}(1 + o(1)), \quad \tau_2 = \frac{g(\varepsilon) + \varepsilon}{p_2 - b(\widehat{x})}(1 + o(1)), \quad \tau_3 = \frac{\varepsilon}{b(\widehat{x}) - p_1}(1 + o(1)),$$

using (31), we get

$$\frac{\tau_1 + \tau_3}{\tau_2} = \frac{p_2 - b(\widehat{x})}{b(\widehat{x}) - p_1} = \frac{\varkappa}{1 - \varkappa},$$

$$\frac{\tau_1+\tau_3}{\tau} = \frac{1}{1+\tau_2/(\tau_1+\tau_3)} = \varkappa, \qquad \frac{\tau_2}{\tau} = \frac{1}{1+(\tau_1+\tau_3)/\tau_2} = 1-\varkappa.$$

Thus,

$$\lim_{\varepsilon\to 0} J(\widehat{x},q^{\varepsilon}) = \frac{1}{\beta}(\varkappa F(p_1)+(1-\varkappa)F(p_2)) = \frac{\widetilde{F}(b(\widehat{x}))}{\beta} = v(\widehat{x}).$$

We see that the strategy (35) satisfies (33), and $v(x) = v_r(x) = v(x)$. The obtained results are summarized below.

Theorem 4 *The value functions* (2), (27), (28) *coincide:* $v = v_r = \widetilde{v}$. *By Theorem* 1, *applied to* (28), v *is strictly increasing, strictly concave and continuously differentiable on* $(0,1)$, *except maybe the point* $\widehat{x}$. *If* $\widetilde{F}$ *is differentiable at* $b(\widehat{x})$, *then* v *is continuously differentiable. The strategy* (32) *is optimal for the relaxed problem* (27).

4. Rational taxation

Assume that a regulator imposes the proportional tax $v'(x)\alpha$ for the fishing intensity α. Then the myopic agents take their optimal strategies from the sets

$$\widehat{\alpha}^i(x) = \arg\max_{u\in[0,\overline{\alpha}^i]} \{f_i(u) - v'(x)u\}.$$

The direct implementation of such feedback controls may cause technical problems, since the related equation (1) can be unsolvable. Instead of continuous change of the tax $v'(X_t)$, a more realistic approach consists in its fixing for some periods of time: $v'(X_{\tau_j})$, $t\in[\tau_j,\tau_{j+1})$. In this case agents also fix their strategies:

$$\alpha^i_{\tau_i} \in \arg\max_{u\in[0,\overline{\alpha}^i]} \{f_i(u) - v'(X_{\tau_j})u\}, \quad t\in[\tau_j,\tau_{j+1}).$$

This scheme results in “step-by-step positional control” (see [18]), defined recursively by the formulas:

$$\begin{aligned}
X_0^{x,\alpha} &= x,\\
\alpha^i_t = \alpha^i_{\tau_j} &\in \arg\max_{u\in[0,\overline{\alpha}^i]} \{f_i(u) - v'(X^{x,\alpha}_{\tau_j})u\}, \quad t\in[\tau_j,\tau_{j+1}), && (36)\\
X_t^{x,\alpha} &= X^{x,\alpha}_{\tau_j} + \int_{\tau_j}^{t} b(X_s^{x,\alpha})\,ds - \sum_{i=1}^{n}\alpha^i_{\tau_j}\cdot(t-\tau_j), \quad t\in[\tau_j,\tau_{j+1}),\\
0 &= \tau_0 < \ldots \tau_j < \ldots, \quad \tau_j\to\infty, \quad j\to\infty, && (37)
\end{aligned}$$

bypassing at the same time the mentioned technical problems.

Theorem 5 *Let $\widetilde{F}'(\widehat{x})$ exist. Then for any* $\varepsilon > 0$, $\delta > 0$ *there exists a sequence* (37) *such that the strategy* (36) *is approximately optimal:* $J_n(x,\alpha) \geqslant v(x) - \varepsilon$ *and stabilizing in the following sense:*

$$|X_t^{x,\alpha} - \widehat{x}| < \delta, \quad t \geqslant \bar{t}(x,\varepsilon,\delta).$$

Proof First note that

$$\widehat{\alpha}^i(z) := \arg \max_{u\in[0,\overline{\alpha}^i]} (f_i(u) - zu) \subset \widetilde{\alpha}^i(z) := \arg \max_{u\in[0,\overline{\alpha}^i]} (\widetilde{f}_i(u) - zu).$$

Indeed, if $u^* \in \widehat{\alpha}^i(z)$, then $-z \in \partial(-f_i)(u^*)$ and $u^* \in \partial(-f_i)^*(-z)$: see [14, Chapter E, Proposition 1.4.3]. But, by (11),

$$\partial(-f_i)^*(-z) = \arg \max_{u\in[0,\overline{\alpha}^i]} (-zu - (-f_i)^{**}(u)) = \arg \max_{u\in[0,\overline{\alpha}^i]} (\widetilde{f}_i(u) - zu) = \widetilde{\alpha}^i(z).$$

Furthermore, from the representation (29) we get

$$\max_{q\in[0,\overline{q}]} \{\widetilde{F}(q) - zq\} = \sum_{i=1}^n \max_{\alpha_i\in[0,\overline{\alpha}^i]} \{\widetilde{f}_i(\alpha_i) - z\alpha_i\}$$

(see also (6)). Thus,

$$\widetilde{q}(z) := \arg \max_{q\in[0,\overline{q}]} (\widetilde{F}(q) - zq) = \sum_{i=1}^n \widetilde{\alpha}^i(z) \supset \sum_{i=1}^n \widehat{\alpha}^i(z). \tag{38}$$

From (25) it then follows that

$$\begin{aligned} b(x) &> \sum_{i=1}^n \widehat{\alpha}^i(v'(x)), \quad x \in (0,\widehat{x}), \\ b(x) &< \sum_{i=1}^n \widehat{\alpha}^i(v'(x)), \quad x \in (\widehat{x},1). \end{aligned} \tag{39}$$

The subsequent argumentation follows the introductory section of [17]. For any $x_0 \in (0,1)$ and any $\alpha_0^i \in \widehat{\alpha}^i(v'(x_0))$ we have

$$\beta v(x_0) = \left(b(x_0) - \sum_{i=1}^n \alpha_0^i\right) v'(x_0) + \sum_{i=1}^n f_i(\alpha_0^i).$$

Put,

$$\psi(x,\alpha) = -\beta v(x) + \left(b(x) - \sum_{i=1}^n \alpha^i\right) v'(x) + \sum_{i=1}^n f_i(\alpha^i)$$

and define the time moment

$$\tau_1 = \inf\{t \geqslant 0 : \psi(X_t^{x_0,\alpha_0}, \alpha_0) < -\beta\varepsilon \text{ or } X_t^{x_0,\alpha_0} > \widehat{x} + \delta\}, \quad x_0 \in (0, \widehat{x}), \tag{40}$$

$$\tau_1 = \inf\{t \geqslant 0 : \psi(X_t^{x_0,\alpha_0}, \alpha_0) < -\beta\varepsilon \text{ or } X_t^{x_0,\alpha_0} < \widehat{x} - \delta\}, \quad x_0 \in (\widehat{x}, 1), \tag{41}$$

$$\tau_1 = \inf\{t \geqslant 0 : \psi(X_t^{x_0,\alpha_0}, \alpha_0) < -\beta\varepsilon \text{ or } X_t^{x_0,\alpha_0} \notin (\widehat{x} - \delta, \widehat{x} + \delta)\}, \quad x_0 = \widehat{x}. \tag{42}$$

For $t \in [0, \tau_1]$ in each of the cases (40), (41), (42) we have respectively

$$X_t^{x_0,\alpha_0} \in [x_0, \widehat{x} + \delta], \quad X_t^{x_0,\alpha_0} \in [\widehat{x} - \delta, x_0], \quad X_t^{x_0,\alpha_0} \in [\widehat{x} - \delta, \widehat{x} + \delta].$$

Assume that x_{k-1}, α_{k-1}, τ_k are defined. Put

$$x_k = X_{\tau_k}^{x_{k-1},\alpha_{k-1}}, \quad \alpha_k^i \in \widehat{\alpha}^i(v'(x_k)),$$

$$\tau_{k+1} = \inf\{t \geqslant \tau_k : \psi(X_t^{x_k,\alpha_k}, \alpha_k) < -\beta\varepsilon \text{ or } X_t^{x_k,\alpha_k} > \widehat{x} + \delta\}, \quad x_k \in (0, \widehat{x}), \tag{43}$$

$$\tau_{k+1} = \inf\{t \geqslant \tau_k : \psi(X_t^{x_k,\alpha_k}, \alpha_k) < -\beta\varepsilon \text{ or } X_t^{x_k,\alpha_k} < \widehat{x} - \delta\}, \quad x_k \in (\widehat{x}, 1), \tag{44}$$

$$\tau_{k+1} = \inf\{t \geqslant \tau_k : \psi(X_t^{x_k,\alpha_k}, \alpha_k) < -\beta\varepsilon \text{ or } X_t^{x_k,\alpha_k} \notin (\widehat{x} - \delta, \widehat{x} + \delta)\}, \quad x_k = \widehat{x}. \tag{45}$$

The function $x \mapsto \psi(x, \alpha)$ is uniformly continuous on any interval $[a, b] \subset (0, 1)$ uniformly in $\alpha \in [0, \overline{q}]$. Thus, there exists δ' such that if

$$|\psi(x, \alpha) - \psi(y, \alpha)| \geqslant \beta\varepsilon, \quad [x, y] \subset [a, b],$$

then $|x - y| \geqslant \delta'$. Assume that $\psi(X_{\tau_{k+1}}^{x_k,\alpha_k}, \alpha_k) = -\beta\varepsilon$. Since $\psi(x_k, \alpha_k) = 0$, we get

$$\delta' \leqslant |X_{\tau_{k+1}}^{x_k,\alpha_k} - x_k| \leqslant \int_{\tau_k}^{\tau_{k+1}} b(X_t^{x_k,\alpha_k})\, dt + \int_{\tau_k}^{\tau_{k+1}} \sum_{i=1}^n \alpha_k^i\, dt \leqslant (\overline{b} + \overline{q})(\tau_{k+1} - \tau_k),$$

where $\overline{b} = \max_{x \in [0,1]} b(x)$. Furthermore, if $\psi(X_{\tau_{k+1}}^{x_k,\alpha_k}) > -\beta\varepsilon$ and $\tau_{k+1} < \infty$, then in any of three cases (43), (44), (45) we have

$$\delta \leqslant |X_{\tau_{k+1}}^{x_k,\alpha_k} - x_k| \leqslant (\overline{b} + \overline{q})(\tau_{k+1} - \tau_k).$$

Thus, the differences $\tau_{k+1} - \tau_k$ are uniformly bounded from below by a positive constant, and the strategy $\alpha = \sum_{k=0}^{\infty} \alpha_k I_{[\tau_k, \tau_{k+1})}(t)$ is well defined for all $t \geqslant 0$. Note, that $X_t^{x_0,\alpha}$ belongs to one of the sets $[x_0, \widehat{x} + \delta]$, $[\widehat{x} - \delta, x_0]$, $[\widehat{x} - \delta, \widehat{x} + \delta]$ for all $t \geqslant 0$.

By the Berge maximum theorem (see [1, Theorem 17.31]) the set-valued mapping $\widehat{\alpha}$ is upper hemicontinuous, hence its graph is closed (see [1, Theorem 17.10]). From (39) it then follows that there is a finite gap between $b(x)$ and $\sum_{i=1}^n \widehat{\alpha}^i(v'(x))$ on $(0, \widehat{x} - \delta) \cup (\widehat{x} + \delta, 1)$. Thus, $|\dot{X}^{\alpha,x_0}|$ is uniformly bounded from below by a positive constant, when $X^{\alpha,x_0} \in (0, \widehat{x} - \delta) \cup (\widehat{x} + \delta, 1)$. This property implies that X^{α,x_0} reaches the neighbourhood $[\widehat{x} - \delta, \widehat{x} + \delta]$ in finite time $\overline{t}(x, \varepsilon, \delta)$. After reaching this neighbourhood, X^{α,x_0} remains in it forever by the construction of α.

It remains to prove that α is ε-optimal. We have

$$-\beta v(X_t^{x_k,\alpha_k})+\left(b(X_t^{x_k,\alpha_k})-\sum_{i=1}^n \alpha_k^i\right)v'(X_t^{x_k,\alpha_k})+\sum_{i=1}^n f_i(\alpha_k^i)\geqslant -\beta\varepsilon,\quad t\in(\tau_k,\tau_{k+1}).$$

After the multiplication on $e^{-\beta t}$ an integration we get

$$e^{-\beta\tau_{k+1}}v(X_{\tau_{k+1}}^{x_k,\alpha_k})-e^{-\beta\tau_k}v(X_{\tau_k}^{x_k,\alpha_k})+\int_{\tau_k}^{\tau_{k+1}} e^{-\beta t}\sum_{i=1}^n f_i(\alpha_k^i)\,dt\geqslant \varepsilon(e^{-\beta\tau_{k+1}}-e^{-\beta\tau_k}).$$

Summing up and passing to the limit we obtain the desired inequality:

$$\int_0^\infty e^{-\beta t}\sum_{i=1}^n f_i(\alpha_t^i)\,dt\geqslant v(x_0)-\varepsilon.$$

□

As an example, consider the problem with n identical agents and assume that their common profit function is linear: $f_i(u)=f(u)=u$, $u\in[0,\overline{\alpha}]$. The HJB equation (9) takes the form

$$\beta v(x)=b(x)v'(x)+n\max_{u\in[0,\overline{\alpha}]}(u-v'(x)u).$$

From (21) it follows that $v'(\widehat{x})=1$. Thus,

$$v'(x)>1,\quad x<\widehat{x},\quad v'(x)<1,\quad x>\widehat{x} \tag{46}$$

and v satisfies the equations

$$\beta v(x)=b(x)v'(x),\quad x<\widehat{x};\qquad \beta v(x)=(b(x)-n\overline{\alpha})v'(x)+n\overline{\alpha},\quad x>\widehat{x}.$$

Solving these equations, by the uniqueness result, given in Lemma 3, we infer that

$$v(x)=\frac{b(\widehat{x})}{\beta}\exp\left(-\int_x^{\widehat{x}}\frac{\beta}{b(y)}\,dy\right),\quad x\in(0,\widehat{x}],$$

$$v(x)=\frac{1}{\beta}(b(\widehat{x})-n\overline{\alpha})\exp\left(\int_{\widehat{x}}^x\frac{\beta}{b(y)-\overline{\alpha}n}\,dy\right)+\frac{1}{\beta}n\overline{\alpha},\quad x\in[\widehat{x},1].$$

For the biomass quantities x below the critical level $\widehat{x}$ the tax $v'(x)$ does not depend on n:

$$v'(x)=\frac{b(\widehat{x})}{b(x)}\exp\left(-\int_x^{\widehat{x}}\frac{\beta}{b(y)}\,dy\right),\quad x\in(0,\widehat{x}].$$

For larger values of x we have

$$v'(x) = \frac{n\overline{\alpha} - b(\widehat{x})}{n\overline{\alpha} - b(x)} \exp\left(-\int_{\widehat{x}}^{x} \frac{\beta}{n\overline{\alpha} - b(y)}\,dy\right), \quad x \in [\widehat{x}, 1].$$

In particular, $v'(x) \to f'(0) = 1$, $n \to \infty$.

Note, that a tax, stimulating an optimal cooperative behavior is by no means unique. For instance, any tax, satisfying (46), can serve this purpose. So, the most interesting quantity is the "critical tax"

$$v'(\widehat{x}) = \widetilde{F}'(b(\widehat{x})). \tag{47}$$

The equality (47) follows from (21). Consider $\widetilde{F}$ as the value function of the elementary problem (29), where the artificial agents with concave revenues $\widetilde{f}_i$ cooperatively distribute some given harvesting intensity q. Formula (47) shows that $v'(\widehat{x})$ is simply the shadow price of the critical growth growth rate $b(\widehat{x})$ within this problem.

We are interested in the dependence of the critical tax $v'(\widehat{x})$ on the size of agent community. Consider again n identical agents with the revenue functions $f_i = f$. If f is linear, the critical tax, as we have seen, does not depend on n. Assume now that f is differentiable and strictly concave. Then by (21) and (38) we get

$$b(\widehat{x}) \in \sum_{i=1}^{n} \arg\max_{u\in[0,\overline{\alpha}]} \{f(u) - v'(\widehat{x})u\}$$

Taking optimal values of u to be equal, we conclude that $v'(\widehat{x}) = f'(b(\widehat{x})/n)$. Thus, $v'(\widehat{x})$ is increasing in n, and $v'(\widehat{x}) \to f'(0)$, $n \to \infty$. Our final result shows that this situation is typical: the critical tax can only increase, when the agent community widens.

Theorem 6 *Denote by F_n, F_{n+m} and v_n, v_{n+m} the cooperative instantaneous revenue functions* (3) *and the value functions* (2)*, corresponding to the agent communities*

$$\{f_i\}_{i=1}^{n} \subset \{f_i\}_{i=1}^{n+m}.$$

Assume that $\widetilde{F}_n'(b(\widehat{x}))$, $\widetilde{F}_{n+m}'(b(\widehat{x}))$ exist. Then

$$v_n'(\widehat{x}) = \widetilde{F}_n'(b(\widehat{x})) \leqslant v_{n+m}'(\widehat{x}) = \widetilde{F}_{n+m}'(b(\widehat{x})).$$

Proof It is enough to consider the case $m = 1$. By the associativity of the infimal convolution we have

$$(-\widetilde{F}_{n+1})(q) = (-\widetilde{F}_n) \oplus (-\widetilde{f}_{n+1})(q).$$

The formula for the subdifferential of an infimal convolution, given in [14, Chapter D, Corollary 4.5.5], implies that

$$\partial(-\widetilde{F}_{n+1})(q) \subseteq \bigcup_{u} \partial(-\widetilde{F}_n)(u) \cap \partial(-\widetilde{f}_{n+1})(q-u) \subseteq \bigcup_{u\in[0,q]} \partial(-\widetilde{F}_n)(u).$$

But since the set-valued mapping $u \mapsto \partial(-\widetilde{F}_{n+1})(u)$ is non-decreasing, we have

$$\partial(-\widetilde{F}_{n+1})(q) \leqslant \partial(-\widetilde{F}_n)(q), \quad q \in [0, \overline{q}].$$

Thus, $\widetilde{F}'_{n+1}(b(\widehat{x})) \geqslant \widetilde{F}'_n(b(\widehat{x}))$. □

A resembling result for discrete time problem was proved in [25, Theorem 3].

References

[1] C.D. ALIPRANTIS and K.C. BORDER: Infinite Dimensional Analysis. A Hitchhiker's Guide. Springer, Berlin, 2006.

[2] R. ARNASON: Fisheries management and operations research. *European J. of Operational Research*, **193**(3), (2009), 741-751.

[3] S.M. ASEEV and A.V. KRYAZHIMSKII: On a class of optimal control problems arising in mathematical economics. *Proc. of the Steklov Institute of Mathematics*, **262**(1), (2008), 10-25.

[4] M. BARDI and I. CAPUZZO-DOLCETTA: Optimal Control and Viscosity Solutions of Hamilton-Jacobi-Bellman Equations. Birkhauser, Boston, 1997.

[5] G. BIRKHOFF and G.-C. ROTA: Ordinary Differential Equations. Wiley, New York, 1989.

[6] C.W. CLARK: Mathematical models in the economics of renewable resources. *SIAM Review*, **21**(1), (1979), 81-99.

[7] C.W. CLARK: Towards a predictive model for the economic regulation of commercial fisheries. *Canadian J. of Fisheries and Aquatic Sciences*, **37**(7), (1980), 1111-1129.

[8] C.W. CLARK: The Worldwide Crisis in Fisheries. Economic Models and Human Behavior. Cambridge University Press, Cambridge, 2006.

[9] M.G. CRANDALL and R. NEWCOMB: Viscosity solutions of Hamilton-Jacobi equations at the boundary. *Proc. of the American Mathematical Society*, **94**(2), (1985), 283-2903.

[10] A.V. DMITRUK and N.V. KUZ'KINA: Existence theorem in the optimal control problem on an infinite time interval. *Mathematical Notes*, **78**(4), (2005), 466-480.

[11] H.S. GORDON: The economic theory of a common-property resource: the fishery. *J. of Political Economy*, **62**(2), (1954), 124-142.

[12] N. Hanley, J.F. Shogren and B. White: *Environmental Economics in Theory and Practice*. Macmillan Education UK, London, 1997.

[13] G. Hardin: The tragedy of the commons. *Science*, **162** 1243-1248, (1968).

[14] J.-B. Hiriart-Urruty and C. Lemaréchal: *Fundamentals of Convex Analysis*. Springer, Berlin, 2001.

[15] V.G. Il'ichev: *Stability, Adaptation and Control in Ecological Systems*. Fizmatlit, Moscow, 2009.

[16] A.D. Ioffe and V.M. Tihomirov: Theory of Extremal Problems. North-Holland, Amsterdam, 1979.

[17] H. Ishii and S. Koike: On ε-optimal controls for state constraint problems. *Annales de l'Institut Henri Poincaré (C) Analyse Non Linéaire*, **17**(4), (2000), 473-502.

[18] N.N. Krasovskii and A.I. Subbotin: *Game-Theoretical Control Problems*. Springer, New York, 1988.

[19] N.V. Long: Dynamic games in the economics of natural resources: A survey. *Dynamic Games and Applications*, **1**(1), (2011), 115-148.

[20] R. McKelvey: Common property and the conservation of natural resources. In: S.A. Levin, T.G. Hallam and L.J. Gross (Eds.) *Applied Mathematical Ecology*, 58-80. Springer, Berlin, 1989.

[21] B.G. Pachpatte: Inequalities for Differential and Integral Equations. Academic Press, San Diego, 1998.

[22] J.P. Rincón-Zapatero and M.S. Santos: Differentiability of the value function in continuous-time economic models. *J. of Mathematical Analysis and Applications*, **394**(1), (2012), 305-323.

[23] R.T. Rockafellar: *Convex Analysis*. Princeton University Press, Princeton, 1970.

[24] R.T. Rockafellar and R.J.-B. Wets: Variational analysis. Springer-Verlag, Berlin, 2009.

[25] D.B. Rokhlin: The derivative of the solution to the Bellman functional equation and the value of bioresources. *Sibirskii Zhurnal Industrial'noi Matematiki*, **3**(1(5)), (2000), 169-181.

[26] H.M. Soner: Optimal control with state-space constraint. I. *SIAM J. on Control and Optimization*, **24**(3), (1986), 552-561.

[27] S.M. SRIVASTAVA: *A Course on Borel Sets*. Springer-Verlag, New York, 1998.

[28] T. STRÖMBERG: The operation of infimal convolution. *Dissertationes Mathematicae*, **352** (1996), 1-58.

[29] A. VILLANI: On Lusin's condition for the inverse function. *Rendiconti del Circolo Matematico di Palermo*, **33**(3), (1984), 331-335.

Archives of Control Sciences
Volume 27(LXIII), 2017
No. 1*, pages 29–39*

State estimation in a decentralized discrete time LQG control for a multisensor system

ZDZISLAW DUDA

In the paper a state filtration in a decentralized discrete time Linear Quadratic Gaussian problem formulated for a multisensor system is considered. Local optimal control laws depend on global state estimates and are calculated by each node. In a classical centralized information pattern the global state estimators use measurements data from all nodes. In a decentralized system the global state estimates are computed at each node using local state estimates based on local measurements and values of previous controls, from other nodes.

In the paper, contrary to this, the controls are not transmitted between nodes. It leads to nonconventional filtration because the controls from other nodes are treated as random variables for each node. The cost for the additional reduced transmission is an increased filter computation at each node.

Key words: multisensor system, LQG problem, Kalman filter

1. Introduction

Multisensor systems find applications in many areas such as aerospace, robotics, image processing, military surveillance, medical diagnosis. The advantage of using these systems over systems with a single sensor results from e.g. improved reliability, robustness, extended coverage, improved resolution e.t.c. In the systems a state estimation problem is one of the critical concerns.

Theoretically, state estimates can be determined by using a conventional Kalman filter in a centralized structure where all process measurements are sent to a central station.

The centralized architecture produces an optimal estimate in a minimum mean square error (MMSE) sense, but it may imply low survivability and requires high processing and communication loads.

Due to limited communication bandwith or reliability constraints fusion algorithms and appropriate architectures (from hierarchical to fully decentralized) are proposed.

The Author is with Silesian University of Technology, Gliwice, Poland, e-mail: Zdzislaw.Duda@polsl.pl

This work has been supported with a grant from the Polish Ministry of Science and High Education.

Received 25.10.2016. Revised 06.02.2017.

In these architecture each node carries out Kalman filtering upon its own measurements and then transmits the local processed data to a fusion center [4, 5, 10] (hierarchical structure) or to other nodes [9, 8] (fully decentralized structure). In fusion nodes a global state estimate is calculated. It may be equivalent to the optimal centralized estimate [4, 5, 10] or suboptimal [1, 2, 3].

In majority papers autonomous systems [1, 2, 3, 6, 12] are considered. A control, if introduced, is a known input [5] or depends on local state estimate [7], only.

In [11] a decentralized Linear-Quadratic-Gaussian (LQG) control problem involving M nodes is considered. Local controls depend on global state estimates. At each node local state estimates are computed using measurement data obtained at that node and values of previous controls from other nodes. The local control law at each node is a linear combination of local state estimates and previous controls transmitted from other nodes.

In this paper a Linear-Quadratic-Gaussian (LQG) problem [11] is considered. Contrary to [11], controls are not transmitted between nodes. It leads to nonconventional local filtration because controls from other nodes should be treated as random variables for each node. The cost for this additional reduced transmission is increased filter computation at each node.

2. Problem formulation

Consider a linear multisensor system described by the equations

$$x_{n+1} = Ax_n + \sum_{j=1}^{M} B^j u_n^j + w_n \tag{1}$$

$$y_n^j = C^j x_n + r_n^j, \quad j = 1, \dots, M \tag{2}$$

where x_n is a state vector, u_n^j is a control vector at node j, y_n^j is a measurement vector at node j ; A, B^j, C^j are the system and observation models, w_n, r_n^j are the state and measurement noises, respectively. It is assumed that $x_0 \sim N(\bar{x}_0, X_0)$, $w_n \sim N(0, W_n)$, $r_n^j \sim N(0, R_n^j)$ and $x_n \in R^k$, $w_n \in R^k$, $y_n^j \in R^{p^j}$, $r_n^j \in R^{p^j}$; $A \in R^{k \times k}$, $C^j \in R^{p_j \times k}$. Additionally, w_n, $r_m^j, j = 1, \dots, M$ are gaussian white noise processes independent of each other and of the gaussian initial state x_0.

The optimal control problem is to find

$$I^o = \min_{\{a_n^j(\vec{y}_n), n=0,\dots,N, j=1,\dots,M\}} E[\frac{1}{2} \sum_{n=0}^{N} (x_n^T Q_n x_n + \sum_{j=1}^{M} u_n^{jT} H^j u_n^j)_{u_n^j = a_n^j(\vec{y}_n)}] \tag{3}$$

subject to the stochastic system (1) where Q_n and H^j are positive semidefinite and positive definite, respectively, symmetric matrices and $\vec{y}_n = \{y_0, \dots, y_n\}, \quad y_i = [y_i^{1T}, \dots, y_i^{MT}]^T$ is the measurement available history.

It is the control problem formulated in a classical information pattern, because control laws are functions of all measurement data.

The solution to the control problem is known [11]. Control laws $a_n^j(\vec{y}_n),\ \ j = 1,\dots,M$, depend on global state estimates based on measurements obtained from all nodes. In [11] a decentralized system is proposed. The global state estimate is obtained as a linear combination of local state estimates based on local measurement information and values of previous controls from all nodes.

The problem formulated in the paper is to compute local state estimates using measurements only at that node. It leads to a decentralized system with an additional reduced data transmission.

3. Solution to the centralized LQG control problem

The solution to the LQG problem [11] has the form

$$u_n^{jo} = S_n^j \hat{x}_{n|n} \tag{4}$$

where the global state estimate $\hat{x}_{n|n}$ is defined as

$$\hat{x}_{n|n} = E(x_n|\vec{y}_n) \tag{5}$$

The quantity y_n is a stacked measurement vector resulting from the eqn. (2) and written in the form

$$y_n = Cx_n + r_n \tag{6}$$

where $y_n = [y_n^{1T},\dots,y_n^{MT}]^T$, $C = [C^{1T},\dots,C^{MT}]^T$, $r_n = [r_n^{1T},\dots,r_n^{MT}]^T$, $R_n = Er_nr_n^T = diag\{R_n^1,\dots,R_n^M\}$.

The control gain S_n^j is

$$S_n^j = -(H^j + B^{jT}\Lambda_{n+1}B^j)^{-1}B^{jT}\Lambda_{n+1}A \tag{7}$$

where Λ_n is propagated backwards in time as

$$\Lambda_n = A^T\Lambda_{n+1}A - \sum_{j=1}^{M} S_n^{jT}(H^j + B^{jT}\Lambda_{n+1}B^j)S_n^j + Q_n \tag{8}$$

The global state estimate $\hat{x}_{n|n}$ is propagated as

$$\hat{x}_{n+1|n+1} \quad = \hat{x}_{n+1|n} + K_{n+1}(y_{n+1} - C\hat{x}_{n+1|n}) \tag{9}$$

where

$$\hat{x}_{n+1|n} = E(x_{n+1}|\vec{y}_n) = A\hat{x}_{n|n} + \sum_{j=1}^{M} B^j u_n^j \tag{10}$$

The Kalman gain K_{n+1} is given as

$$K_{n+1} = P_{n+1|n}C^T(CP_{n+1|n}C^T + R_{n+1})^{-1} \tag{11}$$

where $P_{n+1|n} = E(x_{n+1} - \hat{x}_{n+1|n})(x_{n+1} - \hat{x}_{n+1|n})^T$ has the form

$$P_{n+1|n} = AP_{n|n}A^T + W_n, \quad P_{0|-1} = X_0 \tag{12}$$

The covariance matrix $P_{n+1|n+1} = E(x_{n+1} - \hat{x}_{n+1|n+1})(x_{n+1} - \hat{x}_{n+1|n+1})^T$ is propagated as

$$P_{n+1|n+1} = (\mathbf{1} - K_{n+1}C)P_{n+1|n} \tag{13}$$

or in the information form

$$P^{-1}_{n+1|n+1} = P^{-1}_{n+1|n} + \sum_{j=1}^{M} C^{jT}(R^j_{n+1})^{-1}C^j \tag{14}$$

where $\mathbf{1}$ is the identity matrix.

Using (11) and (13) gives

$$K_{n+1} = P_{n+1|n+1}C^T R^{-1}_{n+1} \tag{15}$$

Then the propagation of the estimate $\hat{x}_{n|n}$ described by (9) can be expressed in the form

$$\hat{x}_{n+1|n+1} = \hat{x}_{n+1|n} + P_{n+1|n+1}\sum_{j=1}^{M} C^{jT}(R^j_{n+1})^{-1}(y^j_{n+1} - C^j\hat{x}_{n+1|n}) \tag{16}$$

The eqn. (4)-(16) form the solution to the LQG problem.

Let us notice that the state estimate (16) with (10) depends on measurements and controls from all nodes. In decentralized systems state estimates and consequently controls should be calculated by each node using measurements available only at that node.

4. Solution to the decentralized LQG problem

In [11] a solution to the decentralized LQG problem is presented. The control laws have the form (4).

The state estimate $\hat{x}_{n|n}$ is divided into two parts

$$\hat{x}_{n|n} = \hat{x}^D_{n|n} + x^C_n \tag{17}$$

where

$$x^C_{n+1} = Ax^C_n + \sum_{j=1}^{M} B^j u^j_n, \quad x^C_0 = \bar{x}_0 \tag{18}$$

and

$$\hat{x}^D_{n+1|n+1} = \sum_{j=1}^{M} [P_{n+1|n+1}(P^j_{n+1|n+1})^{-1}\hat{x}^{Dj}_{n+1|n+1} + h^j_{n+1}] \tag{19}$$

At each node an additional vector h^j_n is calculated as

$$h^j_{n+1} = F_{n+1}h^j_n + G^j_{n+1}\hat{x}^{Dj}_{n+1|n}, \quad h^j_0 = 0 \tag{20}$$

where

$$\begin{aligned} &\hat{x}^{Dj}_{n+1|n} = A\hat{x}^{Dj}_{n|n}, \quad F_n = P_{n|n}P^{-1}_{n|n-1}A \\ &G^j_{n+1} = P_{n+1|n+1}[(P_{n+1|n})^{-1}AP_{n|n}(P^j_{n|n})^{-1}A^{-1} - (P^j_{n+1|n})^{-1}] \end{aligned} \tag{21}$$

and $P^j_{n|n} = E(x^D_n - \hat{x}^{Dj}_{n|n})(x^D_n - \hat{x}^{Dj}_{n|n})^T$ and $P^j_{n|n-1} = E(x^D_n - \hat{x}^{Dj}_{n|n-1})(x^D_n - \hat{x}^{Dj}_{n|n-1})^T$.

The state estimate $\hat{x}^{Dj}_{n|n}$ determined by each node has the form

$$\hat{x}^{Dj}_{n+1|n+1} = A\hat{x}^{Dj}_{n|n} + P^j_{n+1|n+1}C^{jT}(R^j_n)^{-1}(y^j_{n+1} - C^jx^C_{n+1} - C^jA\hat{x}^{Dj}_{n|n}), \ \ \hat{x}^{Dj}_{0|0} = 0 \tag{22}$$

where a covariance matrix $P^j_{n+1|n+1}$ has a classical form.

Using (7), (17) and (19) in (4) the $j-th$ local optimal control law becomes

$$u^{jo}_n = -(H^j + B^{jT}\Lambda_{n+1}B^j)^{-1}B^{jT}\Lambda_{n+1}\{\sum_{l=1}^{M}[P_{n|n}(P^l_{n|n})^{-1}\hat{x}^{Dl}_{n|n} + h^l_n] + x^C_n\} \tag{23}$$

Let us notice that in order to determine the value of the optimal control u^{jo}_n at the $j-th$ node, the p_j dimensional vectors α^{lj}_n defined as

$$\alpha^{lj}_n = B^{jT}\Lambda_{n+1}[P_{n|n}(P^l_{n|n})^{-1}\hat{x}^{Dl}_{n|n} + h^l_n], \quad l = 1,...,M, \ \ l \neq j \tag{24}$$

should be transmitted from other nodes to the node j. Moreover the controls u^l_{n-1} from other nodes must be transmitted too, so that to form (18), (22) and finally (23).

At each node the vector h^j_n must be calculated. Since h^j_n depends on measurements, it should be calculated on-line. The operations in (19) and (20) can be done in parallel.

5. New approach to filtration in the decentralized LQG problem

Let us consider the eqn. (1) in which the control is described by the eqn. (4) i.e.

$$x_{n+1} = Ax_n + B_n\hat{x}_{n|n} + w_n \tag{25}$$

where $B_n = \sum_{j=1}^{M} B^jS^j_n$.

The objective of the local filtration at the $j-th$ node is to compute local estimates using measurements available at that node.

The system (25) can be written in the form

$$x_{n+1} = A_n x_n - B_n \widetilde{x}_{n|n} + w_n \tag{26}$$

where $A_n = A + B_n$ and $\widetilde{x}_{n|n} = x_n - \hat{x}_{n|n}$.

Let a local estimate at the $j-th$ node has the form

$$\hat{x}_n^j = E(x_n|\vec{y}_n^j) \tag{27}$$

where $\vec{y}_n^j = \{y_0^j, ..., y_n^j\}$.

Then the estimate $\hat{x}_{n+1|n+1}^j$ is propagated as

$$\hat{x}_{n+1|n+1}^j = \hat{x}_{n+1|n}^j + K_{n+1}^j (y_{n+1}^j - C^j \hat{x}_{n+1|n}^j) \tag{28}$$

The term $\hat{x}_{n+1|n}^j$ in (28) becomes

$$\hat{x}_{n+1|n}^j = E(x_{n+1}|\vec{y}_n^j) = A_n \hat{x}_{n|n}^j - B_n E(\widetilde{x}_{n|n}|\vec{y}_n^j) \tag{29}$$

We find that

$$\begin{aligned} E(\widetilde{x}_{n|n}|\vec{y}_n^j) \quad &= E[(x_n - \hat{x}_{n|n})|\vec{y}_n^j] = E(x_n|\vec{y}_n^j) - E(\hat{x}_{n|n}|\vec{y}_n^j) = \\ &= E(x_n|\vec{y}_n^j) - E\{[E(x_n|\vec{y}_n)]|\vec{y}_n^j\} = E(x_n|\vec{y}_n^j) - E(x_n|\vec{y}_n^j) = 0 \end{aligned} \tag{30}$$

Thus the last term in (29) is equal to zero and $\hat{x}_{n+1|n}^j$ in (28) has the form

$$\hat{x}_{n+1|n}^j = A_n \hat{x}_{n|n}^j \tag{31}$$

The Kalman gain K_{n+1}^j is

$$K_{n+1}^j = P_{n+1|n}^j C^{jT} (C^j P_{n+1|n}^j C^{jT} + R_{n+1}^j)^{-1} \tag{32}$$

The covariance matrix $P_{n+1|n}^j$ is defined as

$$P_{n+1|n}^j = E(\widetilde{x}_{n+1|n}^j \widetilde{x}_{n+1|n}^{jT}) \tag{33}$$

where $\widetilde{x}_{n+1|n}^j = x_{n+1} - \hat{x}_{n+1|n}^j$.

From (26) and (31) we have

$$\widetilde{x}_{n+1|n}^j \quad = A_n x_n - B_n \widetilde{x}_{n|n} + w_n - A_n \hat{x}_{n|n}^j = A_n \widetilde{x}_{n|n}^j - B_n \widetilde{x}_{n|n} + w_n \tag{34}$$

where $\widetilde{x}^j_{n|n} = x_n - \hat{x}^j_{n|n}$.

Hence $P^j_{n+1|n}$ in (32) has the form

$$\begin{aligned} P^j_{n+1|n} &= E(A_n\widetilde{x}^j_{n|n} - B_n\widetilde{x}_{n|n} + w_n)(A_n\widetilde{x}^j_{n|n} - B_n\widetilde{x}_{n|n} + w_n)^T = \\ &= A_nP^j_{n|n}A^T_n - A_nP^{j*}_{n|n}B^T_n - B_nP^{*j}_{n|n}A^T_n + B_nP_{n|n}B^T_n + W_n \end{aligned} \tag{35}$$

where

$$P^j_{n|n} = E(\widetilde{x}^j_{n|n}\widetilde{x}^{jT}_{n|n}), \qquad P^{j*}_{n|n} = E(\widetilde{x}^j_{n|n}\widetilde{x}^T_{n|n}), \qquad P^{*j}_{n|n} = E(\widetilde{x}_{n|n}\widetilde{x}^{jT}_{n|n}) = (P^{j*}_{n|n})^T \tag{36}$$

should be determined.

The covariance matrix $P^j_{n+1|n+1} = E(\widetilde{x}^j_{n+1|n+1}\widetilde{x}^{jT}_{n+1|n+1})$ in (35) can be found by a classical way and has the form

$$P^j_{n+1|n+1} = (\mathbf{1} - K^j_{n+1}C^j)P^j_{n+1|n} \tag{37}$$

or in an information form

$$(P^j_{n+1|n+1})^{-1} = (P^j_{n+1|n})^{-1} + C^{jT}(R^j_{n+1})^{-1}C^j \tag{38}$$

Using (32) and (37) gives

$$K^j_{n+1} = P^j_{n+1|n+1}C^{jT}(R^j_{n+1})^{-1} \tag{39}$$

By subtracting both sides of (28) from the identity $x_{n+1} = x_{n+1}$ we obtain

$$\widetilde{x}^j_{n+1|n+1} = (\mathbf{1} - K^j_{n+1}C^j)\widetilde{x}^j_{n+1|n} - K^j_{n+1}r^j_{n+1} \tag{40}$$

and similarly to (9)

$$\widetilde{x}_{n+1|n+1} = (\mathbf{1} - K_{n+1}C)\widetilde{x}_{n+1|n} - K_{n+1}r_{n+1} \tag{41}$$

The covariance matrix $P^{j*}_{n+1|n+1} = E(\widetilde{x}^j_{n+1|n+1}\widetilde{x}^T_{n+1|n+1})$ in (35) may be expressed in the form

$$\begin{aligned} P^{j*}_{n+1|n+1} &= E[(\mathbf{1} - K^j_{n+1}C^j)\widetilde{x}^j_{n+1|n} - K^j_{n+1}r^j_{n+1}][(\mathbf{1} - K_{n+1}C)\widetilde{x}_{n+1|n} - K_{n+1}r_{n+1}]^T = \\ &= (\mathbf{1} - K^j_{n+1}C^j)P^{j*}_{n+1|n}(\mathbf{1} - K_{n+1}C)^T + K^j_{n+1}R^{j*}_{n+1}K^T_{n+1} \end{aligned} \tag{42}$$

where $P^{j*}_{n+1|n} = E(\widetilde{x}^j_{n+1|n}\widetilde{x}^T_{n+1|n})$ and $R^{j*}_{n+1} = [R^{j1}_{n+1}, \ldots, R^{jl}_{n+1}, \ldots, R^{jM}_{n+1}]$.

The matrices R^{jl}_{n+1} are defined as $R^{jl}_{n+1} = E(r^j_{n+1}r^{lT}_{n+1}) = 0$ for $j \neq l$ and $R^{jj}_{n+1} = E(r^j_{n+1}r^{jT}_{n+1}) = R^j_{n+1}$

Using (13), (37) and (15), (39) in (42) gives

$$P^{j*}_{n+1|n+1} = \tag{43}$$
$$P^{j}_{n+1|n+1}(P^{j}_{n+1|n})^{-1}P^{j*}_{n+1|n}P^{-1}_{n+1|n}P_{n+1|n+1} + P^{j}_{n+1|n+1}C^{jT}(R^{j}_{n+1})^{-1}\overbrace{R^{j*}_{n+1}R^{-1}_{n+1}C}^{C^j}P_{n+1|n+1}$$

In order to determine $P^{j*}_{n+1|n} = E(\widetilde{x}^{j}_{n+1|n}\widetilde{x}^{T}_{n+1|n})$ in (43) we have from (1) and (10)

$$\widetilde{x}_{n+1|n} = A\widetilde{x}_{n|n} + w_n \tag{44}$$

and from (34)

$$\begin{aligned} P^{j*}_{n+1|n} &= E[A_n\widetilde{x}^{j}_{n|n} - B_n\widetilde{x}_{n|n} + w_n][A\widetilde{x}_{n|n} + w_n]^T = \\ &= A_nP^{j*}_{n|n}A^T - B_nP_{n|n}A^T + W_n \end{aligned} \tag{45}$$

Equations (28), (31), (32), (35), (37), (43) and (45) form the solution to the local filtration problem at the jth node.

Inserting (39) to (28) gives

$$\hat{x}^{j}_{n+1|n+1} - \hat{x}^{j}_{n+1|n} = P^{j}_{n+1|n+1}C^{jT}(R^{j}_{n+1})^{-1}(y^{j}_{n+1} - C^{j}\hat{x}^{j}_{n+1|n}) \tag{46}$$

Multiplying the both sides of the eqn. (46) by $(P^{j}_{n+1|n+1})^{-1}$ we have that

$$(P^{j}_{n+1|n+1})^{-1}(\hat{x}^{j}_{n+1|n+1} - \hat{x}^{j}_{n+1|n}) = C^{jT}(R^{j}_{n+1})^{-1}(y^{j}_{n+1} - C^{j}\hat{x}^{j}_{n+1|n}) \tag{47}$$

Thus

$$C^{jT}(R^{j}_{n+1})^{-1}y^{j}_{n+1} = \tag{48}$$
$$(P^{j}_{n+1|n+1})^{-1}\hat{x}^{j}_{n+1|n+1} - \overbrace{[(P^{j}_{n+1|n+1})^{-1} - C^{jT}(R^{j}_{n+1})^{-1}C^{j}]}^{(P^{j}_{n+1|n})^{-1}(38)}\hat{x}^{j}_{n+1|n}$$

Then the propagation of the estimate $\hat{x}_{n|n}$ described by (16) can be expressed in the form

$$\begin{aligned} \hat{x}_{n+1|n+1} &= [\mathbf{1} - P_{n+1|n+1}\sum_{j=1}^{M}C^{jT}(R^{j}_{n+1})^{-1}C^{j}]\hat{x}_{n+1|n} + \\ &+ P_{n+1|n+1}\sum_{j=1}^{M}(P^{j}_{n+1|n+1})^{-1}\hat{x}^{j}_{n+1|n+1} - P_{n+1|n+1}\sum_{j=1}^{M}(P^{j}_{n+1|n})^{-1}\hat{x}^{j}_{n+1|n} \end{aligned} \tag{49}$$

According to the eqn. (26) the term $\hat{x}_{n+1|n}$ in (49) becomes

$$\hat{x}_{n+1|n} = E(x_{n+1}|\vec{y}_n) = A_n\hat{x}_{n|n} - B_nE(\widetilde{x}_{n|n}|\vec{y}_n) = A_n\hat{x}_{n|n} \tag{50}$$

Let, similarly to [11]

$$\hat{x}_{n+1|n+1} = \sum_{j=1}^{M} [P_{n+1|n+1}(P^j_{n+1|n+1})^{-1}\hat{x}^j_{n+1|n+1} + h^j_{n+1}] \tag{51}$$

where

$$h^j_{n+1} = F_{n+1}h^j_n + G^j_{n+1}\hat{x}^j_{n+1|n} \tag{52}$$

When we substitute (50) and next (51) into the eqn. (49) , we find

$$\begin{aligned}
&\overbrace{\sum_{j=1}^{M} [P_{n+1|n+1}(P^j_{n+1|n+1})^{-1}\hat{x}^j_{n+1|n+1} + h^j_{n+1}]}^{\hat{x}_{n+1|n+1}} = \\
&= [\mathbf{1} - P_{n+1|n+1}\sum_{j=1}^{M} C^{jT}(R^j_{n+1})^{-1}C^j]A_n \overbrace{\sum_{j=1}^{M}[P_{n|n}(P^j_{n|n})^{-1}\hat{x}^j_{n|n} + h^j_n]}^{\hat{x}_{n|n}} + \\
&+P_{n+1|n+1}\sum_{j=1}^{M}(P^j_{n+1|n+1})^{-1}\hat{x}^j_{n+1|n+1} - P_{n+1|n+1}\sum_{j=1}^{M}(P^j_{n+1|n})^{-1}\hat{x}^j_{n+1|n}
\end{aligned} \tag{53}$$

Thus

$$\begin{aligned}
h^j_{n+1} &= P_{n+1|n+1}\overbrace{[(P_{n+1|n+1})^{-1} - \sum_{j=1}^{M} C^{jT}(R^j_{n+1})^{-1}C^j]}^{P^{-1}_{n+1|n}(14)} A_n h^j_n + +P_{n+1|n+1}\{[(P_{n+1|n+1})^{-1} \\
&- \sum_{j=1}^{M} C^{jT}(R^j_{n+1})^{-1}C^j]A_nP_{n|n}(P^j_{n|n})^{-1}A_n^{-1} - (P^j_{n+1|n})^{-1}\}\hat{x}^j_{n+1|n} = \\
&\overbrace{P_{n+1|n+1}(P_{n+1|n})^{-1}A_n}^{F_{n+1}} h^j_n + \\
&+\overbrace{P_{n+1|n+1}[(P_{n+1|n})^{-1}A_nP_{n|n}(P^j_{n|n})^{-1}A_n^{-1} - (P^j_{n+1|n})^{-1}]}^{G^j_{n+1}}\hat{x}^j_{n+1|n}
\end{aligned} \tag{54}$$

Using (51) and (7) in (4) gives

$$u^{jo}_n = -(H^j + B^{jT}\Lambda_{n+1}B^j)^{-1}B^{jT}\Lambda_{n+1}\{\sum_{l=1}^{M}[P_{n|n}(P^l_{n|n})^{-1}\hat{x}^l_{n|n} + h^l_n]\} \tag{55}$$

Let us notice that in order to determine the value of the optimal control u_n^{jo} at the $j-th$ node the p_j dimensional vectors α_n^{lj} defined as

$$\alpha_n^{lj} = B^{jT}\Lambda_{n+1}[P_{n|n}(P_{n|n}^l)^{-1}\hat{x}_{n|n}^l + h_n^l], \quad l = 1,...,M, \ l \neq j \tag{56}$$

should be transmitted from other nodes to the $j-th$ node .

The control laws (23) and (55) have very similar forms and properties discussed in [11].

The main difference is that the latter does not depend on controls from other nodes. Thus contrary to (23) controls need not be transmitted from node to node. However, the cost for this additional reduced transmission is increased filter computation at each node.

6. Conclusions

In the paper the decentralized filtration in LQG control problem is presented. It is shown that the state estimates calculated at each node are updated with current measurement obtained only at that node. Additionally, at each node the vector dependent on past data must be determined. But, the controls need not be transmitted from node to node.

The local state estimation is nonclassical in this sense that it requires some additional calculations to obtain error covariance matrix $P_{n|n}^j$. Fortunately, these calculations do not depend on measurement information and can be done off-line.

The control laws are linear combinations of data calculated at each node. To calculate controls at the jth node only the transmission of the vectors α_n^{lj} from other nodes is needed.

References

[1] K.C. Chang, R.H. Saha and Y. Bar-Shalom: On optimal track to track fusion. *IEEE Trans. on Aerospace and Electronic Systems*, **33**(4), (1997), 1271-1276.

[2] K.C. Chang, Z. Tian and S. Mori: Performance evaluation for MAP state estimate fusion. *IEEE Trans. on Aerospace and Electronic Systems*, **40**(2), (2004), 706-714.

[3] Chen H.M., T. Kirubarajan and Y. Bar-Shalom: Performance limits on track to track fusion versus centralized estimation, *IEEE Trans. on Aerospace and Electronic Systems*, **39**(2), pp. 386-400, (2003).

[4] Z. Duan and X.R. Li: Lossless Linear transformation of sensor data for distributed estimation fusion. *IEEE Trans. on Signal Processing*, **59**(1), (2011), 362-372.

[5] H.HASHMIPOUR, S. ROY and A. LAUB: Decentralized structures for parallel Kalman filtering. *IEEE Trans. on Automatic Control*, **33**(1), (1988), 88-93.

[6] M.E. LIGGINS, C.Y. CHONG, I. KADAR, M. ALFORD, V. VANNICOLA and S. THOMOPOULOS: Distributed fusion architectures and algorithms for target tracking, *Proc. of the IEEE*, **85**(1), (1997), 95-107.

[7] A.G.O. MUTAMBARA and H.F. DURRANT-WHYTE: Estimation and control for a modular wheeled mobile robot. *IEEE Trans. on Control Systems Technology*, **8**(1), (2000) 35-46.

[8] M.S. SCHLOSSER and K. KROSCHEL: Performance analysis of decentralized Kalman filters under communication constraints. *J. of Advances in Information Fusion*, **2**(2), (2007), 65-75.

[9] J. SIJS, M. LAZAR, P.P.J. DEN BOSCH and Z. PAPP: An overview of non-centralized Kalman filters. *Proc. of the 17th IEEE Int. Conf. on Control Applications*, USA, (2008).

[10] E.B. SONG, Y.M. ZHU, J. ZHOU and Z.S. YOU: Optimal Kalman filtering fusion with cross-correlated sensor noises. *Automatica*, **43** (2007), 1450-1456.

[11] J.L. SPEYER: Computation and transmission requirements for a decentralized Linear-Quadratic-Gaussian control problem. *IEEE Trans. on Automatoc Control*, **24**(2), (1979), 266-269.

[12] Y. ZHU, Z. YOU, J. ZHAO, K. ZHANG and X.R. LI: The optimality for the distributed Kalman filtering fusion with feedback. *Automatica*, **37**(2), (2001), 1489-1493.

Archives of Control Sciences
Volume 27(LXIII), 2017
No. 1*, pages 41–62*

Robust H_∞ output feedback control of bidirectional inductive power transfer systems

AKSHYA SWAIN, DHAFER ALMAKHLES, MICHAEL J. NEATH and ALIREZA NASIRI

Bidirectional Inductive power transfer (IPT) systems behave as high order resonant networks and hence are highly sensitive to changes in system parameters. Traditional PID controllers often fail to maintain satisfactory power regulation in the presence of parametric uncertainties. To overcome these problems, this paper proposes a robust controller which is designed using linear matrix inequality (LMI) techniques. The output sensitivity to parametric uncertainty is explored and a linear fractional transformation of the nominal model and its uncertainty is discussed to generate a standard configuration for μ-synthesis and LMI analysis. An H_∞ controller is designed based on the structured singular value and LMI feasibility analysis with regard to uncertainties in the primary tuning capacitance, the primary and pickup inductors and the mutual inductance. Robust stability and robust performance of the system is studied through μ-synthesis and LMI feasibility analysis. Simulations and experiments are conducted to verify the power regulation performance of the proposed controller.

Key words: inductive power transfer, wireless power transfer, robust control, Linear Matrix Inequalities, sensitivity analysis

1. Introduction

Wireless power transfer technology (WPT) is an efficient method of delivering power between two physically isolated systems either through means of a time-varying magnetic field (e.g. Inductive Power Transfer (IPT)) or through the use of electric field coupling (e.g. Capacitive Power Transfer (CPT)). These technologies allow power transfer to take place in environments unsuited for conventional means of energy transfer, and various circuit topologies have been successfully proposed and implemented to cater for a wide range of applications from low power designs for bio-medical implants to high power battery charging systems [27, 5, 17, 14, 16]. Their resilience to harsh external conditions have led to an increase of IPT systems found in areas such as materials handling, renewable energy and heating in recent times [18, 3]. IPT systems for electric

A. Swain (e-mail: a.swain@auckland.ac.nz), the corresponding author, and M.J. Neath (neathmj@gmail.com) are with Department of Electrical and Computer Engineering, The University of Auckland, New Zealand. D. Almakhles (dalmakhles@gmail.com) is with Prince Sultan University, Riyadh, Saudi Arabia. A. Nasiri (nassirym@yahoo.com) is with Hormozgan University, Bandar Abbas, Iran.

Received 4.12.2016.

vehicles (EVs) have been a focal point of interest in recent years, to meet the growing demand for renewable energy. Bidirectional IPT systems are ideal for vehicle-to-grid (V2G) and G2V applications as they are more tamper proof and are able to function in harsh weather conditions [37, 24].

Bidirectional IPT systems suffer significant performance degradation when detuned and thus parallel and series compensations are typically used to improve the power-handling capabilities of IPT systems, causing the systems to behave as high-order resonant networks [29, 26, 11]. As a consequence, IPT systems are complex in nature and are difficult to both design and control when maintained at an operating frequency of 10-100 kHz [36]. Two separate controllers are required to facilitate power flow across the coils, which are dedicated to controlling the converters of either side of the system. In contrast to unidirectional systems, bidirectional IPT systems are even higher order resonant networks and more complex.

In the past, most IPT systems have utilised various types of controllers including directional tuning, fuzzy, bit-stream and simple PI and PID controllers as a means of verifying a model or particular control strategy [7, 6, 9, 10, 8, 12, 13, 31, 32]. These controllers give sub-optimal performance if not correctly tuned and are vulnerable to system disturbances and parametric variations which are prevalent in such systems. Recently the authors in [23] have applied multi-objective genetic algorithms to tune the PID parameters. Such controllers are also associated with tedious tuning processes often involving trial and error, motivating a model based robust controller design approach to overcome such problems.

In recent years, H_∞ controllers have gained popularity as a solution to the low robustness of PID controllers [35, 21]. Robust controllers for uni-directional systems have been developed in [19], where the authors have designed a robust controller for frequency uncertainty. Further, the Linear Matrix Inequality (LMI) framework has been used to design optimal robust controllers which both satisfies robustness as well as the necessary performance parameters [25, 39, 15]. This paper proposes a model based design approach of an H_∞ robust controller for bi-directional IPT systems which can effectively reduce the effects of uncertainties of the system parameters. Due to the complexity of optimal H_∞ controllers, the proposed controller, designed using the LMI method, is reduced to a 2nd order polynomial during the experimental stage. The rest of the paper is organised as follows: Section 2 describes the bidirectional IPT system in detail including the dynamic model of the system . The controller design and synthesis as well as the modelling of uncertainties are described in section 3. Simulation and experimental results are presented in Section 4 with conclusions in Section 5.

2. Bidirectional IPT system

A typical bidirectional IPT system consists of a primary and a secondary side and is shown in Fig. 1. Both sides contain identical circuitry including a converter, an inductor-capacitor-inductor (LCL) resonant network with a series capacitor and dedicated con-

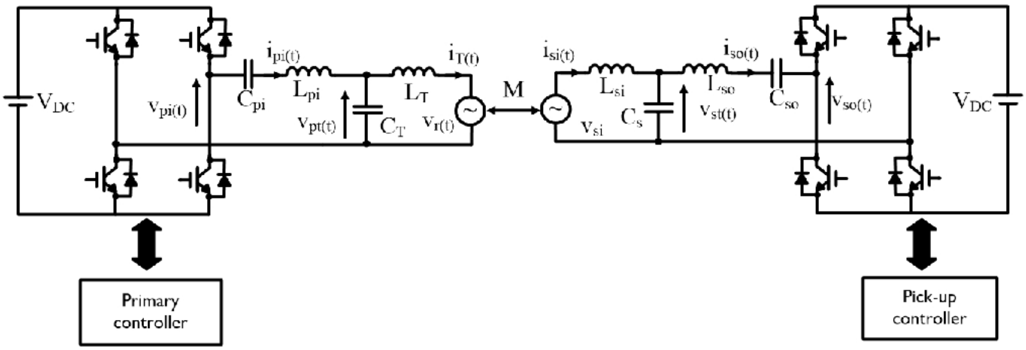

Figure 1: Typical bidirectional IPT system

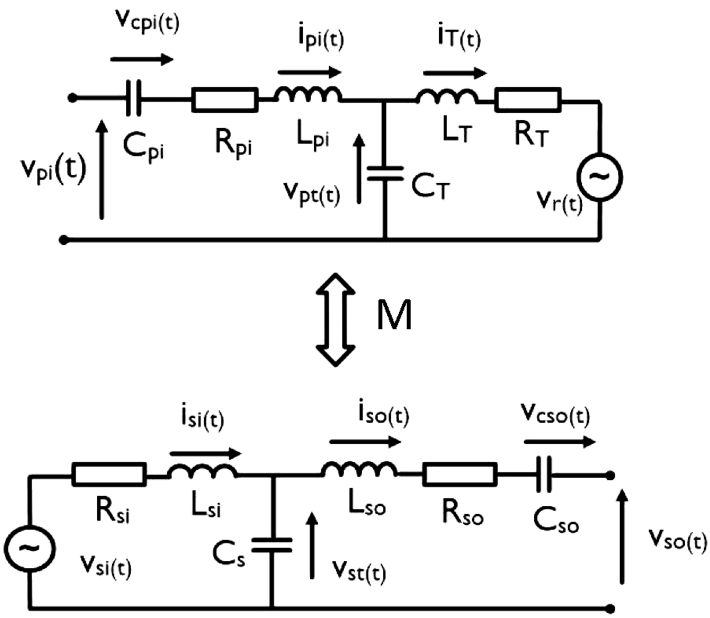

Figure 2: Equivalent circuit of a bidirectional system

troller which operates independently. The primary side converter generate a sinusoidal current at a desired frequency f_0 in the primary winding L_{pt}. Both LCL circuits are tuned to the frequency of the primary track current i_{pt}. A voltage is induced in the secondary pickup coil L_{st} as it is magnetically coupled with the primary. The voltage vectors are controlled by varying the phase angle α which in turn controls the voltage of the system. A phase angle difference of ± 90 degrees results in maximum power transfer, where a leading phase angle constitutes power transfer from the secondary to the primary and likewise a lagging phase angle enables power transfer from the primary to the secondary.

2.1. Dynamic model

Fig. 2 shows the bidirectional IPT system represented in schematic form. The dynamic model of this circuit developed in [34, 30, 33] is described as :

$$x = \begin{bmatrix} x_1 & x_2 & x_3 & x_4 & x_5 & x_6 & x_7 & x_8 \end{bmatrix}^T = \begin{bmatrix} i_{pi} & v_{cpi} & v_{pt} & i_T & i_{so} & v_{cso} & v_{st} & i_{si} \end{bmatrix}^T$$

where:

i_{pi} – current through the primary side inductor L_{pi}
v_{cpi} – voltage across the primary input capacitor C_{pi}
v_{pt} – voltage across primary side capacitor C_T
i_T – current through track inductor L_T
i_{so} – current through the pick-up side inductor L_{so}
v_{cso} – voltage across the pick-up output capacitor C_{so}
v_{st} – voltage across the pick-up side capacitor C_s
i_{si} – current through the pick-up side inductor L_{si}

Let the input vector u be denoted as:

$$u = \begin{bmatrix} u_1 & u_2 \end{bmatrix}^T = \begin{bmatrix} v_{pi} & v_{so} \end{bmatrix}^T$$

where $u_1 = v_{pi}$ is the input voltage applied at the primary side. Note that this voltage is essentially the output voltage of the primary side converter and $u_2 = v_{so}$= voltage at the pick-up side. Following the basic principles of circuit theory, the dynamic model can be expressed by the 8 differential equations as follows:

$$\begin{aligned}
\dot{x}_1 &= -\frac{R_{pi}}{L_{pi}}x_1 - \frac{1}{L_{pi}}x_2 - \frac{1}{L_{pi}}x_3 + \frac{1}{L_{pi}}u_1 \\
\dot{x}_2 &= \frac{1}{C_{pi}}x_1 \\
\dot{x}_3 &= \frac{1}{C_T}x_1 - \frac{1}{C_T}x_4 \\
\dot{x}_4 &= \gamma\left[\frac{1}{L_T}x_3 - \frac{R_T}{L_T}x_4 - \beta x_7 - \beta R_{si}x_8\right] \\
\dot{x}_5 &= -\frac{R_{so}}{L_{so}}x_5 - \frac{1}{L_{so}}x_6 + \frac{1}{L_{so}}x_7 - \frac{1}{L_{so}}u_2 \\
\dot{x}_6 &= \frac{1}{C_{so}}x_5 \\
\dot{x}_7 &= -\frac{1}{C_s}x_5 + \frac{1}{C_s}x_8 \\
\dot{x}_8 &= \gamma\left[\beta x_3 - \beta R_T x_4 - \frac{1}{L_{si}}x_7 - \frac{R_{si}}{L_{si}}x_8\right]
\end{aligned} \tag{1}$$

where

$$\beta = \frac{M}{L_{si}L_T}, \quad \gamma = \frac{1}{1-M\beta}$$

This can be expressed in the standard state space form as :

$$\dot{x} = Ax + Bu \tag{2}$$

where the system matrix A is given by

$$A = \begin{bmatrix} \frac{-R_{pi}}{L_{pi}} & -\frac{1}{L_{pi}} & -\frac{1}{L_{pi}} & 0 & 0 & 0 & 0 & 0 \\ \frac{1}{C_{pi}} & 0 & 0 & 0 & 0 & 0 & 0 & 0 \\ \frac{1}{C_T} & 0 & 0 & -\frac{1}{C_T} & 0 & 0 & 0 & 0 \\ 0 & 0 & \frac{\gamma}{L_T} & -\frac{\gamma R_T}{L_T} & 0 & 0 & -\gamma\beta & -\gamma\beta R_{si} \\ 0 & 0 & 0 & 0 & -\frac{R_{so}}{L_{so}} & -\frac{1}{L_{so}} & \frac{1}{L_{so}} & 0 \\ 0 & 0 & 0 & 0 & \frac{1}{C_{so}} & 0 & 0 & 0 \\ 0 & 0 & 0 & 0 & -\frac{1}{C_s} & 0 & 0 & \frac{1}{C_s} \\ 0 & 0 & \gamma\beta & -\gamma\beta R_T & 0 & 0 & -\frac{\gamma}{L_{si}} & -\frac{\gamma R_{si}}{L_{si}} \end{bmatrix}$$

and the input matrix B is given by

$$B = \begin{bmatrix} \frac{1}{L_{pi}} & 0 & 0 & 0 & 0 & 0 & 0 & 0 \\ 0 & 0 & 0 & 0 & -\frac{1}{L_{so}} & 0 & 0 & 0 \end{bmatrix}^T \tag{3}$$

Considering the track current $i_T = x_4$ and pick-up current $i_{so} = x_5$ as outputs, the output equation can be written as:

$$y = Cx \tag{4}$$

where

$$y = \begin{bmatrix} y_1 & y_2 \end{bmatrix}^T = \begin{bmatrix} i_T & i_{so} \end{bmatrix}^T, \quad C = \begin{bmatrix} 0 & 0 & 0 & 1 & 0 & 0 & 0 & 0 \\ 0 & 0 & 0 & 0 & 1 & 0 & 0 & 0 \end{bmatrix} \tag{5}$$

The relative gain array (RGA) analysis performed in [30] suggests strong interaction between output y_1 and input u_1 as well as between output y_2 and input u_2. From this it can be seen that the system can be controlled using a decentralized approach. It should also be noted that this is the ideal control configuration as it will allow the primary and secondary sides to be controlled independently without the need for communication.

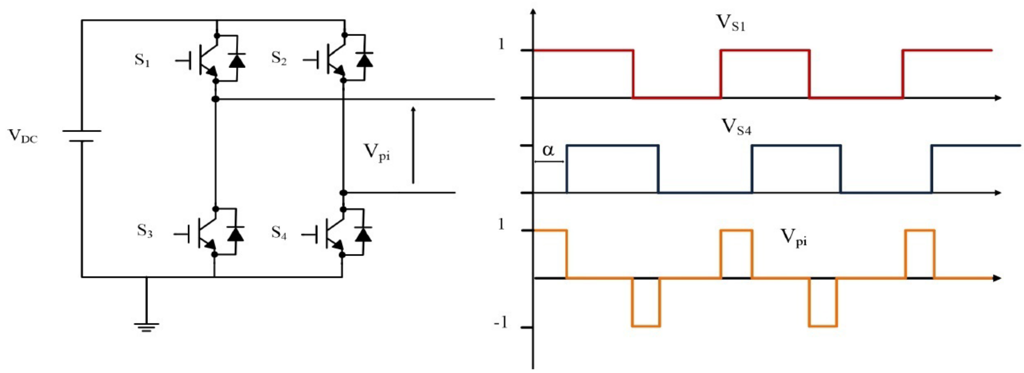

Figure 3: Waveforms for H-Bridge switching

3. Bidirectional IPT pickup-side controller

Robustness is a crucially important component of control theory, as real engineering systems are vulnerable to external disturbances, measurement noise and modeling uncertainties. In terms of IPT systems, uncertainties and disturbances may cause frequency drifts, loss of efficiency or instability. One typical source of uncertainty is the discrepancy between the mathematical model and the physical system.

As inferred from the relative gain array analysis, decentralized control is an acceptable method for obtaining the desired response. Therefore, the proposed controller ensures the control of the secondary side only, whilst the primary side controller is operated at a fixed phase angle using an open-loop controller. The pickup controller regulates the output power P_{si} by varying the voltage v_{si} applied to the secondary side's resonant network as [23]:

$$P_{si} = \frac{M}{L_{st}} \frac{\|v_{pi}\|}{\omega Lpt} \|v_{si}\| \sin(\theta) \tag{6}$$

Voltage v_{si} can be controlled by varying the secondary side phase angel α_s. The voltage produced by the pick up converter can be expressed in terms of α_s as :

$$v_{si} = V_{sin} \frac{4}{\sqrt{2}\pi} \sin(\alpha_s) \tag{7}$$

where V_{sin} is the dc voltage of the active load supplied by the pickup-side converter. Fig. 3 shows how the interaction between the angle α and the input switching signals. It can be seen from this that variations in αchange the output voltage V_{pi} by varying its duty cycle.

3.1. Singular value sensitivity

The concept of sensitivity is very useful in the analysis and controller design for feedback systems [22, 1, 2]. An important issue in designing a controller for an IPT system is the sensitivity of outputs to parameter variations. It is therefore appropriate to conduct a sensitivity analysis of the system to quantify the effect of variations of system parameters on the overall system model and provide better insight on controller behaviour when exposed to disturbances.

Singular value sensitivity is an effective method for quantifying the effect the parametric uncertainties on the system model. Suppose the transfer function matrix (TFM) of the nominal system is $G_0(j\omega)$. Let the TFM of the real system be $G'(j\omega)$. Then,

$$\Delta G(j\omega) = G^{'}(j\omega) - G_0(j\omega) \tag{8}$$

$G_0(j\omega)$ differs from $G^{'}(j\omega)$, by a variation in parameter p by an amount Δp. The sensitivity of a particular value σ from its nominal value σ_0 due to variations of a paramenter p is defined as:

$$S_p^{\sigma}(j\omega) = \frac{\Delta\sigma}{\sigma_0} \cdot \frac{p}{\Delta p} \tag{9}$$

For a perturbed system, the limits of the output are bounded by $\bar{\sigma}(G^{'}(j\omega))$ and $\underline{\sigma}(G^{'}(j\omega))$. Similarly the maximum and minimum deviations of the output are bounded by $\bar{\sigma}(\Delta G(j\omega))$ and $\underline{\sigma}(\Delta G(j\omega))$. Table 1 shows the singular value sensitivities for a range of variations in system parameters, where the percentage change in maximum value $\Delta\sigma(\%)$ is defined by

$$\Delta\sigma(\%) = \frac{\bar{\sigma}(G^{'}(j\omega)) - \bar{\sigma}(G_0(j\omega))}{\bar{\sigma}(G_0(j\omega))} \times 100 \tag{10}$$

The magnitude of the sensitivity of the maximum singular values is defined as:

$$\left\| S_p^{\sigma}(j\omega) \right\| (\%) = \left\| \frac{\bar{\sigma}(G'(j\omega)) - \bar{\sigma}(G_0(j\omega))}{\bar{\sigma}(G_0(j\omega))} \right\| \cdot e \left\| \frac{p}{\Delta p} \right\| \tag{11}$$

Table- 1 shows parameters computed by varying the primary tuning capacitance C_T, primary track inductance L_T and secondary inductance L_{si} at 20kHz. It can be concluded that bidirectional IPT systems are very sensitive to changes in the tuning capacitance, which can be attributed to the fact that C_T is used as the tuning capacitance for both inductors of the LCL circuit. The sensitivity of the system to variations in the pickup inductance is lower for the same reason as well as due to changes in the magnetic coupling. This further validates the need for a robust controller that adequately deals with parametric uncertainties.

3.2. Modelling of uncertain systems

In many robust design problems, the uncertainties include unstructred uncertainties such as unmodelled dynamics and parameter variations. Many dynamic perturbations that occur in different parts of a system can be lumped into one single perturbation block Δ. Through the use of linear fractional transformations (LFTs), the uncertain parts can

Table 1: Sensitivity of singular value for variations in L_T , L_{si} and C_T for bidirectional IPT system

	% change in parameter	$\triangle\overline{\sigma}(\%)$	$S_p^{\overline{\sigma}}(\%)$
L_T	-20	5.99	14.98
	-10	2.92	14.6
	10	-2.47	13.85
	20	-5.37	13.42
L_{si}	-20	2.69	6.725
	-10	0.95	4.75
	10	-0.54	2.7
	20	-0.76	1.94
C_T	-20	-12.7	63.37
	-10	-6.83	68.29
	10	8.022	80.22
	20	17.6	87.83

be taken out of the dynamics and the whole system can be arranged in the standard linear fractional transformation $F_u(M,\Delta)$ [4].

In a realistic system, the three physical parameters C_T,L_T and L_{si} are not exactly known. However, it can be assumed that these values are within certain known intervals, represented as:

$$\begin{aligned} C_T &= C_{T_0}(1 + p_c\delta_c) \\ L_T &= C_{T_0}(1 + p_t\delta_t) \\ L_{si} &= L_{si_0}(1 + p_s\delta_s) \end{aligned} \tag{12}$$

where C_{T_0}, L_{T_0}, and L_{si_0} are the nominal values for C_T,L_T and L_{si} respectively. p_c,p_t,p_s and δ_c,δ_t,δ_s represent the relative perturbations on these parameters. In the present study, it is assumed that $C_{T_0} = 2.49\mu F$, $L_{T_0} = 22.84\mu H$,$L_{si_0} = 23.49\mu H$, $p_c = 0.2$,$p_t = 0.4$ and $p_s = 0.4$ and $-1 \leqslant \delta_c\delta_t\delta_s \leqslant 1$. This represents $\pm 40\%$ uncertainty in the primary and pickup inductors L_T and L_{si} and $\pm 20\%$ uncertainty in the primary tuning capacitance C_T. Variations in L_T and L_{si} also vary the mutual inductance M according to

$$M = k\sqrt{L_T L_{si}} \tag{13}$$

and can be modelled by an LFT formulation in terms of β, as can variations in parameters $\frac{1}{C_T}$, $\frac{1}{L_T}$ and $\frac{1}{L_{si}}$ in terms of p , δ and their nominal values. Many dynamic perturbations that occur in different parts of a system can be lumped into one single perturbation block Δ. Through the use of linear fractional transformations (LFTs), the uncertain parts can be taken out of the dynamics and the whole system can be arranged in the standard linear fractional transformation [4, 28] as shown in Fig 4, where the block Δ denotes the model uncertainty and G_{mod} denotes the nominal model which is dependent on the existing state space model as well as on C_{T_0}, L_{T_0}, L_{si_0} and β_0 .

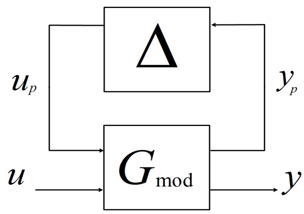

Figure 4: Uncertain model of the Bi-directional IPT system

The dynamic behavior of the nominal system can be described as:

$$\begin{aligned}
&\dot{x} = Ax(t) + B_1 u_p(t) + B_2 u(t)\\
&y_p(t) = C_1 x(t) + D_{11}(t) + D_{12} u(t)\\
&y(t) = C_2 x(t) + D_{12} u_p(t) + D_{22} u(t)
\end{aligned} \tag{14}$$

where $x \in \mathbf{R}^n$ is the state variable vector, $u \in \mathbf{R}^m$ is the system input, $y \in \mathbf{R}^r$ is the measurement output and $u_p \in \mathbf{C}^p$ and $y_p \in \mathbf{C}^p$ are uncertainty signals described by

$$\begin{aligned}
u_p &= \begin{bmatrix} u_{c1} & u_{c2} & u_{L1} & u_{L2} & u_{s1} & u_{s2} & u_{b1} & u_{b2} & u_{b3} & u_{b4} \end{bmatrix}^T\\
&= \begin{bmatrix} \delta_{c1} y_{c1}\\ \delta_{c2} y_{c2}\\ \delta_{L1} y_{L1}\\ \delta_{c2} y_{c2L2}\\ \delta_{s1} y_{s1}\\ \delta_{s2} y_{s2}\\ \delta_{b1} y_{b1}\\ \delta_{b2} y_{b2}\\ \delta_{b3} y_{b3}\\ \delta_{b4} y_{b4} \end{bmatrix}
\end{aligned} \tag{15}$$

$$y_p = \begin{bmatrix} y_{c1} & y_{c2} & y_{L1} & y_{L2} & y_{s1} & y_{s2} & y_{b1} & y_{b2} & y_{b3} & y_{b4} \end{bmatrix}^T$$

$$= \begin{bmatrix} -p_c u_{c1} + \frac{1}{C_{T_0}} x_1 \\ -p_c u_{c2} + \frac{1}{C_{T_0}} x_4 \\ -p_L u_{L1} + \frac{\gamma}{L_{T_0}} x_3 \\ -p_L u_{L2} + R_T \frac{\gamma}{L_{T_0}} x_4 \\ -p_s u_{s1} + R_T \frac{\gamma}{L_{si_0}} x_7 \\ -p_s u_{s2} + R_{si} \frac{\gamma}{L_{si_0}} x_8 \\ \gamma\beta_0 x_7 \\ \gamma\beta_0 R_T x_4 \\ \gamma\beta_0 x_3 \\ \gamma\beta_0 R_{si} x_8 \end{bmatrix} \tag{16}$$

The matrices A,$B_2 = B$ and $C_2 = C$ are the system, input and output matrices respectively and B_1,C_1 and D are given by

$$B_1 = \begin{bmatrix} 0 & 0 & 0 & 0 & 0 & 0 & 0 & 0 & 0 & 0 \\ 0 & 0 & 0 & 0 & 0 & 0 & 0 & 0 & 0 & 0 \\ -p_c & p_c & 0 & 0 & 0 & 0 & 0 & 0 & 0 & 0 \\ 0 & 0 & -p_l & p_l & 0 & 0 & -p_b & 0 & 0 & p_b \\ 0 & 0 & 0 & 0 & 0 & 0 & 0 & 0 & 0 & 0 \\ 0 & 0 & 0 & 0 & 0 & 0 & 0 & 0 & 0 & 0 \\ 0 & 0 & 0 & 0 & 0 & 0 & 0 & 0 & 0 & 0 \\ 0 & 0 & 0 & 0 & p_s & p_s & 0 & -p_b & -p_b & 0 \end{bmatrix} \tag{17}$$

$$C1 = \begin{bmatrix} \frac{1}{C_{T_0}} & 0 & 0 & 0 & 0 & 0 & 0 & 0 \\ 0 & 0 & 0 & \frac{1}{C_{T_0}} & 0 & 0 & 0 & 0 \\ 0 & 0 & \frac{\gamma}{L_{T_0}} & 0 & 0 & 0 & 0 & 0 \\ 0 & 0 & 0 & \gamma\frac{R_T}{L_{T_0}} & 0 & 0 & 0 & 0 \\ 0 & 0 & 0 & 0 & 0 & 0 & \frac{\gamma}{L_{si_0}} & 0 \\ 0 & 0 & 0 & \gamma\beta_0 R_T & 0 & 0 & 0 & 0 \\ 0 & 0 & \gamma\beta_0 & 0 & 0 & 0 & 0 & 0 \\ 0 & 0 & 0 & 0 & 0 & 0 & 0 & \gamma\beta_0 R_{si} \end{bmatrix} \tag{18}$$

$$D_{11} = \begin{bmatrix} -p_c & 0 & 0 & 0 & 0 & 0 \\ 0 & -p_c & 0 & 0 & 0 & 0 \\ 0 & 0 & -p_l & 0 & 0 & 0 \\ 0 & 0 & 0 & -p_l & 0 & 0 \\ 0 & 0 & 0 & 0 & -p_s & 0 \\ 0 & 0 & 0 & 0 & 0 & -p_s \end{bmatrix} \tag{19}$$

$$D_{12} = D_{21}^T = 0_{(10\times 2)}, \qquad D_{22} = 0_{(2\times 2)} \tag{20}$$

The block diagram of the closed loop system is shown in Fig-5 where d is the disturbance on the system output with finite energy. W_1 is a weighting function which is selected to tailor the tracking requirement and similarly W_2 is used to ensure good noise rejection. The weighting functions are generally used because it is often undesirable

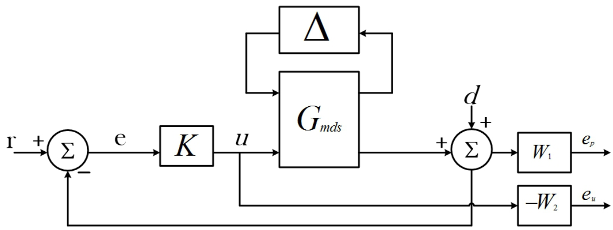

Figure 5: Block diagram of closed-loop system structure

and unfeasible to minimize the sensitivity over all frequencies. The weighting functions are chosen by the designer to tailor the tracking requirement and are usually high gain low pass filters. By applying the weights, instead of minimizing the sensitivity function alone, the weight W_1 is applied and $\| W_1 S \|_\infty$ is minimized. Similarly for good noise rejection, a control weighting function W_2 is used such that $\| W_2 KS \|_\infty$ is minimized [28, 4].

To obtain a good control design, it is necessary to select suitable weighting functions. The performance and control weighting functions that have been used in this work are given in the form [28]

$$W_1 = \frac{\beta(\alpha s^2 + 2\zeta\omega_c\sqrt{\alpha}s + \omega^2)}{(\beta s^2 + 2\zeta_2\omega_c\sqrt{\beta}s + \omega^2)} \tag{21}$$

$$W_2 = \frac{s^2 + 2\frac{w_{bc}}{\sqrt{M_u}} + \frac{\omega_{bc}^2}{M_u}}{\varepsilon s^2 + 2\sqrt{\varepsilon}\omega_{bc}s + \omega_{bc}^2} \tag{22}$$

where β is the d.c gain of the function which controls the disturbance rejection,α is the high frequency gain which controls the response peak overshoot, ζ_1 and ζ_2 are the damping ratios of the cross over frequency, ω_{bc} is the controller bandwidth, M_u is the peak magnitude of the sensitivity function and ε is a parameter chosen to be a small value which lies usually in the range 0.01 to 0.1.

3.3. Robust control design using Linear Matrix Inequalities

The formulation of the H_∞ synthesis problem can achieve a set of desired controllers by resolving a convex optimization problems with a set of linear matrix inequality (LMI) constraints in the form [38, 20].

$$F(x) \triangleq F_0 + \sum_{i=1}^{m} x_i F_i < 0 \tag{23}$$

Affine parameter dependent models are well suited for Lyapunov based analysis and synthesis, and can be used to analyse the stability and the performance of the uncertain systems. The objective of the output feedback controller is to satisfy the following properties:

1. It should be a stabilizing controller K, such that the system is always stable for any perturbations under the condition $\| \Delta \|_\infty \leqslant 1$
2. The H_∞ norm of the transfer function $T_{dz}(s)$ from the variable d to z should be less than 1, namely

$$\left\| \begin{matrix} \mathrm{T}_{de_p}(s) \\ \mathrm{T}_{de_u}(s) \end{matrix} \right\|_\infty < 1 \tag{24}$$

The H_∞ performance can be optimized by solving the following LMI problem:

$$\begin{aligned}
&\begin{bmatrix} N_{21} & 0 \\ 0 & I \end{bmatrix}^T \begin{bmatrix} A^T X + XA & XB_1 & C_1^T \\ B_1^T X & -\gamma I & D_{11}^T \\ C_1 & D_{11} & -\gamma I \end{bmatrix} \begin{bmatrix} N_{21} & 0 \\ 0 & I \end{bmatrix} < 0 \\
&\begin{bmatrix} N_{12} & 0 \\ 0 & I \end{bmatrix}^T \begin{bmatrix} AY + XA^T & YC_1^T & B_1 \\ C_1 X & -\gamma I & D_{11} \\ B_1^T & D_{11}^T & -\gamma I \end{bmatrix} \begin{bmatrix} N_{12} & 0 \\ 0 & I \end{bmatrix} < 0 \\
&\begin{bmatrix} X & I \\ I & Y \end{bmatrix}^T \geqslant 0
\end{aligned} \tag{25}$$

where N_{12} and N_{21} denote bases of null spaces of $\left(B_2^T, D_{12}^T\right)$ and (C_2, D_{21}) respectively. These terms are used to evaluate the parts that cannot be reflected by the measured output and cannot be affected by the control input. By solving the above LMI problem, the two positive definite matrices X and Y are found such that

$$X - Y^{-1} = X_2 X_2^T \tag{26}$$

Then, by applying the singular value decomposition to (26), we get the matrix $X_2 \in \mathbf{R}^{n \times n_k}$, where n_k can be the rank of $X - Y^{-1}$. Further a matrix X_c is constructed using X and X_2 as:

$$X_c = \begin{bmatrix} X & X_2^T \\ X_2 & I \end{bmatrix} \tag{27}$$

To solve a H_∞ synthesis controller, a matrix K composed by all unknown coefficient matrices is defined as:

$$K = \begin{bmatrix} A_k & B_k \\ C_k & D_k \end{bmatrix} \tag{28}$$

Lastly, a LMI, which is only dependant on the matrix K, will be be solved and this is given by

$$H_{X_C} + P_{X_C}^T KQ + Q^T K^T P_{X_C} < 0 \tag{29}$$

For inequality (29), the matrices H_{X_C},P_{X_C} and Q are all known and certain, having the forms of

$$H_{X_C} = \begin{bmatrix} A_0^T X_c + X_c A_0 & X_c B_0 & C_0^T \\ B_0^T X_c & -I & D_{11}^T \\ C_0 & D_{11} & -I \end{bmatrix} \tag{30}$$

$$P_{X_C} = \begin{bmatrix} \overline{B}^T X_c & 0 & \overline{D}^T \end{bmatrix} \tag{31}$$

$$Q = \begin{bmatrix} \overline{C} & D_{21} & 0 \end{bmatrix} \tag{32}$$

where A_o, B_o, C_o, $\overline{B}$, $\overline{C}$, $\overline{D}_{12}$ and $\overline{D}_{21}$ are respectively equal to

$$A_o = \begin{bmatrix} A & 0 \\ 0 & 0 \end{bmatrix}^T, \quad B_o = \begin{bmatrix} B_1 \\ 0 \end{bmatrix}, \quad C_o = \begin{bmatrix} C_1 & 0 \end{bmatrix}, \quad \overline{B} = \begin{bmatrix} 0 & B_2 \\ I & 0 \end{bmatrix}$$

$$\overline{C} = \begin{bmatrix} 0 & I \\ C_2 & 0 \end{bmatrix}, \quad \overline{D}_{12} = \begin{bmatrix} 0 & D_{12} \end{bmatrix}, \quad \overline{D}_{21} = \begin{bmatrix} 0 \\ D_{21} \end{bmatrix}$$

The H_∞ synthesis problem can be transformed into a feasibility problem of a linear matrix inequality system only dependent on the control parameters to be solved. Thus it is easy to achieve an H infinity output feedback controller based on the LMI method.

4. Results

To demonstrate the effectiveness of the robust controller, a 1kW bidirectional IPT prototype shown in Fig. 9 was built as a benchmark. The various parameters of the prototype are shown in Table 2. Before performing the experiments, initial simulations were carried out where the step response of the system, controlled both with PID and H_∞ controllers, were compared. The simulations were then performed again with altered system parameters and finally conducted on the prototype. The phase shift θ is held constant at 90° and phase angle α is varied on the pick up side controller to regulate power flow between the primary and secondary coils.

4.1. Simulations

The response time of the H_∞ controller is investigated using PLECS, a MATLAB simulation-based software package. At time $t = 0$, a step change in reference voltage of ± 1.0kW is applied to the system corresponding to power flowing to and from the

Table 2: Parameters of Bidirectional IPT prototype converter

Parameter	Value
$V_{DC,1} = V_{DC,2}$	150V
$L_{pi} = L_{so}$	46.5μH
L_T	22.84μH
L_{si}	23.49μH
$C_T = C_s$	2.47μF
$C_{pi} = C_{so}$	2.53μF
M	5μH
f_0	20kHz

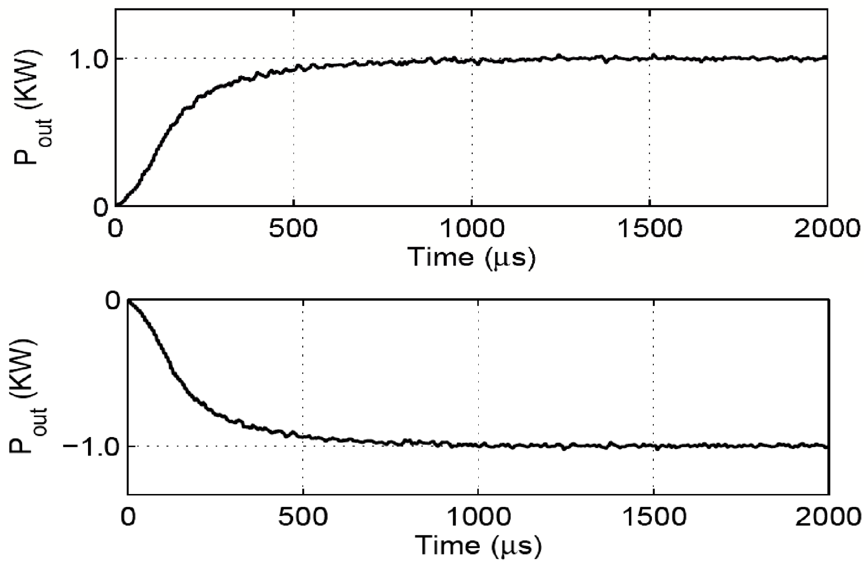

Figure 6: Power regulation performance of robust controller in forward and reversed direction

primary and secondary. Variations in C_T,L_T and L_{si} of 40% were introduced into the system. Fig. 6 shows the step response of the nominal system in forward and reverse direction.

The gain of the H_∞ controller designed using the methods described before can be represented as:

$$K(s) = \frac{U(s)}{E(s)} = \frac{\sum_{i=0}^{13} b_i s^i}{\sum_{j=0}^{13} a_i s^i} \tag{33}$$

where $a_0 = 0, a_1 = 5\times10^5, a_2 = 1.4\times10^5, a_3 = 1.1\times10^{49}, a_4 = 8.4\times10^{44}, a_5 = 3.0\times10^{40}$, $a_6 = 4.0\times10^{35}, a_7 = 1.2\times10^{31}, a_8 = 5.7\times10^8, a_9 = 1.7\times10^{21}, a_{10} = 2.6\times10^{10}, a_{11} = 7.4\times10^{11}, a_{12} = 3.6\times10^4$, $b_0 = 3.2\times10^{54}, b_1 = 9.2\times10^{51}, b_2 = 6.3\times10^{48}, b_3 = 1.2\times10^{45}, b_4 = 8.5\times10^{40}, b_5 = 2.4\times10^{36}$, $b_6 = 4.0\times10^{31}, b_7 = 9.32\times10^{26}, b_8 = 5.6\times10^{21}, b_9 = 1.2\times10^{17}, b_{10} = 2.5\times10^{10}, b_{11} = 5.4\times10^6, b_{12} = 3.6\times10^4, b_{13} = 7.2\times10^{-5}$.

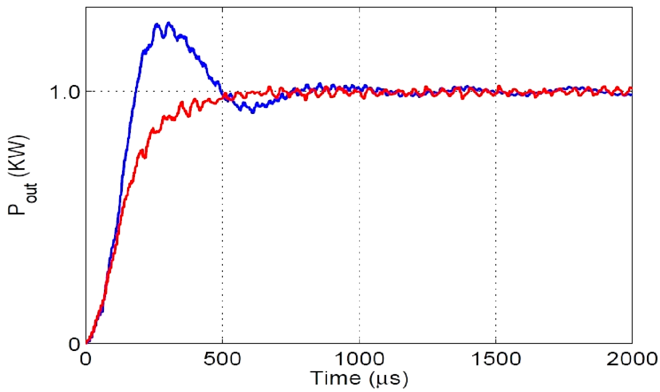

Figure 7: Comparison of power regulation for PID (blue) and robust (red) control systems with 40% variation in primary tuning capacitance C_T

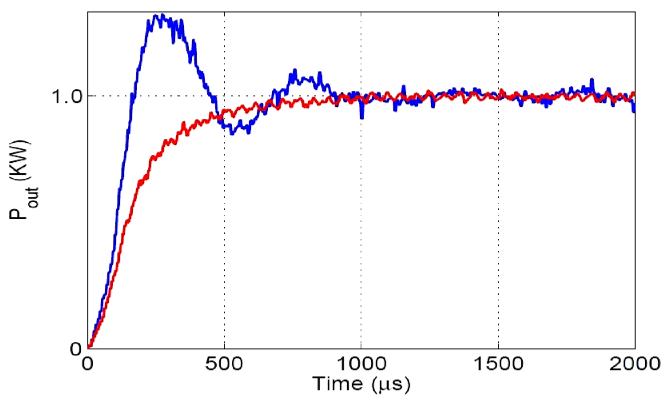

Figure 8: Comparison of power regulation for PID (blue) and robust (red) control systems with 40% variation in primary and pickup tuning inductances L_T and L_{si}

As shown in Figs 7 and 8, the PID controller shows significant decrease in performance in the presence of parametric disturbances. Both cases show increased overshoot and oscillations when a variation of 40% is introduced to the tuning capacitor and inductors, while the robust controller experiences no significant variations. Results for reverse direction are similar in nature and therefore not shown.

4.2. Experimental

To verify the results obtained from the MATLAB simulations, experiments were conducted on the prototype bidirectional IPT system, using a Texas Instruments TMS28335 microcontroller. The prototype is capable of transferring approximately 1kW of power over a 48mm air gap with 85% efficiency. The gain of the controller given in (33) in the discrete domain , when sampled at a rate of 40 kHz is given by

$$K(z) = \frac{U(z)}{E(z)} = \frac{\sum_{i=0}^{13} b_i z^i}{\sum_{j=0}^{13} a_i z^i} \tag{34}$$

where $a_0 = -0.4, a_1 = 1.7, a_2 = -3.2, a_3 = 5.3, a_4 = -8.0, a_5 = 9.6, a_6 = -10.8, a_7 = 11.7, a_8 = -10.2, a_9 = 8.9, a_{10} = -7.0, a_{11} = 4.0, a_{12} = -2.4, a_{13} = 1, b_0 = -1.9 \times 10^{-5}, b_1 = 9.2 \times 10^{-5}, b_2 = -1.9 \times 10^{-4}, b_3 = 3 \times 10^{-4}, b_4 = -4.8 \times 10^{-4}, b_5 = 5.8 \times 10^{-4}, b_6 = -6.5 \times 10^{-4}, b_7 = 7.3 \times 10^{-4}, b_8 = -6.4 \times 10^{-4}, b_9 = 5.5 \times 10^{-4}, b_{10} = -4.5 \times 10^{-10}, b_{11} = 2.6 \times 10^{-4}, b_{12} = -1.6 \times 10^{-4}, b_{13} = 7.2 \times 10^{-5}$

Fig. 10 shows the step response of 1kW in the forward direction. Due to the specifications of the prototype, the maximum possible variation that can be safely applied to the system is 25%. Figs 11 and 12 show the response of the system under 25% parameter variation in tuning capacitance C_T and tuning inductor L_T and L_{si} respectively. It is evident from these results that there is no significant variations from the nominal system as shown by the simulation results in Section 4.1 and thus validating the performance capabilities of the robust controller.

In order to improve the settling time of the controller, a second experiment was performed using a reduced second order controller, based on the Hankel singular value (SV) based reduction algorithm. Hankel SV's can be used to determine the dominant energy states of a stable system, which are preserved while states of lower energy are removed. Fig. 13 shows the results of the second order reduced order controller in comparison with the H$_\infty$robust controller for the nominal system. It can be seen that reducing the order of the controller results in some improvement in the settling time of the controller.

5. Conclusions

Due to their high order and nonlinear nature, the performance of bidirectional IPT systems degrade significantly with changes in systems parameters when controlled with conventional PID controllers. Therefore, a robust H_∞ controller has been designed to reduce the effects of parametric uncertainties on power regulation as well as to eliminate tedious tuning procedures associated with PID controllers. Several objective functions including settling time, rise time and peak overshoot, were minimized using LMI techniques to obtain the optimal H_∞ controller whist maintaining robust stability and tracking. Simulations using MATLAB as well as experimental tests were conducted to verify the response of the robust controller.

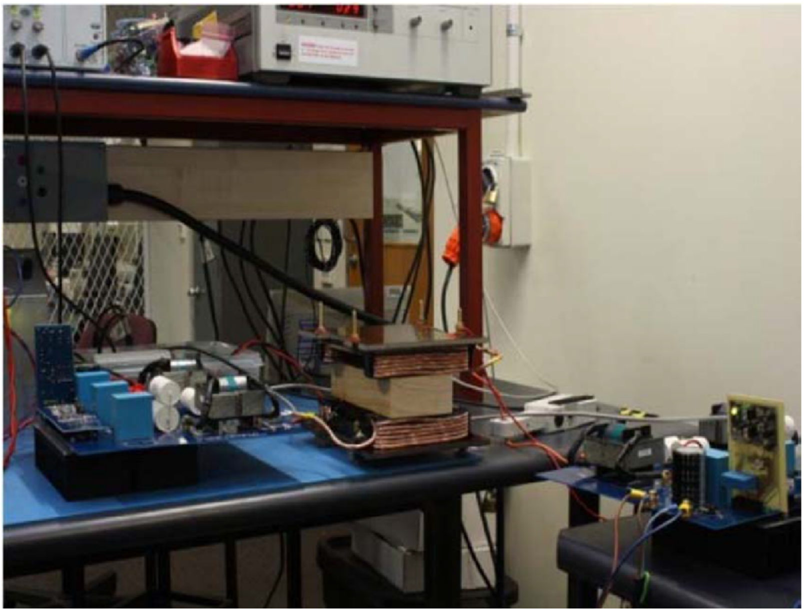

Figure 9: Prototype Bidirectional IPT system used for verification

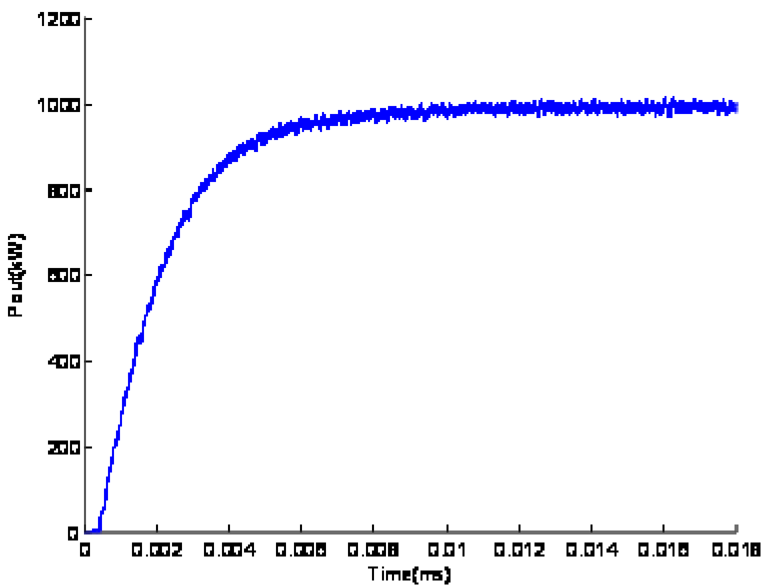

Figure 10: Experimental results of robust controller for nominal system

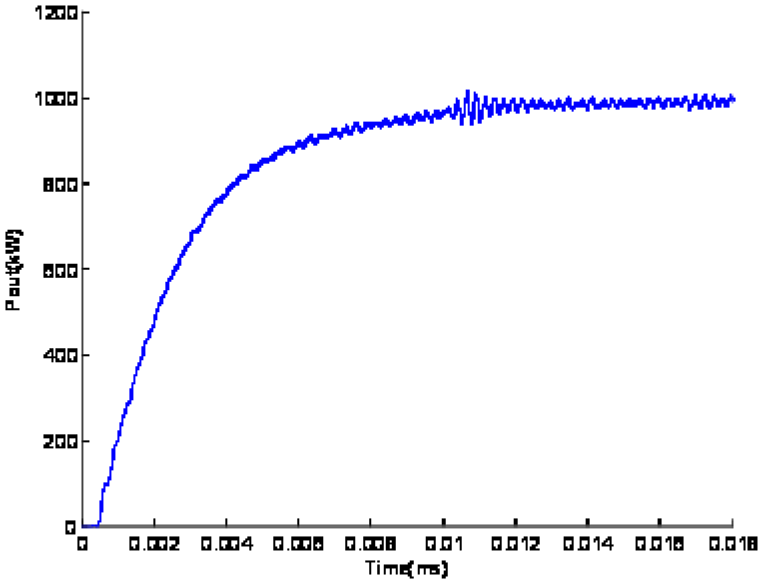

Figure 11: Experimental result of robust controller for system with 25% C_T variation

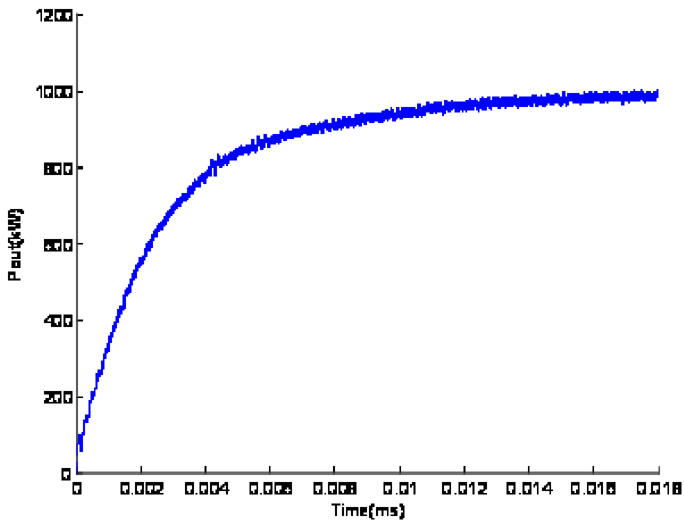

Figure 12: Experimental result of robust controller for system with 25% L_T and L_{si} variation

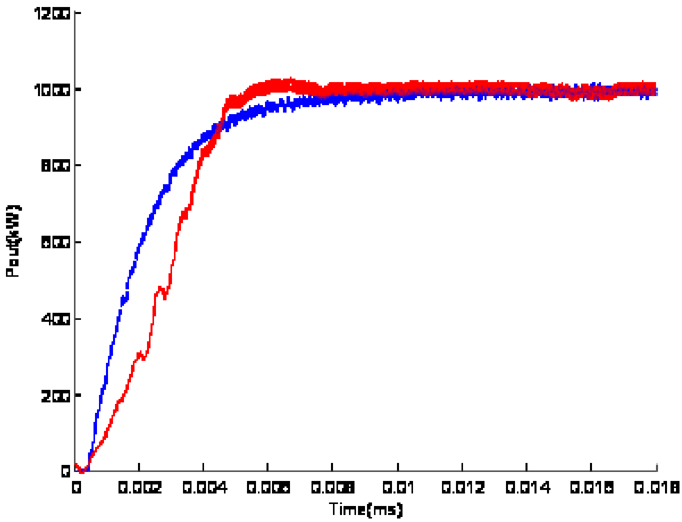

Figure 13: Experimental result of robust controller (blue) and reduced order (2nd order) robust controller (red) for nominal system

References

[1] G.J. BALAS, A.K. PACKARD, M.G. SAFONOV and R.Y. CHIANG: Next generation of tools for robust control. In *Proc. of the American Control Conf.*, **6** (2004), 5612-5615.

[2] J. DOYLE and G. STEIN: Multivariable feedback design: Concepts for a classical/modern synthesis. *IEEE Trans. on Automatic Control*, **26**(1), (1981), 4-16.

[3] A. W. GREEN and J. T. BOYS: 10 kHz inductively coupled power transfer-concept and control. In *Fifth Int. Conf. on Power Electronics and Variable-Speed Drives*, (1994), 694-699.

[4] DA-WEI GU, P. PETKOV and M. KONSTANTINOV: Robust Control Design with MATLAB. Springer-Verlag London, ISBN-10: 1852339837, 2005.

[5] HAO HAO, G.A. COVIC and J.T. BOYS: A parallel topology for inductive power transfer power supplies. *IEEE Transactions on Power Electronics*, **29**(3), (2014), 1140-1151.

[6] JR-UEI WILLIAM HSU, AIGUO PATRICK HU, P. SI and AKSHYA K. SWAIN: Power flow control of a 3-D wireless pick-up . In *2nd IEEE Conf. on Industrial Electronics and Applications*, (2007), 2172-2177.

[7] JR-UEI WILLIAM HSU, AIGUO PATRICK HU and AKSHYA SWAIN: A wireless power pickup based on directional tuning control of magnetic amplifier. *IEEE Trans. on Industrial Electronics*, **56**(7), (2009), 2771-2780.

[8] JR-UEI WILLIAM HSU, AIGUO PATRICK HU and AKSHYA SWAIN: Fuzzy logic based directional full-range tuning control of wireless power pickups . *IET Power Electronics*, **5**(6), (2012), 773-781.

[9] JR-UEI WILLIAM HSU, AIGUO PATRICK HU and AKSHYA K. SWAIN: Fuzzy based directional tuning controller for a wireless power pick-up . In *EEE Region 10 Conference*, (2008).

[10] JR-UEI WILLIAM HSU, AKSHYA K SWAIN and AIGUO PATRICK HU: Implicit adaptive controller for wireless power pick-ups . In *6th IEEE Conf. on Industrial Electronics and Applications*, (2011), 514-519.

[11] C.-Y. HUANG, J.T. BOYS and G.A. COVIC: LCL pickup circulating current controller for inductive power transfer systems. *IEEE Trans. on Power Electronics*, **28**(4), (2013), 2081-2093.

[12] LIANG HUANG, A. PATRICK HU and AKSHYA SWAIN: A New Resonant Compensation Method for Improving the Performance of Capacitively Coupled Power Transfer System . In *IEEE Energy Conversion Congress and Exposition*, (2014), 870-875.

[13] LIANG HUANG, A. PATRICK HU and AKSHYA SWAIN: Comparison of Two High Frequency Converters for Capacitive Power Transfer . In *IEEE Energy Conversion Congress and Exposition*, (2014), 5437-5443.

[14] LIANG HUANG, AIGUO PATRICK HU and AKSHYA SWAIN: An overview of capacitively coupled power transfer-a new contactless power transfer solution . In *8th IEEE Conf. on Industrial Electronics and Applications*, (2013), 461-465.

[15] J.V. INGLES, P. GARCES and R. LEYVA: Robust LMI control of a buck-boost converter with low ripple propagation. In *20th Mediterranean Conf. on Control Automation*, (2012), 1272-1277.

[16] S.M. ASIF IQBAL, U.K. MADAWALA, D.J.THRIMAWITHANA and AKSHYA K. SWAIN: A Bi-directional inductive power transfer system with individually controlled tracks and pick-ups . In *IEEE Energy Conversion Congress and Exposition Asia*, (2013), 1059-1064.

[17] N.A. KEELING, J.T. BOYS and G.A. COVIC: Unity power factor inductive power transfer pick-up for high power applications. In *34th Annual Conf. of IEEE Industrial Electronics*, (2008), 1039-1044.

[18] GE LI, YINGUI ZHOU, HAITIAN WANG, PENG FU and LIANG CAO: Compact power supplies for tokamak heating. *IEEE Transactions on Dielectrics and Electrical Insulation*, **19**(1), (2012), 233-238.

[19] YAN-LING LI, YUE SUN and XIN DAI: μ-synthesis for frequency uncertainty of the ICPT system. *IEEE Transactions on Industrial Electronics*, **60**(1), (2013), 291-300.

[20] YANN-LING LI, YUE SUN and XIN DAI: Robust control for an uncertain LCL resonant ICPT system using LMI method. *Control Engineering Practice*, **21**(1), (2013), 31-41.

[21] RENQUAN LU, SHUKUI LI and LIN XUE: Robust H_∞; optimal speed control of DC motor using lmi approach. In *Control and Decision Conf.*, (2008), 4350-4354.

[22] B. MORGAN JR.: Sensitivity analysis and synthesis of multivariable systems. *IEEE Trans. on Automatic Control*, **11**(3), (1966), 506-512.

[23] M.J. NEATH, A.K. SWAIN, U.K. MADAWALA and D.J. THRIMAWITHANA: An optimal PID controller for a bidirectional inductive power transfer system using multiobjective genetic algorithm. *IEEE Transactions on Power Electronics*, **29**(3), (2014), 1523-1531.

[24] M.J. NEATH, A.K. SWAIN, U.K. MADAWALA, D.J. THRIMAWITHANA and D.M. VILATHGAMUWA: Controller synthesis of a bidirectional inductive power interface for electric vehicles. In *IEEE Third Int. Conf. on Sustainable Energy Technologies*, (2012), 60-65.

[25] C. OLALLA, R. LEYVA, A. EL-AROUDI and I. QUEINNEC: Robust LQR control for PWM converters: An LMI approach. *IEEE Trans. on Industrial Electronics*, **56**(7), (2009), 2548-2558.

[26] G. SCHEIBLE, D. DZUNG, J. ENDRESEN and JAN-ERIK FREY: Unplugged but connected [design and implementation of a truly wireless real-time sensor/actuator interface]. *IEEE Industrial Electronics Magazine*, **1**(2), (2007), 25-34.

[27] PING SI, A.P. HU, S. MALPAS and D. BUDGETT: A frequency control method for regulating wireless power to implantable devices. *IEEE Trans. on Biomedical Circuits and Systems*, **2**(1), (2008), 22-29.

[28] S. SKOGESTAD and I. POSTLETHWAITE: Multivariable Feed Back Control: Analysis and Design. Wiley, second edition, 2005.

[29] J.P.C. SMEETS, T.T. OVERBOOM, J.W. JANSEN and E.A. LOMONOVA: Comparison of position-independent contactless energy transfer systems. *IEEE Trans. on Power Electronics*, **28**(4), (2013), 2059-2067.

[30] A.K. SWAIN, M.J. NEATH, U.K. MADAWALA and D.J. THRIMAWITHANA: A dynamic multivariable state-space model for bidirectional inductive power transfer systems. *IEEE Trans. on Power Electronics*, **27**(11), (2012), 4772-4780.

[31] AKSHYA SWAIN, DHAFER ALMAKHLES, YOUFENG HOU, NITISH PATEL and UDAYA MADAWALA: A sigma-delta modulator based PI controller for bi-directional inductive power transfer system, . In *2nd IEEE Southern Power Electronics Conf.*, (2017), 1-5.

[32] AKSHYA SWAIN, DHAFER ALMAKHLES, NATHAN PYLE, HOSSEIN MEHRABI and AIGUO PATRICK HU: Single-bit modulator based controller for capacitive power transfer system. In *2nd IEEE Southern Power Electronics Conf.*, (2017), 1-5.

[33] AKSHYA SWAIN, SRIKANTH DEVARAKONDA and UDAYA MADAWALA: Modelling, sensitivity analysis and controller synthesis of multi pick-up bi-directional inductive power transfer systems. *IEEE Trans. on Industrial Informatics*, **10**(2), (2014), 1372-1380.

[34] AKSHYA K. SWAIN, MICHAEL J. NEATH, U.K. MADAWALA and D.J.THRIMAWITHANA: A dynamic model for bi-directional inductive power transfer systems. In *37th IEEE Conf. on Industrial Electronics Society*, (2011), 1024-1029.

[35] G. WILLMANN, D.F. COUTINHO, L. F A PEREIRA and F.B. LIBANO: Multiple-loop H_∞ control design for uninterruptible power supplies. *IEEE Trans. on Industrial Electronics*, **54**(3), (2007), 1591-1602.

[36] H.H. WU, A. GILCHRIST, K. SEALY, P. ISRAELSEN and J. MUHS: A review on inductive charging for electric vehicles. In *Int. Electric Machines Drives Conf.*, (2011), 143-147.

[37] M. YILMAZ and P.T. KREIN: Review of the impact of vehicle-to-grid technologies on distribution systems and utility interfaces. *IEEE Trans. on Power Electronics*, **28**(12), (2013), 5673-5689.

[38] LIU YU-ZHONG, LIN LU and LI YAN: H_∞ dynamical output feedback control of switched systems with delayed perturbations. In *Control and Decision Conf.*, (2009), 881-884.

[39] LAN ZHOU, JIN HUA SHE, MIN WU and YONG HE: LMI-based design method of robust modified repetitive-control systems. In *8th IEEE Int. Conf. on Control and Automation*, (2010), 440-445.

Archives of Control Sciences
Volume 27(LXIII), 2017
No. 1*, pages 63–76*

An adaptive control scheme for hyperbolic partial differential equation system (drilling system) with unknown coefficient

HAMED SHIRINABADI FARAHANI, HEIDAR ALI TALEBI and MOHAMMAD BAGHERMENHAJ

The adaptive boundary stabilization is investigated for a class of systems described by second-order hyperbolic PDEs with unknown coefficient. The proposed control scheme only utilizes measurement on top boundary and assume anti-damping dynamics on the opposite boundary which is the main feature of our work. To cope with the lack of full state measurements, we introduce Riemann variables which allow us reformulate the second-order in time hyperbolic PDE as a system with linear input-delay dynamics. Then, the infinite-dimensional time-delay tools are employed to design the controller. Simulation results which applied on mathematical model of drilling system are given to demonstrate the effectiveness of the proposed control approach.

Key words: drilling systems, adaptive control, hyperbolic partial differential equation, wave equation, boundary control

1. Introduction

We investigate boundary stabilization for a class of linear second-order hyperbolic PDE system with uncertainty coefficient on a finite space domain. The general issue addressed in this paper is how to deal with the wave in a one-dimensional form, as considered e.g. when modeling the dynamics of an elastic slope vibrating around its rest position. Particularly, we consider the wave equation describing the dynamics of the deformation denoted by $z(x,t)$.The research activities in boundary control field were devoted to parabolic PDEs in the early 2000s [1]. In recent years, however, more attention has been given to the hyperbolic PDEs and in particular to the stabilization of such dynamics [2-5].Many physical systems can be described by first-order hyperbolic PDEs, such as traffic flow, heat exchangers [20].Subsequently, in [6] systems with unknown input delay, i.e., an important class of infinite dimensional systems with first-order hyperbolic PDE dynamics is tackled. In [18-19] sufficient condition for exponential stability

The Authors are with Amirkabir University of Technology, Tehran, Iran. H. Talebi is the corresponding author, e-mail: alit@aut.ac.ir. Other e-mails: h.shirinabadi@aut.ac.ir and menhaj@aut.ac.ir

Received 5.06.2016. Revised 25.08.2016.

for various class of nonlinear first-order hyperbolic PDE system is given. In [21], back-stepping approaches have been used for first-order hyperbolic PDEs to achieve stability.

To the best of our knowledge, adaptive output-feedback boundary control problem has not yet been developed for the second-order hyperbolic PDEs especially when the dynamics are unstable, namely the wave equation. Wave and beam equations have been addressed in [7- 9], however, the dynamics are assumed to be stable.In [10], adaptive boundary control of unstable wave equation is studied by measuring all state $z(x,t)x \in [0,1]$ which is not feasible in real application. Recently in [17], an adaptive control law for wave equation is designed by measuring down and top boundary, simultaneously.

This paper is devoted to the boundary stabilization of uncertain hyperbolic PDE system. Here, we introduce the main ideas for back-stepping control of hyperbolic PDEs, the most basic of which is the wave equation . The main distinguished feature of a wave equation is that it is second order in time.

We consider mathematical model of drilling system [11], as a case study, which described (in linear form) by the second-order in time hyperbolic PDE subject to boundary conditions with unmatched parametric uncertainty.

We use the modified Riemann variables to reformulate the plant model as a linear input-delay model cascaded with a transport equation opposite of the input propagation direction. This structure allows us to reconstruct the delayed bottom velocity from top-boundary measurement. The Lyapunov methodology is then used for stability analysis. Both control and parameter estimation approaches utilize top-boundary measurement only, which is the main feature of our work. Toward this objective, first an invertible infinite-dimensional back-stepping transformation is introduced to transform the original system into a target system, from which it is much easier to design the desired controller and implement the performance analysis.Then, for the target system, a dynamic compensation for the unknown parameter is given by an adaptive technique and projection operator. Subsequently, based on this technique and the certainty equivalence principle, an adaptive controller is constructed to stabilize the target system in a certain sense. Finally, by the invertibility of the infinite-dimensional back-stepping transformation, the controller designed for the target system can stabilize the original system in the foregoing sense.

The rest of the paper is organized as follows. In Sec. 2, we introduce the mathematical modeling of drilling system and then present adaptive controller in Sec. 3 followed by the statement of the main stability theorem and its proof. We finally end our paper with a numerical simulations to illustrate the effectiveness of our proposed approach in Sec. 4. Concluding remarks and possible further research lines are presented in Sec. 5.

Notation: $||\ ||_{L^2}$ denotes the norm in $L^2(0,1)$ space, defined by $||u||^2_{L^2(0,1)} = \int_0^1 |u|^2 dx$ for all functions $u \in L^2(0,1)$. Similarly, $H^2(0,1)$ is the set of functions $u \in H^2(0,1)$ such that $\int_0^1 |u|^2 + |u_x|^2 + |u_{xx}^2 dx$ is finite. (u_x stands for the partial derivative of the function u with respect to x). Also, for $(a,b) \in R^2$ such that $a < b$, we define the standard projection operator on the interval $[a,b]$ as a function of two scalar arguments f (denoting the parameter being updated) and g (denoting the nominal update law) as

$$Proj_{[a,b]}(f,g) = g \begin{cases} 0 & \text{if} \quad f = a \text{ and } g < 0 \\ 0 & \text{if} \quad f = b \text{ and } g > 0 \\ 1 & \quad\text{otherwise.} \end{cases}$$

2. Mathematical modeling

To evaluate the performance of the proposed adaptive control approach, we consider a drilling system model [11], shown in Fig. 1. The main process of oil well drilling, which is depicted in Fig.1, includes in creation of a narrow deep hole in the ground until the oil reservoir is reached [11]. This system consists of a bit, tool for cutting rock, drill pipes, drill collars and rotatory table which provides torque on drill pipe for penetrating into ground.

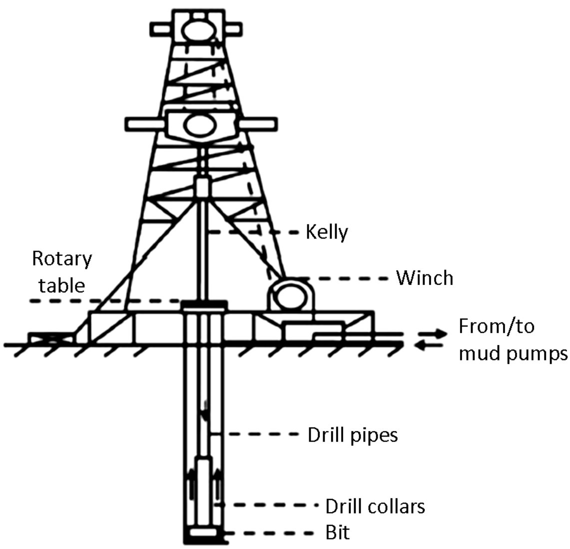

Figure 1: Drilling system

A distributed parameter model of drilling system is described by the second-order hyperbolic PDEs as follow [11]:

$$GJ\frac{\partial^2\theta(\xi,t)}{\partial\xi^2} - I\frac{\partial^2\theta(\xi,t)}{\partial t^2} - \beta\frac{\partial\theta(\xi,t)}{\partial t} = 0, \quad \xi \in [0,L], \ \ t \geqslant 0 \tag{1}$$

with boundary conditions

$$I_B \frac{\partial^2\theta}{\partial t^2}(0,t) = GJ\frac{\partial\theta}{\partial\xi}(0,t) + T\left(\frac{\partial\theta}{\partial t}(0,t)\right) \tag{2}$$

$$GJ\frac{\partial\theta}{\partial\xi}(L,t) = \Omega(t) \tag{3}$$

where $\theta(\xi,t) : [0,L]\times R^+ \to R$ (angle of rotation) and $\frac{\partial\theta}{\partial t}(\xi,t)$ (angular velocity) are the system states with $\left(\theta(\cdot,0), \frac{\partial\theta}{\partial t}(\cdot,0)\right) \in H_1([0,L])\times L_2([0,L])$, $\frac{\partial\theta}{\partial t}$ and $\frac{\partial\theta}{\partial\xi}$ denote the partial derivatives of $\theta(\xi,t)$ with respect to t and ξ, respectively, $T\left(\frac{\partial\theta}{\partial t}(0,t)\right)$ is the torque which is a nonlinear function of the bit speed which is uncertain, and $\Omega(t) : R^+ \to R$ is the control law coming from the rotor, I is the inertia, G is the shear modulus and J is the geometrical moment of inertia.

In the sequel, the damping coefficient β is assumed to be zero and without loss of generality, L is assumed to be equal one. By choosing $q = \frac{dT}{d\frac{\partial\theta}{\partial t}}\left(\left(\frac{\partial\theta}{\partial t}\right)^{ref}\right)$ (called anti-damping coefficient) where $\left(\frac{\partial\theta}{\partial t}\right)^{ref}$ is a given angular velocity to be achieved, the distributed mathematical model reduces to the unidimensional wave equation

$$\frac{\partial^2\theta(\xi,t)}{\partial\xi^2} = \rho^2\frac{\partial^2\theta(\xi,t)}{\partial t^2}; \quad \xi\in[0,1],\ t\geqslant 0; \rho = \sqrt{\frac{I}{GJ}} \tag{4}$$

$$\frac{\partial^2\theta}{\partial t^2} = c\frac{\partial\theta}{\partial\xi}(0,t) + cq\frac{\partial\theta}{\partial t}(0,t); \quad c = \frac{GJ}{I_B} \tag{5}$$

$$\frac{\partial\theta}{\partial\xi}(1,t) = g\Omega(t) = U(t); \quad g = \frac{1}{GJ}. \tag{6}$$

Our objective is to design a feedback law $U(t)$ to ensure dissipativity of the system, despite uncertainty in anti-damping coefficient $q > 0$, which does not employ the entire distributed state, but only the top boundary value measurement. We only measure angular velocity of the top boundary i.e. signal $\frac{\theta}{t}(1,\cdot)$, for all time. This assumption arises in a new formulation in which we need only the velocity at the boundary for all time. The main challenge here is instability of dynamics (5) with unmatched parametric uncertainty, since q acts on the lower boundary while the controller is applied on the opposite boundary. To deal with parameter uncertainties, as common in adaptive control approach, we assume that there exist a fixed and known constants $Q_{\min}$, $Q_{\max}$ such that $Q_{\min} < q < Q_{\max}$, $\forall x\in[0,1]$.

First, without loss of generality we assume $\rho^2 = 1$ and reformulate the plant (4)-(6) by introducing Riemann variables $u(\xi,t) = \frac{\partial\theta(\xi,t)}{\partial t} - \frac{\partial\theta(\xi,t)}{\partial\xi}$ and $v(\xi,t) = \frac{\partial\theta(\xi,t)}{\partial t} + \frac{\partial\theta(\xi,t)}{\partial\xi}$ as follows:

$$\frac{\partial u(\xi,t)}{\partial t} = -\frac{\partial u(\xi,t)}{\partial \xi} \tag{7}$$

$$\frac{\partial v(\xi,t)}{\partial t} = \frac{\partial v(\xi,t)}{\partial \xi} \tag{8}$$

$$v(1,t) = \frac{\partial \theta}{\partial t}(1,t) + U(t) = W(t) \tag{9}$$

$$\frac{\partial^2 \theta}{\partial t^2}(0,t) - c(1-q)\frac{\partial \theta}{\partial t}(0,t) = cv(0,t) \tag{10}$$

$$u(0,t) = 2\frac{\partial \theta}{\partial t}(0,t) - v(0,t). \tag{11}$$

ODE equation (10) can be represented in standard state space form as:

$$\dot{X}(t) = \begin{bmatrix} \dot{x}_1(t) \\ \dot{x}_2(t) \end{bmatrix} = \begin{bmatrix} 0 & 1 \\ 0 & c(q-1) \end{bmatrix} \begin{bmatrix} x_1(t) \\ x_2(t) \end{bmatrix} + \begin{bmatrix} 0 \\ c \end{bmatrix} v(0,t) \tag{12}$$

where $x_1(t) = \theta(0,t)$ and $x_2(t) = \frac{\partial \theta}{\partial t}(0,t)$ are the states of linear ODE system (10). It is obvious that this system is unstable for $q > 1$.The control objective is to design $v(1,t)$ and in turns $U(t)$ (from (9)) to achieve asymptotic stability of (10).

3. The proposed adaptive control design

In this section, similar to [10] we present an infinite dimensional back-stepping transformation, using which system (5) is transformed into a target system. Then, based on this transformation, our proposed adaptive controller is designed, which can stabilize the original system in the desired sense. If q is known, the back-stepping transformation $(x_2(t),u,v) \to (x_2(t),u,\omega)$ is given as follows:

$$\omega(\xi,t) = v(\xi,t) - (1-c-q)\left[\int_0^\xi k(\xi,y)v(y,t)dy + \lambda(\xi)\frac{\partial \theta}{\partial t}(0,t)\right] \tag{13}$$

where kernel $k(\xi,y)$ and $\lambda(\xi)$ are to be designed later.

Now, by taking the derivative of ω, we obtain:

$$\frac{\partial \omega(\xi,t)}{\partial \xi} = \tag{14}$$

$$\frac{\partial v(\xi,t)}{\partial \xi} - (1-c-q)\left[k(\xi,\xi)v(\xi,t)dy + \int_0^\xi \frac{\partial k(\xi,y)}{\partial \xi}v(y,t)dy + \lambda'(\xi)\frac{\partial \theta}{\partial t}(0,t)\right]$$

$$\frac{\partial\omega(\xi,t)}{\partial t} = \frac{\partial v(\xi,t)}{\partial t} - (1-c-q)\left[k(\xi,y)\frac{\partial}{\partial t}v(y,t)dy + \lambda(\xi)\frac{\partial^2\theta}{\partial t^2}(0,t)\right]. \tag{15}$$

Then, using integration by part, and using (10), we can get

$$\begin{aligned}\frac{\partial\omega(\xi,t)}{\partial t} = \frac{\partial v(\xi,t)}{\partial t} - (1-c-q)\Bigg[&k(\xi,\xi)v(\xi,t) - k(\xi,0)v(0,t) - \\ &-\int_0^\xi \frac{\partial k(\xi,y)}{\partial y}v(y,t)dy + \lambda(\xi)\left(c(q-1)\frac{\partial\theta}{\partial t}(0,t) + cv(0,t)\right)\Bigg].\end{aligned} \tag{16}$$

In case where q is known, the target system is given by [10]:

$$\frac{\partial\omega(\xi,t)}{\partial t} = \frac{\partial\omega(\xi,t)}{\partial\xi} \tag{17}$$

$$\omega(1,t) = 0. \tag{18}$$

Then, by substituting (14) and (16) into (17) and using (18), we can get

$$\frac{\partial k(\xi,y)}{\partial y} + \frac{\partial k(\xi,y)}{\partial\xi} = 0 \tag{19}$$

$$\lambda'(\xi) - c(q-1)\lambda(\xi) = 0 \tag{20}$$

$$k(\xi,0) = c. \tag{21}$$

The solution of the PDE (19) and ODE (20) can then be given as:

$$k(\xi,y) = ce^{c(q-1)(\xi-y)} \tag{22}$$

$$\lambda(\xi) = e^{c(q-1)\xi}. \tag{23}$$

In [10], the ODE system with input delay was modeled as a first order hyperbolic PDE and the back-stepping transformation used to design the controller, however, the adaptive case has not been addressed.

In case where the damping factor q is unknown, the back-stepping transformation (13) can be changed to:

$$\omega(\xi,t) = v(\xi,t) - (1-c-\hat{q})\left[\int_0^\xi \hat{k}(\xi,y,t)v(y,t)dy + \hat{\lambda}(\xi,t)x_2(t)\right] \tag{24}$$

where $\hat{q}$ is the estimate of unknown q.

Taking the time derivative of the transformation (24) and using the dynamics (8)-(12) we obtain

$$\frac{\partial\omega(\xi,t)}{\partial t}=\frac{\partial v(\xi,t)}{\partial t}-\int_0^{\xi}\frac{\partial k(\xi,y,t)}{\partial t}v(y,t)dy-\int_0^{\xi}k(\xi,y,t)\frac{\partial v(y,t)}{\partial t}dy-\lambda(\xi)\dot{x}_2(t)=$$

$$\frac{\partial v(\xi,t)}{\partial \xi}-\int_0^{\xi}\frac{\partial k(\xi,y,t)}{\partial t}v(y,t)dy-\int_0^{\xi}k(\xi,y,t)\frac{\partial v(\xi,t)}{\partial \xi}dy-\lambda(\xi)\left(c(q-1)x_2(t)+cv(0,t)\right).$$

Then, using integration by parts and taking the derivative of (24) with respect to x and noting that

$$\frac{\partial k(\xi,y,t)}{\partial t}+\frac{\partial k(\xi,y,t)}{\partial y}=0,$$

the original system (7)-(12) can be transformed into following target system:

$$\dot{x}_2(t)=-cc_0x_2(t)+c\omega(0,t)+c\widetilde{q}(t)x_2(t) \tag{25}$$

$$\frac{\partial\omega(\xi,t)}{\partial t}=\frac{\partial\omega(\xi,t)}{\partial\xi}-c\widetilde{q}(t)x_2(t)\lambda(\xi)+\dot{\hat{q}}(t)f(\xi,t) \tag{26}$$

$$\omega(1,t)=0 \tag{27}$$

$$\frac{\partial u(\xi,t)}{\partial t}=-\frac{\partial u(\xi,t)}{\partial\xi} \tag{28}$$

Where $\widetilde{q}(t)=q-\hat{q}(t)$ and $\hat{q}(t)$ is the estimate of unknown parameter q, and $f(\xi,t)$ is defined as:

$$f(\xi,t)=\left(\frac{1}{1-c_0-\hat{q}(t)}-c\xi\right)\lambda(\xi)x_2(t)-c\int_0^{\xi}k(\xi,y,t)(\xi-y)v(y,t)dy+$$

$$+\left(\frac{1}{1-c_0-\hat{q}(t)}\right)\int_0^{\xi}k(\xi,y,t)v(y,t)dy.$$

Now, by plugging the transformation (24) into (27) and using (8-10), after a lengthy but straightforward computation we obtain

$$\hat{k}(\xi,y,t)=ce^{c(\hat{q}(t)-1)(\xi-y)} \tag{29}$$

$$\hat{\lambda}(\xi)=e^{c(\hat{q}(t)-1)\xi}. \tag{30}$$

Given the back-stepping transformation (24), the following theorem states the main contribution of the paper which summarizes the proposed control law, adaptation rule and stability proof.

Theorem 7 (Stability of the target system (17) and (18)). *Consider the target system* (25)-(28)*. Then, by using control law* (38)*, and adaptation law* (36)*, the zero equilibrium of target system is exponentially stable in the sense of the following system norm:*

$$Y(t) = \left(\left|\left| \frac{\partial \omega(\cdot,t)}{\partial t} \right|\right|_{L^2(0,1)} \left|\left| \frac{\partial \omega(\cdot,t)}{\partial \xi} \right|\right|_{L^2(0,1)} + |x_2(t)|^2 \right)^{\frac{1}{2}}. \tag{31}$$

Proof Consider the following candidate Lyapunov function

$$V(t) = E(t) + \frac{\widetilde{q}(t)^2}{\gamma} \tag{32}$$

where

$$E(t) = \log \left[1 + (x_2(t))^2 + \int_0^1 e^{\xi} \omega(\xi,t)^2 d\xi + \int_0^1 e^{1-\xi} u(\xi,t)^2 d\xi \right]. \tag{33}$$

In the sequel, we will omit the arguments when the notation is obvious. The time derivative of $V(t)$ is given by:

$$\dot{V}(t) = \frac{1}{1+\psi(t)} \left[2x_2 \frac{\partial x_2}{\partial t} + \int_0^1 2e^{\xi} \omega \frac{\partial \omega}{\partial t} d\xi + \int_0^1 2e^{1-\xi} u \frac{\partial u}{\partial t} d\xi \right] - \frac{2}{\gamma_q} \dot{\hat{q}}(t) \widetilde{q}(t) \tag{34}$$

where

$$\psi(t) = (x_2(t))^2 + \int_0^1 e^{\xi} \omega(\xi,t)^2 d\xi + \int_0^1 e^{1-\xi} u(\xi,t)^2 d\xi. \tag{35}$$

Using Young and Cauchy-Schwartz inequalities yields in:

$$\exists \widetilde{M} > 0 \;\; s.t. \;\; \left| 2\dot{\widetilde{q}}(t) \int_0^1 e^{\xi} \omega(\xi,t) f(\xi,t) d\xi \right| \leqslant \gamma_q \widetilde{M} \left(x_2(t)^2 + ||\omega(t)||^2 \right). \tag{36}$$

Then by choosing the following adaptation law

$$\dot{\hat{q}}(t) = \frac{a\gamma_q}{1+\psi(t)} Proj_{[Q_{\min},Q_{\max}]} \{ g(t,\hat{q}(t)), \hat{q}(t) \} \tag{37}$$

where

$$g(t,\hat{q}(t)) = x_2(t) \left(x_2(t) + (\hat{q}(t) + c_0 - 1) \in_(t-1)^t f(\tau) e^{(\tau - t + 1)(c(\hat{q}(t)-1)+1)} d\tau \right)$$

and by using property of projection operator together with (26)-(29), equality (34) can be expressed as:

$$\dot{V}(t) \leqslant -frack\psi(t) \left(x_2(t)^2 + ||\omega(\xi,t)||^2 + ||u(\xi,t)||^2 \right); \quad k > 0. \tag{38}$$

Finally, plugging (24) into (28) imposes the following control law:

$$\begin{aligned} v(1,t) = W(t) &= (1-c-\hat{q}(t))\left[\int_0^1 \hat{k}(1,y,t)v(y,t)dy + \hat{\lambda}(\xi)x_2(t)\right] = \\ &= (1-c-\hat{q}(t))\left[\int_0^1 ce^{c(\hat{q}-1)(1-y)}W(t+y-1)dy + e^{a(\hat{q}-1)\xi}x_2(t)\right]. \end{aligned} \tag{39}$$

To finish, by suitable change of variable $t+y-1=\tau$ the control law can be expressed as follows:

$$W(t) = (1-c-\hat{q}(t))\left[\int_{(} t-1)^{t} ce^{c(\hat{q}-1)(1-y)}W(\tau)d\tau + e^{a(\hat{q}-1)\xi}x_2(t)\right]. \tag{40}$$

□

Now consider the following inverse back-stepping transformation $(x_2(t),u,\omega) \to (x_2(t),u,v)$ as

$$v(\xi,t) = \omega(\xi,t) - (c_0+\hat{q}-1)\int_0^{\xi} m(\xi,y,t)\omega(y,t)dy - \rho(\xi)x_2(t) \tag{41}$$

where kernel $m(\xi,y,t)$ and $\rho(\xi)$ can be computed by applying Laplace transformation in ξ to both sides of (24) and using (30-31) can be expressed as follows:

$$m(\xi,y,t) = ce^{cc_0(\xi-y)} \tag{42}$$

$$\rho(\xi) = e^{cc_0\xi}. \tag{43}$$

Corollary 1 (Stability of the original system) *Consider the plant* (4-6)*, control law* (38)*, and adaptation law* (36)*, here exist* M_0*,* $N_0 > 0$ *such that* $E(t) \leqslant M_0(e^{N_0E(0)}-1)$.

Proof We consider the following Lyapunov function candidate

$$E(t) = (q-\hat{q}(t))^2 + \int_0^1 \left[\frac{\partial\theta}{\partial\xi}(\xi,t)\right]^2 d\xi + \int_0^1 \left[\frac{\partial\theta}{\partial t}(\xi,t)\right]^2 d\xi + x_2(t)^2. \tag{44}$$

Notice that

$$\frac{\partial\theta(\xi,t)}{\partial t} = \frac{u(\xi,t)+v(\xi,t)}{2}$$

and

$$\frac{\partial\theta(\xi,t)}{\partial\xi} = \frac{v(\xi,t)-u(\xi,t)}{2}.$$

Time differentiation of $E(t)$ yields in

$$\dot{E}(t) = -2\dot{\hat{q}}(t) + \int_0^1 \left(\frac{\partial v}{\partial t}(\xi,t) - \frac{\partial u}{\partial t}(\xi,t)\right)\left(\frac{v(\xi,t)-u(\xi,t)}{2}\right)d\xi +$$
$$+ \int_0^1 \left(\frac{\partial v}{\partial t}(\xi,t) + \frac{\partial u}{\partial t}(\xi,t)\right)\left(\frac{v(\xi,t)+u(\xi,t)}{2}\right)d\xi + 2x_2(t)\dot{x}_2(t).$$

Then plugging parameter update law (37) and calculate control law noticing that by (9) $U(t) = v(1,t) - \frac{\partial \theta}{\partial t}(1,t)(1,t)$, using (36) and applying Young and Cauchy-Schwartz inequalities, it can be seen that there exist M_0, $N_0 > 0$ such that

$$E(t) \leqslant M_0(e^{N_0 E(0)} - 1). \tag{45}$$

□

4. Simulation results

In this section, we present numerical simulation to illustrate the effectiveness of the proposed controller. Similar to [11] we focus on trajectory of the form $\theta^{ref}(\xi,t) = -T(\omega_r)\xi + \omega_r t + u_0$ where $\omega_r \equiv \frac{\partial \theta^{ref}(\xi,t)}{\partial t}$ is uniform rotatory speed with the reference control input $\bar{U} = -T(\omega_r)$.

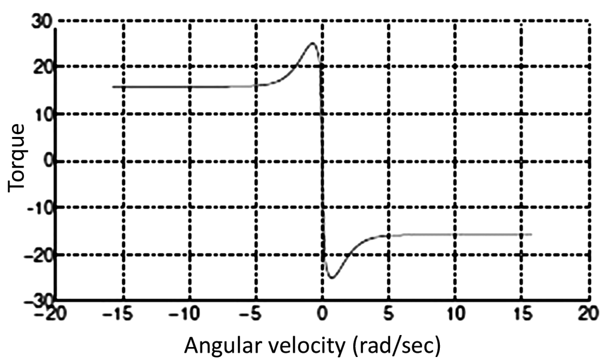

Figure 2: Function presenting rock-on-bit friction

Our objective is to design an adaptive controller that exponential stability of system (4)-(6) be guaranteed.

According to our proposed scheme, we consider only a measurement of top velocity $\omega(t) = \frac{\partial \theta}{\partial t}(1,t)$. The parameters of the model used in simulations are taken from [12] to ease performance comparisons and gathered in Tab. 1.

Table 3: List of parameter used in simulations

Symbol	Description	Value
L	Length of the drillpipe	2000 m
I_d	Inertia of the drillpipe per unit length	0.095 kg
I_b	Inertia of the BHA	311 kgm^2
G	Shear modulus	79.310^9 kgm^2
J	Geometric moment of inertia	1.1910^{-5} m^4
β	Drill string damping	0
T_{tobdyn}	Torque on the bit parameter	7500 N
$\alpha_1, \alpha_2, \alpha_3$	Friction parameters	5.5, 2.2, 3500
c_b	Viscous damping torque at the bit	0.03 Nm sec/rad

Velocity reference is chosen $\frac{\partial\theta^{ref}(\xi,t)}{\partial t} = 3$. Therefore the unknown parameter $q = 0.21$. Initial parameter's estimate is $\hat{q}(0) = 0.25$. The parameter estimate evolution is depicted in Fig. 3. By control input as depicted in Fig. 4 where adaptive control is turned on at $t = 9$ sec, stabilization of the drill string using back-stepping controller is achieved and shown in Fig. 5. It means that by control law (39) the stick-slip vibrations of drill string are reduced. Also in Fig. 5, the velocity at surface follows a similar trend delayed by 0.5 sec which corresponds to the time needed for the control law to propagate back to the surface. As shown in Fig. 3, the estimate of q converges but not to the unknown parameter, even if stabilization is satisfied.

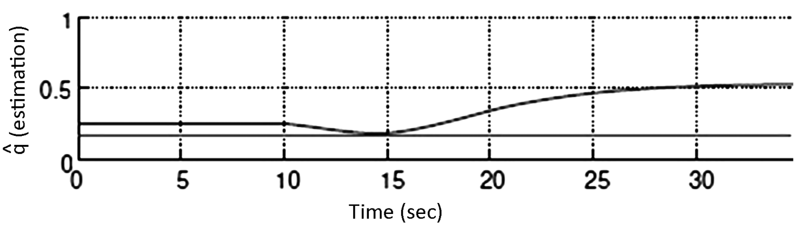

Figure 3: Parameter estimate evolution

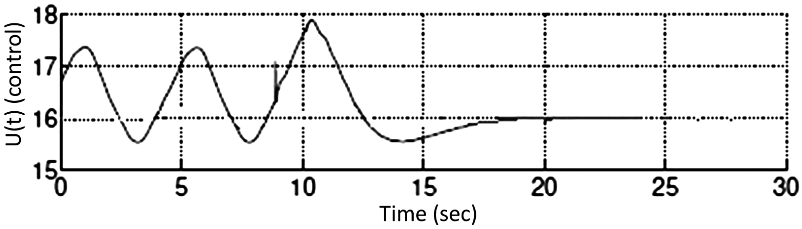

Figure 4: Control signal: input-adaptive controller is turned on after 9 sec

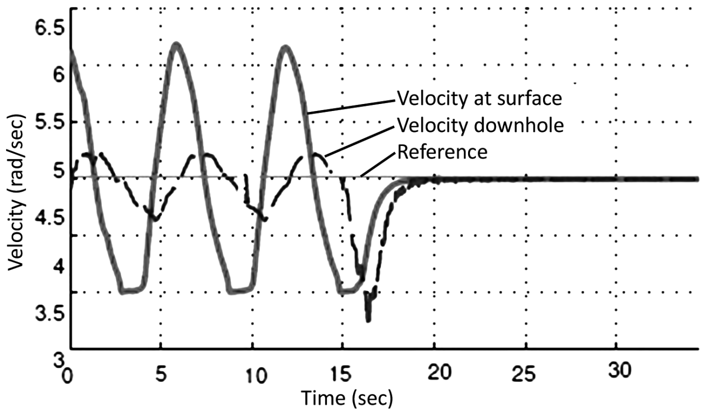

Figure 5: Velocity evolution: adaptive controller turned on after 9 sec

5. Conclusion

In this paper, we consider a class of second-order hyperbolic partial differential equation (wave equation) with unknown coefficient and propose an adaptive controller. The achievement of this new control method is that it does not require the measurements of the entire system state but only of top boundary values. The extension of this technique to other types of boundary conditions,is a topic of the further work.

References

[1] A. BALOGH, W.-J. LIU and M. KRSTIC: Stability enhancement by boundary control in 2D channel flow. *IEEE Trans on Automatic Control*, **46** (2001), 1696-1711.

[2] J.-M. CORON, G. BASTIN and B. D'ANDREA NOVEL: . Dissipative boundary conditions for one-dimensional nonlinear hyperbolic systems. *SIAM J. on Control and Optimization*, **47** (2008), 1460-1498.

[3] J.-M. CORON, B. D'ANDREA NOVEL and G. BASTIN: A strict Lyapunov function for boundary control of hyperbolic systems of conservation laws. *IEEE Trans. on Automatic Control*, **52** (2007), 2-11.

[4] J.-M. CORON, R. VAZQUEZ, M. KRSTIC and G. BASTIN: .Local exponential H_2 stabilization of a 2×2 quasilinear hyperbolic system using backstepping. *SIAM J. on Control and Optimization*, **51** (2013), 2005-2035.

[5] H. SHIRINABADI and H.A. TALEBI: Lyapunov stability analysis of special class of PDE systemsControl. *2nd Int. Conf. on Instrumentation and Automation*, (2011), 648-653.

[6] D. BRESCH-PIETRI and M. KRSTIC: Adaptive trajectory tracking despite unknown input delay and plant parameters. *Automatica*, **45** (2009), 2074Ű2081.

[7] T. KOBAYASHI: Low-gain adaptive stabilization of infinite-dimensional second-order systems. *J. Mathematical Analysis and Applications*, **275** (2002), 835-849.

[8] T. KOBAYASHI: Adaptive stabilization of infinite-dimensional semilinear second-order systems. *IMA J. Mathematical Control and Information*, **20** (2003), 137-152.

[9] T. KOBAYASHI: Stabilization of infinite-dimensional second-order systems by adaptive PI controllers. *Mathematical Methods in the Applied Sciences*, **24** (2001), 513-527.

[10] M. KRSTIC: Adaptive control of an anti-stable wave PDE. *Dynamics of Continuous, Discrete and Impulsive Systems*, **17** (2010), 853-882.

[11] B.SALDIVAR, S.MONDI, J.JACQUES and L.V. RASVAN: Stick-slip oscillations in oill well drilings: Distributed parameter and neutral type retarded model approaches. *18th IFAC World Congress*, Italy, (2011).

[12] QI-ZHI ZHANG, YU-YAO HE, LIN LI and NURZAT: Sliding mode control of rotary drilling system with stick slip oscillation. *Int. Workshop on Intelligent Systems and Applications*, China, (2010), 1-4.

[13] P.A. IOANNOU and B. FIDAN: Adaptive Control Tutorial. Society for Industrial Mathematics, 2006.

[14] A. SERRARENS, M. VAN DE MOLENGRAFT, J. KOK and L. VAN DEN STEEN: H_∞ control for suppressing stick-slip in oil well drillstrings. *IEEE Control Systems*, **18**(2), (1998), 19-30.

[15] C. SAGERT, F. DI MEGLIO, M. KRSTIC and P. ROUCHON: Backstepping and flatness approaches for stabilization of the stick-slip phenomenon for drilling. *IFAC Symp. on System, Structure and Control*, 2013.

[16] M. KRISTIC: Boundary Control of PDEs: A Course on Backstepping Designs. Society for Industrial Mathematics, 2008.

[17] D. PIETRI and M. KRISTIC: Output-feedback adaptive control of wave PDE with boundary anti-damping. *Automatica*, **50** (2014), 1407-1415.

[18] C. PRIEU and F. MAZENC: ISS-Lyapunov function for time varying hyperbolic systems of balance law. *Mathematics of Control, Signals, and Systems*, **24** (2012), 111-134.

[19] F. CASTILLO, E. WITRANT, C. PRIEURE and L. DUGRAD: Dynamic boundary stabilization of hyperbolic systems. *Proc. 51st IEEE Conf. on Decision and Control*, Maui, USA, (2012).

[20] D. BRESCH-PIETRI and M. KRSTIC: Delay-adaptive predictor feedback for systems with unknown long actuator delay. *IEEE Trans. on Automatic Control*, **55**(9), (2010), 2106-2112.

[21] M. KRSTIC and A. SMYSHLYAEV: Backstepping boundary control for first-order hyperbolic PDEs and application to systems with actuator and sensor delays. *Systems and Control Letters*, **57**(9), (2008), 750-758.

Archives of Control Sciences
Volume 27(LXIII), 2017
No. 1*, pages 77–89*

Pointwise observation of the state given by complex time lag parabolic system

ADAM KOWALEWSKI

Various optimization problems for linear parabolic systems with multiple constant time lags are considered. In this paper, we consider an optimal distributed control problem for a linear complex parabolic system in which different multiple constant time lags appear both in the state equation and in the Neumann boundary condition. Sufficient conditions for the existence of a unique solution of the parabolic time lag equation with the Neumann boundary condition are proved. The time horizon T is fixed. Making use of the Lions scheme [13], necessary and sufficient conditions of optimality for the Neumann problem with the quadratic performance functional with pointwise observation of the state and constrained control are derived. The example of application is also provided.

Key words: distributed control, parabolic system, time lags, pointwise observation.

1. Introduction

Various optimization problems associated with the optimal control of distributed parabolic systems with lags appearing in the boundary conditions have been studied recently in Refs. [1] - [11] and [12], [16], [17].

In this paper, we consider an optimal distributed control problem for a linear complex parabolic system in which different multiple constant time lags appear both in the state equation and the Neumann boundary condition.

Such complex systems constitute in a linear approximation, a universal mathematical model for many diffusion processes.

Sufficient conditions for the existence of a unique solution of such time lag parabolic equations with the Neumann boundary conditions involving multiple time lags are proved.

In this paper, we restrict our considerations to the case of the distributed control for the Neumann problem. Consequently, we formulate the following optimal control problem. We assume that the performance functional has the quadratic form with pointwise

The Author is with AGH University of Science and Technology, Institute of Automatics and Biomedical Engineering, 30-059 Cracow, al.Mickiewicza 30, Poland, e-mail: ako@agh.edu.pl.

This work was carried out within the research programme AGH University of Science and Technology, No. 11.11.120.396.

Received 26.10.2016.

observation of the state. Moreover, the time horizon is fixed in our optimization problem. Finally, we impose some constraints on the distributed control. Making use of the Lions framework [13] necessary and sufficient conditions of optimality with the quadratic performance functional with pointwise observation of the state and constrained control are derived for the Neumann problem. The example of application is also provided.

2. Existence and uniqueness of solutions

Consider now the distributed-parameter system described by the following parabolic lag equation

$$\frac{\partial y}{\partial t}+A(t)y+\sum_{i=1}^{m} y(x,t-h_i)=v \quad x\in\Omega, t\in(0,T) \tag{1}$$

$$y(x,t')=\Phi_0(x,t') \qquad x\in\Omega, t'\in[-\Upsilon,0) \tag{2}$$

$$y(x,0)=y_0(x) \qquad x\in\Omega \tag{3}$$

$$\frac{\partial y}{\partial\eta_A}=\sum_{s=1}^{l} y(x,t-k_s)+u \qquad x\in\Gamma, t\in(0,T) \tag{4}$$

$$y(x,t')=\Psi_0(x,t') \qquad x\in\Gamma, t'\in[-\Upsilon,0) \tag{5}$$

where: $\Omega\subset R^n$ is a bounded, open set with boundary Γ , which is a C^∞ - manifold of dimension $n-1$. Locally, Ω is totally on one side of Γ . $\frac{\partial y}{\partial\eta_A}$ is a normal derivative at Γ, directed towards the exterior of Ω,

$$y\equiv y(x,t;v), \qquad v\equiv v(x,t), \qquad u\equiv u(x,t),$$
$$Q=\Omega\times(0,T), \qquad \bar{Q}=\bar{\Omega}\times[0,T],$$
$$Q_0=\Omega\times[-\Upsilon,0), \qquad \Sigma=\Gamma\times(0,T),$$
$$\Sigma_0=\Gamma\times[-\Upsilon,0),$$

h_i, k_s are specified positive numbers representing time lags such that $0\leqslant h_1<h_2<\ldots<h_m$ for $i=1,\ldots,m$ and $0\leqslant k_1<k_2<\ldots<k_l$ for $s=1,\ldots,l$ respectively, Φ_0,Ψ_0 are initial functions defined on Q_0 and Σ_0 respectively. Moreover, $\Upsilon=\max\{h_m,k_l\}$.

The operator $A(t)$ has the form

$$A(t)y=-\sum_{i,j=1}^{n}\frac{\partial}{\partial x_i}\left(a_{ij}(x,t)\frac{\partial y(x,t)}{\partial x_j}\right) \tag{6}$$

and the functions $a_{ij}(x,t)$ satisfy the condition

$$\sum_{i,j=1}^{n} a_{ij}(x,t)\Phi_i\Phi_j\geqslant\alpha\sum_{i=1}^{n}\Phi_i^2 \qquad \alpha>0, \tag{7}$$

$$\forall (x,t) \in \bar{Q}, \ \forall \Phi_i \in R$$

where: $a_{ij}(x,t)$ are real C^∞ functions defined on $\bar{Q}$ (closure of Q). The equations (1) - (5) constitute a Neumann problem.

First we shall prove sufficient conditions for the existence of a unique solution of the mixed initial-boundary value problem (1) - (5) for the case where $v \in L^2(Q)$.

For this purpose, for any pair of real numbers $r,s \geqslant 0$, we introduce the Sobolev space $H^{r,s}(Q)$ ([14], Vol. 2, p.6) defined by

$$\left.\begin{array}{l} H^{r,s}(Q) = H^0(0,T;H^r(\Omega)) \cap H^s(0,T;H^0(\Omega)) \\ \text{which is a Hilbert space normed by} \\ \left(\int\limits_0^T \| y(t) \|^2_{H^r(\Omega)} dt + \| y \|^2_{H^s(0,T;H^0(\Omega))} \right)^{\frac{1}{2}} \end{array}\right\} \tag{8}$$

where: the spaces $H^r(\Omega)$ and $H^s(0,T;H^0(\Omega))$ are defined in Chapter 1 ([14], Vol.1) respectively.

Consequently, some properties and central theorems for the functions $y \in H^{r,s}(Q)$ are given in [7], [10] and [14].

The existence of a unique solution for the mixed initial-boundary value problem (1) - (5) on the cylinder Q can be proved using a constructive method, i.e., first, solving (1) - (5) on the subcylinder Q_1 and in turn on Q_2, etc. until the procedure covers the whole cylinder Q. In this way the solution in the previous step determines the next one.

For simplicity, we introduce the following notations:

$$E_j \triangleq ((j-1)\lambda, j\lambda) \text{ where } \lambda = \min\{h_1, k_1\}, \quad Q_j = \Omega \times E_j,$$

$$\Sigma_j = \Gamma \times E_j \ \text{ for } \ j = 1, \ldots K \, .$$

Using the results of Section 14 ([13], pp. 182-185) we can prove the following result.

Lemma 1 *Let*

$$v \in L^2(Q) \tag{9}$$

$$f_j \in L^2(Q_j) \tag{10}$$

where

$$f_j(x,t) = v(x,t) - \sum_{i=1}^{m} y_{j-1}(x, t-h_i)$$

$$y_{j-1}(\cdot, (j-1)\lambda) \in L^2(\Omega) \tag{11}$$

$$q_j \in H^{1/2,1/4}(\Sigma_j) \tag{12}$$

where

$$q_j(x,t) = \sum_{s=1}^{l} y_{j-1}(x, t-k_s) + u(x,t).$$

Then, there exists a unique solution $y_j \in H^{2,1}(Q_j)$ for the mixed initial-boundary value problem (1)*,* (4)*,* (11)*.*

Proof: We observe that for $j = 1$,

$$\sum_{i=1}^{m} y_{j-1}\big|_{Q_0}(x, t-h_i) = \sum_{i=1}^{m} \Phi_0(x, t-h_i) \quad \text{and}$$

$$\sum_{s=1}^{l} y_{j-1}\big|_{\Sigma_0}(x, t-k_s) = \sum_{s=1}^{l} \Psi_0(x, t-k_s).$$

Then the assumptions (10), (11) and (12) are fulfilled if we assume that $\Phi_0 \in H^{2,1}(Q_0)$, $y_0 \in L^2(\Omega)$, $u \in H^{1/2,1/4}(\Sigma)$ and $\Psi_0 \in H^{1/2,1/4}(\Sigma_0)$. These assumptions are sufficient to ensure the existence of a unique solution $y_1 \in H^{2,1}(Q_1)$. Next for $j = 2$ we have to verify that $f_2 \in L^2(Q_2)$, $y_1(\cdot, \lambda) \in L^2(\Omega)$ and $q_2 \in H^{1/2,1/4}(\Sigma_2)$. It is easy to notice that the condition (10) follows from the fact that $y_1 \in H^{2,1}(Q_1)$ and $v \in L^2(Q)$. Really, from the Theorem 3.1 ([14], Vol.1, p.19) we can prove that $y_1 \in H^{2,1}(Q_1)$ implies that the mapping $t \to y_1(\cdot, t)$ is continuous from $[0, \lambda] \to H^1(\Omega) \subset L^2(\Omega)$, hence $y_1(\cdot, \lambda) \in L^2(\Omega)$. Then using the Trace Theorem ([14], Vol. 2, p.9) we can verify that $y_1 \in H^{2,1}(Q_1)$ implies that $y_1 \to y_1\Big|_{\Sigma_1}$ is a linear, continuous mapping of $H^{2,1}(Q_1) \to H^{1/2,1/4}(\Sigma)$. Assuming that $v \in H^{1/2,1/4}(\Sigma)$, the condition $q_2 \in H^{1/2,1/4}(\Sigma_2)$ is fulfilled. Then, there exists a unique solution $y_2 \in H^{2,1}(Q_2)$. We shall now summarize the foregoing result for any Q_j, $j = 3, \ldots, K$.

Theorem 1 *Let y_0, Φ_0, Ψ_0, u and v be given with $y_0 \in L^2(\Omega), \Phi_0 \in H^{2,1}(Q_0), \Psi_0 \in H^{1/2,1/4}(\Sigma_0)$, $u \in H^{1/2,1/4}(\Sigma)$ and $v \in L^2(Q)$. Then, there exists a unique solution $y \in H^{2,1}(Q)$ for the mixed initial-boundary value problem* (1) – (5)*. Moreover, $y(\cdot, j\lambda) \in L^2(\Omega)$ for $j = 1, \ldots, K$.*

3. Problem formulation. Optimization theorems

We shall now formulate the optimal distributed control problem for the Neumann problem. Let us denote by $U = L^2(Q)$ the space of controls. The time horizon T is fixed in our problem.

Let $x^1, \ldots, x^\mu$ be points of Ω. We assume that the observation is $\{y(x^j, t; v)\}$, $1 \leqslant j \leqslant \mu$ - provided we can attach a meaning to this.

If we now assume that the coefficients of the operator A in the equation (1) are sufficiently regular, then from the Theorem 1 it follows that

$$y(v) \in H^{2,1}(Q). \tag{13}$$

Hence, $y(v) \in L^2(0,T;H^2(\Omega))$ and $y(x^j,t)$ has meaning (and "$t \to y(x^j,t)$" $\in L^2(0,T)$) if

$$H^2(\Omega) \subset C^0(\Omega) \tag{14}$$

which is true if (and only if)

$$\frac{1}{2} - \frac{2}{n} < 0 \quad \text{i.e.} \quad n \leqslant 3\,.$$

Hence we make the standing hypothesis that the dimension is $n \leqslant 3$.

Then the observation

$$Cy(v) = \{y(x^j,t;v)\} \in (L^2(0,T))^\mu \tag{15}$$

The cost function is now given

$$I(v) = \lambda_1 \parallel Cy(v) - z_d \parallel^2_{(L^2(0,T))^\mu} + \lambda_2 \int\limits_Q (Nv)v\,dxdt \tag{16}$$

If $z_d = \{z_{d1}, \ldots, z_\mu\}$,

$$I(v) = \lambda_1 \sum_{j=1}^{\mu} \int\limits_0^T \mid y(x^j,t;v) - z_{dj}(t) \mid^2 dt + \lambda_2 \int\limits_Q (Nv)v\,dxdt \tag{17}$$

where: $\lambda_i \geqslant 0$, $\lambda_1 + \lambda_2 > 0$; $z_{dj}(t)$ are given elements in $L^2(0,T)$ and N is a positive, linear operator on $L^2(Q)$ into $L^2(Q)$.

Finally, we assume the following constraint on controls $v \in U_{ad}$, where

$$U_{ad} \text{ is a closed, convex subset of } U \tag{18}$$

Let $y(x,t;v)$ denote the solution of the mixed initial-boundary value problem (1)- (5) at (x,t) corresponding to a given control $v \in U_{ad}$. We note from the Theorem 1 that for any $v \in U_{ad}$ the performance functional (17) is well-defined since $y(v) \in H^{2,1}(Q)$. The solving of the formulated optimal control problem is equivalent to seeking a $v_0 \in U_{ad}$ such that $I(v_0) \leqslant I(v)\ \ \forall v \in U_{ad}$. Then from the Theorem 1.3 ([13], p. 10) it follows that for $\lambda_2 > 0$ a unique optimal control v_0 exists; moreover, v_0 is characterized by the following condition

$$I'(v_0) \cdot (v - v_0) \geqslant 0 \qquad \forall v \in U_{\mathrm{ad}} \tag{19}$$

Using the form of the cost function given by (17) we can express (19) in the following form

$$\lambda_1 \sum_{j=1}^{\mu} \int\limits_0^T (y(x^j,t;v_0) - z_{dj}(t))(y(x^j,t;v) - y(x^j,t;v_0))dt +$$

$$+\lambda_2 \int\limits_Q N v_0 (v - v_0) dxdt \geqslant 0 \qquad \forall v \in U_{ad} \tag{20}$$

To simplify (20), we introduce the adjoint equation and for every $v \in U_{ad}$, we define the adjoint variable $p = p(v) = p(x,t;v)$ as the solution of the equation

$$\begin{gathered} -\frac{\partial p(v)}{\partial t} + A^*(t)p(v) + \sum_{i=1}^{m} p(x,t+h_i;v) = \lambda_1 \sum_{j=1}^{\mu} (y(x^j,t;v) - z_{dj}(t)) \otimes \delta(x-x^j) \\ x \in \Omega, t \in (0, T-\Upsilon) \end{gathered} \tag{21}$$

$$\begin{gathered} -\frac{\partial p(v)}{\partial t} + A^*(t)p(v) = \lambda_1 \sum_{j=1}^{\mu} (y(x^j,t;v) - z_{dj}(t)) \otimes \delta(x-x^j) \\ x \in \Omega, t \in (T-\Upsilon, T) \end{gathered} \tag{22}$$

$$p(x,T;v) = 0 \qquad x \in \Omega \tag{23}$$

$$\frac{\partial p(v)}{\partial \eta_{A^*}}(x,t) = \sum_{s=1}^{l} p(x,t+k_s;v) \qquad x \in \Gamma, t \in (0, T-\Upsilon) \tag{24}$$

$$\frac{\partial p(v)}{\partial \eta_{A^*}}(x,t) = 0 \qquad x \in \Gamma, t \in (T-\Upsilon, T) \tag{25}$$

where

$$\left.\begin{aligned} & g(t) \otimes \delta(x-x^j) \ \text{ is the distribution,} \\ & \Psi \to \int_0^T g(t)\Psi(x^j,t)dt, \ \Psi \in \mathcal{D}(Q) \\ & A^*(t)p = -\sum_{i,j=1}^{n} \frac{\partial}{\partial x_j}\left(a_{ij}(x,t)\frac{\partial p}{\partial x_i}\right) \end{aligned}\right\} \tag{26}$$

The existence of a unique solution for the problem (21) - (25) on the cylinder Q can be proved using a constructive method. It is easy to notice that for given z_d and v , problem (21) - (25) can be solved backwards in time starting from $t = T$, i.e., first, solving (21) - (25) on the subcylinder Q_K and in turn on Q_{K-1} , etc. until the procedure covers the whole cylinder Q . For this purpose, we may apply Theorem 1 (with an obvious change of variables) to problem (21) - (25) (with reversed sense of time, i.e., $t' = T - t$).

Lemma 2 *Let the hypothesis of Theorem 1 be satisfied. Then, for given* $z_{dj}(t) \in L^2(0,T)$ *and any* $v \in L^2(Q)$*, there exists a unique solution* $p(v) \in H^{2,1}(Q)$ *for the problem* (21) - (25) *defined by transposition*

$$\int\limits_Q p(v_0)\left(\frac{\partial \Psi}{\partial t} + A\Psi\right) dxdt = \sum_{j=1}^{\mu} \int_0^T \left(y(x^j,t;v_0) - z_{dj}(t)\right) \Psi(x^j,t)dt \tag{27}$$

$$\forall \Psi \in H^{2,1}(Q), \quad \Psi\Big|_{\Sigma} = 0, \quad x \in \Gamma,\ t \in (0,T) \quad \text{and} \quad \Psi(x,T) = 0.$$

Remark 1 *The right hand side of* (27) *is a continuous linear form on* $H^{2,1}(Q)$ *if* $n \leqslant 3$.

Consequently, after transformations the first component on the left-hand side of (20) can be rewriten as

$$\lambda_1 \sum_{j=1}^{\mu} \int_0^T (y(x^j,t;v_0) - z_{dj}(t))(y(x^j,t;v) - y(x^j,t;v_0))dt = \int_Q p(v_0)(v - v_0)\, dxdt \tag{28}$$

Substituting (28) into (20) we obtain

$$\int_Q (p(v_0) + \lambda_2 N v_0)(v - v_0)\, dxdt \geqslant 0, \quad \forall v \in U_{ad} \tag{29}$$

Theorem 2 *For the problem* (1) - (5) *with the performance functional* (17) *with* $z_{dj}(t) \in L^2(0,T)$ *and* $\lambda_2 > 0$ *and with constraints on controls* (18)*, there exists a unique optimal control* v_0 *which satisfies the maximum condition (29).*

Consider now the particular case where $U_{ad} = L^2(Q)$. Thus the maximum condition (29) is satisfied when

$$v_0 = -\lambda_2^{-1} N^{-1} p(v_0) \tag{30}$$

We must notice that the conditions of optimality derived above (Theorem 2) allow us to obtain an analytical formula for the optimal control in particular cases only (e.g. there are no constraints on controls). This results from the following: the determining of the function $p(v_0)$ in the maximum condition from the adjoint equation is possible if and only if we know y_0 which corresponds to the control v_0. These mutual connections make the practical use of the derived optimization formulas difficult. Therefore we resign from the exact determining of the optimal control and we use approximation methods.

In the case of performance functional (17) with $\lambda_1 > 0$ and $\lambda_2 = 0$, the optimal control problem reduces to the minimizing of the functional on a closed and convex subset in a Hilbert space. Then, the optimization problem is equivalent to a quadratic programming one (Ref. [10]) which can be solved by the use of the well-known algorithms, e.g. Gilbert's (Ref. [10]).

The practical application of Gilbert's algorithm to an optimal control problem for a parabolic system with boundary condition involving a time lag is presented in [12]. Using Gilbert's algorithm, a one-dimensional numerical example of the plasma control process is solved.

4. Example

Making use of the results of [13], we shall express the optimal control (30) in the feedback form.

For this purpose we consider the following set of equations with $\varepsilon \in (0,T)$:

$$\begin{cases} \dfrac{\partial y}{\partial t} + A(t)y + \displaystyle\sum_{i=1}^{m} y(x,t-h_i) + \lambda_2^{-1} N^{-1} p = 0 & \text{for } t-h_i \geqslant \varepsilon \\ \dfrac{\partial y}{\partial t} + A(t)y + \displaystyle\sum_{i=1}^{m} \Phi_\varepsilon(x,t-h_i) + \lambda_2^{-1} N^{-1} p = 0 & \text{for } t-h_i < \varepsilon \end{cases} \tag{31}$$

$$(x,t) \in \Omega \times (\varepsilon, T)$$

$$\begin{cases} -\dfrac{\partial p}{\partial t} + A^*(t)p + \displaystyle\sum_{i=1}^{m} p(x,t+h_i) \; - \; \lambda_1 y = -\lambda_1 z_d & \\ & \text{for } (x,t) \in \Omega \times (\varepsilon, T-\Upsilon) \\ -\dfrac{\partial p}{\partial t} + A^*(t)p - \lambda_1 y = -\lambda_1 z_d & \text{for } (x,t) \in \Omega \times (T-\Upsilon, T) \end{cases} \tag{32}$$

with boundary conditions

$$\frac{\partial y}{\partial \eta_A}(x,t) = \begin{cases} \displaystyle\sum_{s=1}^{l} y(x,t-k_s) + u(x,t) & \text{for } t-k_s \geqslant \varepsilon \\ \displaystyle\sum_{s=1}^{l} \Psi_\varepsilon(x,t-k_s) + u(x,t) & \text{for } t-k_s < \varepsilon \end{cases} \tag{33}$$

$$(x,t) \in \Gamma \times (\varepsilon, T)$$

$$\frac{\partial p}{\partial \eta_{A^*}}(x,t) = \begin{cases} \displaystyle\sum_{s=1}^{l} p(x,t+k_s) & \text{for } (x,t) \in \Gamma \times (\varepsilon, T-\Upsilon) \\ 0 & \text{for } (x,t) \in \Gamma \times (T-\Upsilon, T) \end{cases} \tag{34}$$

and with initial and final conditions

$$\begin{cases} y(x,\varepsilon) = y_\varepsilon(x) & x \in \Omega \\ p(x,T) = 0 & x \in \Omega \end{cases} \tag{35}$$

where: $y_\varepsilon \in H^1(\Omega)$, Φ_ε and Ψ_ε are given function defined on $\Omega \times [\varepsilon - \Upsilon, \varepsilon)$ and $\Gamma \times [\varepsilon - \Upsilon, \varepsilon)$ respectively, that is $\Phi_\varepsilon \in H^{2,1}(\Omega \times [\varepsilon - \Upsilon, \varepsilon))$ and $\Psi_\varepsilon \in H^{1/2,1/4}(\Gamma \times [\varepsilon - \Upsilon, \varepsilon))$.

We shall consider problem (31) - (35) subject to (1) for $t \in (\varepsilon, T)$ and $U_{ad} = L^2(Q)$. The performance functional is given by

$$I_\varepsilon(v) = \lambda_1 \int_\varepsilon^T \int_\Omega |\, y(x,t;v) - z_d \,|^2 \, dxdt + \lambda_2 \int_\varepsilon^T \int_\Omega (Nv)v \, dxdt \tag{36}$$

Then the problem (31)-(36) with $\lambda_2 > 0$ has a unique optimal control in the form (30). Also it is easy to verify that (31) - (35) has a unique solution

$$\{y,p\} \in H^{2,1}(\Omega \times (\varepsilon,T)).$$

Proposition 1 *Let $\{y,p\}$ be solution of* (31) - (35) *with* $\varepsilon = 0$. *We define σ_ε, the system "state" at time ε, by the triplet $(y(\cdot,\varepsilon),\Phi_\varepsilon,\Psi_\varepsilon)$, where*

$$\Phi_\varepsilon(\cdot,t') = \begin{cases} \Phi_0(\cdot,t') & \text{for } t' \in \hat{E}_\varepsilon = [-\Upsilon,0) \cap [\varepsilon-\Upsilon,\varepsilon) \\ y(\cdot,t')|_\Omega & \text{for } t' \in [\varepsilon-\Upsilon,\varepsilon) - \hat{E}_\varepsilon \end{cases} \tag{37}$$

$$\Psi_\varepsilon(\cdot,t') = \begin{cases} \Psi_0(\cdot,t') & \text{for } t' \in \hat{E}_\varepsilon = [-\Upsilon,0) \cap [\varepsilon-\Upsilon,\varepsilon) \\ y(\cdot,t')|_\Gamma & \text{for } t' \in [\varepsilon-\Upsilon,\varepsilon) - \hat{E}_\varepsilon \end{cases} \tag{38}$$

Then, for all triplets $\varepsilon \leqslant t$ in $(0,T)$,

$$p(\cdot,t) = P(t,\varepsilon)\sigma_\varepsilon + r_\varepsilon(\cdot,t) \tag{39}$$

where $P(t,\varepsilon)$ and $r_\varepsilon(\cdot,t)$ are determined by the following procedure

First we solve the set of equations

$$\begin{cases} \dfrac{\partial\alpha}{\partial t} + A(t)\alpha + \displaystyle\sum_{i=1}^{m} \alpha(x,t-h_i) + \lambda_2^{-1}N^{-1}\beta = 0 \\ \text{for } \ t-h_i \geqslant \varepsilon \\ \\ \dfrac{\partial\alpha}{\partial t} + A(t)\alpha + \displaystyle\sum_{i=1}^{m} \Phi_\varepsilon(x,t-h_i) + \lambda_2^{-1}N^{-1}\beta = 0 \\ \text{for } \ t-h_i < \varepsilon \end{cases} \tag{40}$$

$$(x,t) \in \Omega \times (\varepsilon,T)$$

$$\begin{cases} -\dfrac{\partial\beta}{\partial t} + A^*(t)\beta + \displaystyle\sum_{i=1}^{m} \beta(x,t+h_i) \ -\lambda_1\alpha = 0 & \\ & \text{for } \ (x,t) \in \Omega \times (\varepsilon, T-\Upsilon) \\ -\dfrac{\partial\beta}{\partial t} + A^*(t)\beta - \lambda_1\alpha = 0 & \text{for } \ (x,t) \in \Omega \times (T-\Upsilon, T) \end{cases} \tag{41}$$

with boundary conditions

$$\frac{\partial\alpha}{\partial\eta_A}(x,t) = \begin{cases} \displaystyle\sum_{s=1}^{l} \alpha(x,t-k_s) & \text{for } t-k_s \geqslant \varepsilon \\ \displaystyle\sum_{s=1}^{l} \Psi_\varepsilon(x,t-k_s) & \text{for } t-k_s < \varepsilon \end{cases} \tag{42}$$

$$(x,t) \in \Gamma \times (\varepsilon, T)$$

$$\frac{\partial \beta}{\partial \eta_{A^*}}(x,t) = \begin{cases} \sum_{s=1}^{l} \beta(x, t+k_s) & \text{for } (x,t) \in \Gamma \times (\varepsilon, T-\Upsilon) \\ 0 & \text{for } (x,t) \in \Gamma \times (T-\Upsilon, T) \end{cases} \tag{43}$$

and with initial and final conditions

$$\begin{cases} \alpha(x,\varepsilon) = y(x,\varepsilon) & x \in \Omega \\ \beta(x,T) = 0 & x \in \Omega \end{cases} \tag{44}$$

then

$$P(t,\varepsilon)\sigma_\varepsilon = \beta(\cdot,t) \tag{45}$$

Next we solve the set of equations

$$\begin{cases} \frac{\partial \kappa}{\partial t} + A(t)\kappa + \sum_{i=1}^{m} \kappa(x, t-h_i) \ + \lambda_2^{-1} N^{-1}\delta = 0 \\ \qquad\qquad\qquad\qquad\qquad\qquad \text{for } \ t-h_i \geqslant \varepsilon \\ \frac{\partial \kappa}{\partial t} + A(t)\kappa + \lambda_2^{-1} N^{-1}\delta = 0 \quad \text{for } \ t-h_i < \varepsilon \end{cases} \tag{46}$$

$$(x,t) \in \Omega \times (\varepsilon, T)$$

$$\begin{cases} -\frac{\partial \delta}{\partial t} + A^*(t)\delta + \sum_{i=1}^{m} \delta(x, t+h_i) \ - \lambda_1 \kappa = -\lambda_1 z_d \\ \qquad\qquad\qquad\qquad\qquad\qquad \text{for } \ (x,t) \in \Omega \times (\varepsilon, T-\Upsilon) \\ -\frac{\partial \delta}{\partial t} + A^*(t)\delta - \lambda_1 \kappa = -\lambda_1 z_d \quad \text{for } \ (x,t) \in \Omega \times (T-\Upsilon, T) \end{cases} \tag{47}$$

with boundary conditions

$$\frac{\partial \kappa}{\partial \eta_A}(x,t) = \begin{cases} \sum_{s=1}^{l} \kappa(x, t-k_s) + v(x,t) & \text{for } t-k_s \geqslant \varepsilon \\ v(x,t) & \text{for } t-k_s < \varepsilon, \end{cases} \tag{48}$$

$$(x,t) \in \Gamma \times (\varepsilon, T)$$

$$\frac{\partial \delta}{\partial \eta_{A^*}}(x,t) = \begin{cases} \sum_{s=1}^{l} \delta(x, t+k_s) & \text{for } (x,t) \in \Gamma \times (\varepsilon, T-\Upsilon) \\ 0 & \text{for } (x,t) \in \Gamma \times (T-\Upsilon, T) \end{cases} \tag{49}$$

and with initial and final conditions

$$\begin{cases} \kappa(x,\varepsilon) = 0 & x \in \Omega \\ \delta(x,T) = 0 & x \in \Omega \end{cases} \tag{50}$$

then

$$r_\varepsilon(x,t) = \delta(x,t) \tag{51}$$

Setting $\varepsilon = t$ in (39) and substituting the result into (30) we obtain

$$v_0(\cdot,t) = -\lambda_2^{-1} N^{-1} \left(P(t,t), \sigma_t + r_t(\cdot,t) \right), \qquad t \in (0,T) \tag{52}$$

Let us assume that N is the identity operator on $L^2(Q)$. Then using of Schwartz's Kernel Theorem [15], it is easy to prove that the optimal feedback control (52) can be expressed in the following form

$$\begin{aligned} v_0(x,t) = -\lambda_2^{-1} \Bigg\{ & \int_\Omega K_0(x,x',t) y(x',t) dx' + \\ & + \int_{t-\Upsilon}^{t} \int_\Omega K_1(x,x',t,t') \Phi_t(x',t') dx' dt' + \\ & + \int_{t-\Upsilon}^{t} \int_\Gamma K_2(x,x',t,t') \Psi_t(x',t') d\Gamma dt' + r_t(x,t) \Bigg\} \end{aligned} \tag{53}$$

where $\{K_0, K_1, K_2\}$ is the kernel of $P(t,t)$.

5. Conclusions

The results presented in the paper can be treated as a generalization of the results concerning pointwise observation of state given by parabolic systems with the Neumann boundary conditions involving multiple time delays obtained in [11] and by the parabolic equations with the homogeneous Dirichlet boundary conditions obtained in [13] onto the case of different multiple constant time lags appearing both in the parabolic state equations and in the Neumann boundary conditions.

Sufficient conditions for the existence of a unique solution of such time lag parabolic equations with the Neumann boundary conditions involving multiple constant time lags are proved (Lemma 1 and Theorem 1). The optimal control is characterized by using the adjoint equation (Lemma 2). The necessary and sufficient conditions of optimality are derived for a linear quadratic problem (1)-(5), (17), (18) (Theorem 2). The optimal control is obtained in the feedback form (Example).

We can also obtain estimates and a sufficient condition for the boundedness of solutions for such parabolic time lag systems with specified forms of feedback control.

Finally, we can consider optimal control problems of time lag hyperbolic systems with pointwise observation of the state.

The ideas mentioned above will be developed in forthcoming papers.

References

[1] G. Knowles: Time-optimal control of parabolic systems with boundary conditions involving time delays. *J. Optimization Theory and Applications*, **25**(4), (1978), 563-574.

[2] A. Kowalewski: Optimal control with initial state not a priori given and boundary condition involving a delay. *Lecture Notes in Control and Information Sciences*, **95**, (1987), 94-108, Springer-Verlag, Berlin-Heidelberg.

[3] A. Kowalewski: Boundary control of distributed parabolic system with boundary condition involving a time-varying lag. *Int. J. Control*, **48**(6), (1988), 2233-2248.

[4] A. Kowalewski: Feedback control for a distributed parabolic system with boundary condition involving a time-varying lag. *IMA J. Mathematical Control and Information*, **7**(2), (1990), 143-157.

[5] A. Kowalewski: Optimality conditions for a parabolic time delay system. Lecture Notes in Control and Information Sciences, **144**, (1990), 174-183, Verlag, Berlin-Heidelberg.

[6] A. Kowalewski: Optimal control of parabolic systems with time-varying lags. *IMA J. Mathematical Control and Information*, **10**(2), (1993), 113-129.

[7] A. Kowalewski: Optimal control of distributed parabolic systems with multiple time time-varying lags. *Int. J. Control*, **69** (3), (1998), 361-381.

[8] A. Kowalewski: Optimizaton of parabolic systems with deviating arguments. *Int. J. Control*, **72**(11), (1999), 947-959.

[9] A. Kowalewski: Optimal control of time delay parabolic systems. *Optimization*, **50**(1-2), (2001), 205-232.

[10] A. Kowalewski: Optimal Control of Infinite Dimensional Distributed Parameter Systems with Delays. University of Mining and Metallurgy Press, Cracow 2001.

[11] A. Kowalewski: Pointwise observation of the state given by the parabolic system with boundary condition involving multiple time delays. *Archives of Control Sciences*, **26**(2), (2016), 189-197.

[12] A. Kowalewski and J. Duda: On some optimal control problem for a parabolic system with boundary condition involving a time-varying lag. *IMA J. Mathematical Control and Information*, **9**(2), (1992), 131-146.

[13] J.L. Lions: Optimal control of systems governed by partial differential equations. Springer-Verlag, Berlin-Heidelberg, 1971.

[14] J.L. LIONS and E. MAGENES: Non-homogeneous boundary value problems and applications. **1** and **2**, Springer-Verlag, Berlin-Heidelberg, 1972.

[15] L. SCHWARTZ: Teorie de Distributions. Hermann, Paris, 1957.

[16] P.K.C. WANG: Optimal control of parabolic systems wih boundary conditions involving time delays. *SIAM J. Control*, **13**(2), (1975), 274-293.

[17] K.H. WONG: Optimal control computation for parabolic systems with boundary conditions involving time delays. *J. Optimization Theory and Applications*, **53**(3), (1987), 475-507.

Archives of Control Sciences
Volume 27(LXIII), 2017
No. 1*, pages 91–118*

New perspectives of analog and digital simulations of fractional order systems

ABDELFATAH CHAREF, MOHAMED CHAREF, ABDELBAKI DJOUAMBI and ALINA VODA

In the recent decades, fractional order systems have been found to be useful in many areas of physics and engineering. Hence, their efficient and accurate analog and digital simulations and numerical calculations have become very important especially in the fields of fractional control, fractional signal processing and fractional system identification. In this article, new analog and digital simulations and numerical calculations perspectives of fractional systems are considered. The main feature of this work is the introduction of an adjustable fractional order structure of the fractional integrator to facilitate and improve the simulations of the fractional order systems as well as the numerical resolution of the linear fractional order differential equations. First, the basic ideas of the proposed adjustable fractional order structure of the fractional integrator are presented. Then, the analog and digital simulations techniques of the fractional order systems and the numerical resolution of the linear fractional order differential equation are exposed. Illustrative examples of each step of this work are presented to show the effectiveness and the efficiency of the proposed fractional order systems analog and digital simulations and implementations techniques.

Key words: adjustable fractional operators, Charef approximation, fractional differential equation, fractional integrator, fractional systems

1. Introduction

The subject of fractional order systems has gained considerable importance in the recent decades due mainly to their numerous applications in various fields of applied science and engineering [10], [23], [24], [33]. Nowadays well known concepts in the fields of control system, signal processing and identification are being extended for the development of their fractional order counterparts as emerging topics [2], [12], [30], [31], [34]. Hence, the fractional order systems efficient, reliable and accurate simulations and numerical calculations have become very important research topics. The considerable

A. Charef (corresponding author; e-mail: afcharef@yahoo.com) and M. Charef are with Laboratoire de Traitement du Signal Département d'Electronique, Université des Frères Mentouri - Constantine, Route Ain El-bey, Constantine 25011, Algeria. A. Djouambi is with Département d'Electronique, Université Larbi Ben M'Hidi, Oum-El-Bouaghi 04000, Algeria. A. Voda is with Université Grenoble Alpes, CNRS, GIPSA-lab, F-38000 Grenoble, France.

Received 19.01.2017.

attention given to such systems is to establish a fractional system theory so it may be accessible to the general science and engineering communities.

A major problem with fractional systems is their time domain simulations which are more difficult compared to the regular systems because they are basically infinite dimensional systems due to their fractional orders. This is challenging and researchers working in this domain have developed different interesting methods to simulate them. There are broadly two major approaches for the time domain simulations of the fractional order systems: analytical and numerical methods. The purpose of the analytical method is to obtain an explicit expression for the general responses of the fractional order systems. Yet, analytical responses are often not simple to obtain. Only some closed form analog or digital approximation expressions of the responses of the fractional systems have been developed [3], [4], [5], [14], [16], [20], [25], [27], [28]. On the contrary, the goal of the numerical method is the development of a robust and stable numerical scheme for the responses of the fractional order systems. A great deal of effort has been expended in this research axis leading to a variety of techniques. But, there is no proposed efficient numerical method which simultaneously achieves speed, accuracy, and ease of simulation. Two types of numerical approaches have been developed for the simulation of the fractional order systems. The first method is based on the digital approximation of the irrational analog transfer function of the fractional order system leading to a recurrent equation. The digital approximation can be obtained by indirect or direct discretization. In indirect discretization technique two steps are required, first analog frequency domain fitting of the irrational analog transfer function is made then one of the s to z transform methods such as Euler, Tustin or Al-Alaoui is used for the discretization. The direct discretization method is based on the application of power series in the z domain of the Euler operator, Tustin operator or Al-Alaoui operator to the fractional differentiation of the irrational analog transfer function of the fractional system [1], [9], [15], [17], [18], [24], [29], [36]. The most used direct discretization is the Grunwald-Letnikov definition of the fractional differentiation [24]. Fractional differential equations have also been the focus of many mathematicians. Consequently, considerable attention has been given to their numerical solutions [11], [19], [21], [22], [32], [35]. However, these methods may not be interesting from an engineering approach at least in terms of simulation and implementation of fractional systems.

In this article, new simulations and numerical calculations perspectives of the fractional order systems based on an adjustable fractional order structure of the fractional integrator are considered. First, using Charef's approximation method [6], we will derive an adjustable fractional order rational function approximation of the analog fractional integrator s^{-m} (m is any real positive number) where the poles of the rational function are calculated only one time for $m = 0.5$, which means that they are completely independent of the parameter m [7]. Analog and digital simulation structures made up of two parts will be derived to simulate the fractional order integrator s^{-m} for any real positive number m. The right part is a fixed structure designed only once for $m = 0.5$ and it will be used for any fractional order $m > 0$. The left part is a structure composed of an ensemble of functions depending on the fractional order m only. Then, the proposed simulation structure of the fractional integrator will be used to derive analog and digital simulations of the fractional order systems represented by linear fractional differential equations. At last, the numerical solution of the linear fractional order differential equations is obtained. Illustrative examples of this work are presented to show the effectiveness and the efficiency of the proposed analog and digital simulations techniques and resolution of the fractional order systems.

2. Fractional order integrator: adjustable fractional order structure

The analog fractional order integrator is represented by the following irrational transfer function:

$$G_I(s) = \frac{1}{s^m}, \quad \text{for} \quad m > 0. \tag{1}$$

In a given frequency band of interest $[\omega_L, \omega_H]$ and a given integer number N, the rational function approximation of the fractional order operator $G_I(s)$ can be expressed by the following equation [6], [8], [13]:

$$G_I(s) = \frac{1}{s^m} \cong \frac{1}{(\omega_c)^m} \frac{\prod_{i=1}^{N-1}\left[1+\frac{s}{z_i(m)}\right]}{\prod_{i=1}^{N}\left[1+\frac{s}{p_i(m)}\right]} \tag{2}$$

the poles $p_i(m)$ (for $i = 1, 2, \ldots, N$) and the zeros $z_i(m)$ (for $i = 1, 2, \ldots, (N-1)$) of the above approximation are given as:

$$p_i(m) = \omega_c 10^{\left(\frac{2i-1-m}{m(1-m)}\right)\varepsilon}, \quad z_i(m) = \omega_c 10^{\left(\frac{2i-1+m}{m(1-m)}\right)\varepsilon} \tag{3}$$

where

$$\varepsilon = \frac{m(1-m)}{2\left(N+\frac{1-m}{2}\right)}\left[\log_{10}(\omega_{\max}/\omega_c)\right]$$

is the approximation error and the frequencies ω_c and $\omega_{\max}$ such that $\omega_c = \gamma\omega_L$ (for $10^{-5} \leqslant \gamma \leqslant 1$) and $\omega_{\max} = \theta\omega_H$ (for $1 \leqslant \theta \leqslant 10^5$).

The rational function of equation (2) can be decomposed as:

$$G_I(s) = \frac{1}{s^m} \cong \sum_{i=1}^{N} \frac{h_i(m)}{\left(1+\frac{s}{p_i(m)}\right)} \tag{4}$$

where the residues $h_i(m)$ (for $i = 1, 2, \ldots, N$) are calculated as:

$$h_i(m) = \frac{1}{(\omega_c)^m} \frac{\prod_{j=1}^{N-1}\left(1-\frac{p_i(m)}{z_j(m)}\right)}{\prod_{\substack{j=1\\ j\neq i}}^{N}\left(1-\frac{p_i(m)}{p_j(m)}\right)}. \tag{5}$$

The adjustable fractional order structure of the rational function approximation of the fractional integrator is realized such that all the poles p_i (for $i = 1,2,\dots,N$) are completely independent of the fractional order m. It has been shown in [7] that the best value of the parameter m used to calculate the poles $p_i(m)$ is $m = 0.5$. So, equation (4) is rewritten as:

$$G_I(s) = \frac{1}{s^m} \cong \sum_{i=1}^{N} \frac{h_i(m)}{\left(1+\frac{s}{p_i}\right)} \tag{6}$$

where the poles $p_i = p_i(m = 0.5)$ (for $i = 1,2,\dots,N$) are given as:

$$p_i = \omega_c 10^{(8i-6)\,\varepsilon}. \tag{7}$$

In the rational function approximation of equation (2), the error and the frequency ω_c normally depend on the fractional order m. But, ε) and ω_c are calculated for $m = 0.5$ which means that $\varepsilon = \varepsilon(0.5)$ and $\omega_c = \omega_c(0.5)$. For $m \neq 0.5$, $\varepsilon(m)$ and $\omega_c(m)$ have to be adjusted to guarantee that $p_1(0.5) = p_1(m)$. From [6], $\varepsilon(m) = 4m(1-m)\varepsilon$ and $\omega_c(m) = \omega_c 10^{[4m-2]\varepsilon}$. So, the fixed poles p_i (for $i = 1,2,\dots,N$) and the zeros $z_i(m)$ (for $i = 1,2,\dots,(N-1)$) of equation (3) are given as:

$$p_i = \omega_c 10^{(8i-6)\,\varepsilon}, \quad z_i(m) = \omega_c 10^{(8i-4+4m)\,\varepsilon}. \tag{8}$$

Then, using the expressions of the poles and the zeros of equation (8) the residues $h_i(m)$ (for $i = 1,2,\dots,N$) of equation (5) are derived as:

$$h_i(m) = \frac{1}{\left[\omega_c 10^{(4m-2)\,\varepsilon}\right]^m} \frac{\prod\limits_{j=1}^{N-1}\left(1-10^{8(i-j-m)\,\varepsilon}\right)}{\prod\limits_{\substack{j=1^N \\ j\neq i}}\left(1-10^{8(i-j)\,\varepsilon}\right)}. \tag{9}$$

2.1. Adjustable fractional order structure recap

In a given frequency band of interest $[\omega_L, \omega_H]$ and a given integer number N, we have:

$$G_I(s) = \frac{1}{s^m} \cong \sum_{i=1}^{N} \frac{h_i(m)}{\left(1+\frac{s}{p_i}\right)}, \quad \text{for } m > 0 \tag{10}$$

the fixed poles p_i and the residues $h_i(m)$ (for $i = 1,2,\dots,N$) of the approximation are given as:

$$p_i = \omega_c 10^{(8i-6)\,\varepsilon}, \quad h_i(m) = \frac{1}{\left[\omega_c 10^{(4m-2)\,\varepsilon}\right]^m} \frac{\prod\limits_{j=1}^{N-1}\left(1-10^{8(i-j-m)\,\varepsilon}\right)}{\prod\limits_{\substack{j=1^N \\ j\neq i}}\left(1-10^{8(i-j)\,\varepsilon}\right)} \tag{11}$$

where $\varepsilon = \frac{1}{(8N+2)}\left[\log_{10}\left(\frac{\omega_{\max}}{\omega_c}\right)\right]$, $\omega_c = \gamma\omega_L$, $(10^{-5} \leqslant \gamma \leqslant 1)$ and $\omega_{\max} = \theta\omega_H$, $(1 \leqslant \theta \leqslant 10^5)$.

2.2. Analog simulation

The rational function approximation of the fractional integrator s^{-m} of equation (10) is:

$$\frac{Y(s)}{E(s)} = G_I(s) = \frac{1}{s^m} \cong \sum_{i=1}^{N} \frac{h_i(m)}{\left(1+\frac{s}{p_i}\right)}. \tag{12}$$

The output of the fractional integrator is then given by:

$$Y(s) = \sum_{i=1}^{N} \frac{h_i(m)}{1+\frac{s}{p_i}} E(s) = \sum_{i=1}^{N} (h_i(m)E(s)) \frac{1}{1+\frac{s}{p_i}} = \sum_{i=1}^{N} V_i(s) \tag{13}$$

with

$$V_i(s) = (h_i(m)E(s)) \left(\frac{1}{1+\frac{s}{p_i}}\right), \quad \text{for } i = 1,2,\ldots,N.$$

In the time domain, for $i = 1,2,\ldots,N$, $v_i(t)$ is simulated by the first order differential equation

$$\frac{dv_i(t)}{dt} = -p_i v_i(t) + p_i (h_i(m)e(t)).$$

Then the analog simulation of the fractional order integrator s^{-m} is given as:

$$\left\{ \begin{array}{l} y(t) = \displaystyle\sum_{i=1}^{N} v_i(t) \\ \dfrac{dv_i(t)}{dt} = -p_i v_i(t) + (p_i h_i(m))\ e(t) \end{array} \right\}, \quad \text{for } m > 0 \text{ and } i = 1,\ 2,\ \ldots,\ N \tag{14}$$

Fig. 1 shows the analog simulation of the fractional integrator s^{-m} using equation (14). The right part of the simulation structure representing the second expression of equation (14) is a fixed structure made of first order sub-systems which are completely independent of the fractional order m. So, it can be used for the simulation of the fractional integrator of any fractional order $m > 0$. The left part is a structure composed of an ensemble of functions depending on the fractional order m only.

2.3. Digital simulation

The analog simulation of the fractional integrator s^{-m} is given in equation (14). So, the digital simulation of the fractional integrator can be obtained from equation (14) as follows:

$$y(k) = \sum_{i=1}^{N} v_i(k) \tag{15}$$

and from the second expression of equation (14), we have (for $i = 1,2,\ldots,N$):

$$V_i(s) = \frac{1}{1+\frac{s}{p_i}} (h_i(m))\, E(s). \tag{16}$$

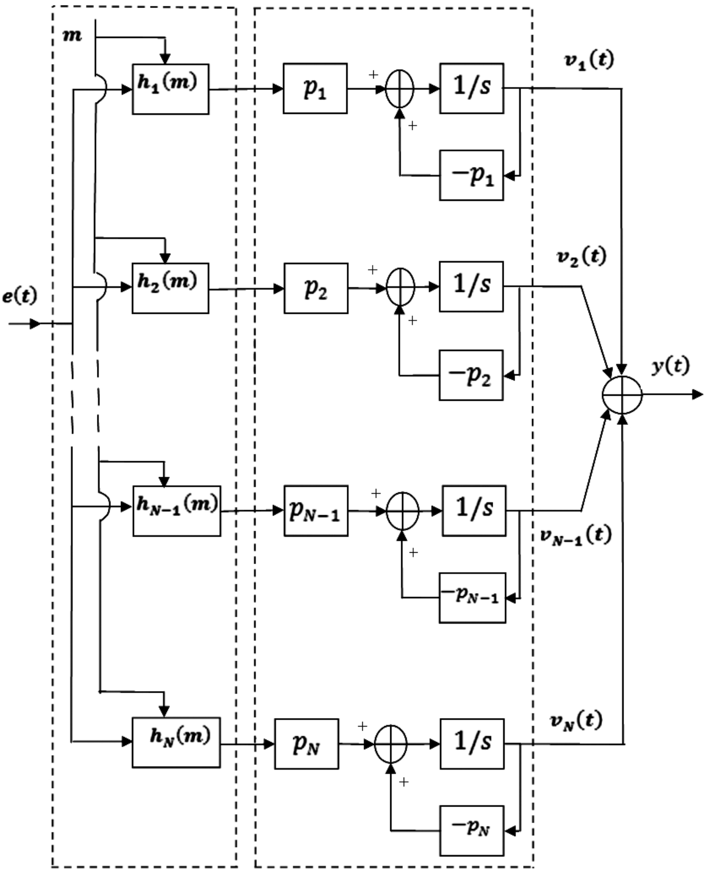

Figure 1: Proposed analog simulation of the fractional integrator s^{-m} $(m > 0)$

The $\mathcal{Z}$ transform of the analog transfer function

$$\frac{1}{1+\frac{s}{p_i}}, \quad \text{for } \ i = 1,2,\ldots,N \tag{17}$$

of equation (16) with zero order hold (ZOH) is obtained as follows [26]:

$$\mathcal{Z}\left\{(ZOH)\left(\frac{1}{1+\frac{s}{p_i}}\right)\right\} = (1-z^{-1})\mathcal{Z}\left\{\frac{1}{s\left(1+\frac{s}{p_i}\right)}\right\} = \frac{(1-\delta_i)z^{-1}}{1-\delta_i z^{-1}} \tag{18}$$

where $\delta_i = exp(-Tp_i)$ (for $i = 1,2,\ldots,N$) with T the sampling period. So, from equations (16) and (18) we can write that (for $i = 1,2,\ldots,N$):

$$V_i(z) = \left(\frac{(1-\delta_i)z^{-1}}{1-\delta_i z^{-1}}\right)(h_i(m))\,E(z). \tag{19}$$

Rearranging equation (19), we will get (for $i = 1,2,\ldots,N$):

$$V_i(z) = \delta_i z^{-1} V_i(z) + (1-\delta_i)\ (h_i(m))\ \left(z^{-1}E(z)\right). \tag{20}$$

In the time domain, $v_i(k)$ (for $i = 1,2,\ldots,N$) is given as:

$$v_i(k) = \delta_i v_i(k-1) + \ (h_i(m))\,(1-\delta_i)\ e(k-1) \tag{21}$$

Then, the digital simulation of the fractional integrator s^{-m} (for $m > 0$) is given as follows:

$$\begin{cases} y(k) = \sum\limits_{i=1}^{N} v_i(k) \\ v_i(k) = \delta_i v_i(k-1) + \ (h_i(m))\,(1-\delta_i)\ e(k-1)\ , \quad \text{for } i = 1,\ 2,\ \ldots,\ N \end{cases} \tag{22}$$

Fig. 2 shows the digital simulation of the fractional integrator s^{-m} (for $m > 0$). Because it is derived from the analog one the digital simulation structure is also made of two parts. The right part representing the second expression of equation (22) is a fixed structure which can be used for the digital simulation of the fractional integrator of any fractional order $m > 0$. The left part is a structure composed of the same ensemble of functions of the analog structure.

2.4. Illustrative example

To show the effectiveness and the usefulness of the proposed method, we will consider the rational function approximation of the analog fractional order integrators $s^{-0.63}$ and $s^{-1.74}$ in the frequency band $[\omega_L,\ \omega_H] = [0.001\,\text{rad/s},\ 100\,0\,\text{rad/s}]$ for $N = 20$. From equation (10), we get:

$$\frac{1}{\mathrm{s}^{0.63}} \cong \sum_{\mathrm{i}=1}^{20} \frac{\mathrm{h_i}(0.63)}{1+\frac{s}{p_i}} \tag{23}$$

$$\frac{1}{s^{1.74}} \cong \sum_{i=1}^{20} \frac{h_i(1.74)}{1+\frac{s}{p_i}}. \tag{24}$$

For $\omega_c = 0.001$, $\omega_L = 10^{-6}$ and $\omega_{\max} = 1000$ and $\omega_H = 10^6$ we have $\varepsilon = 0.0741$. Then, from equation (11), the poles and the residues (for $i = 1,2,\ldots,20$) are:

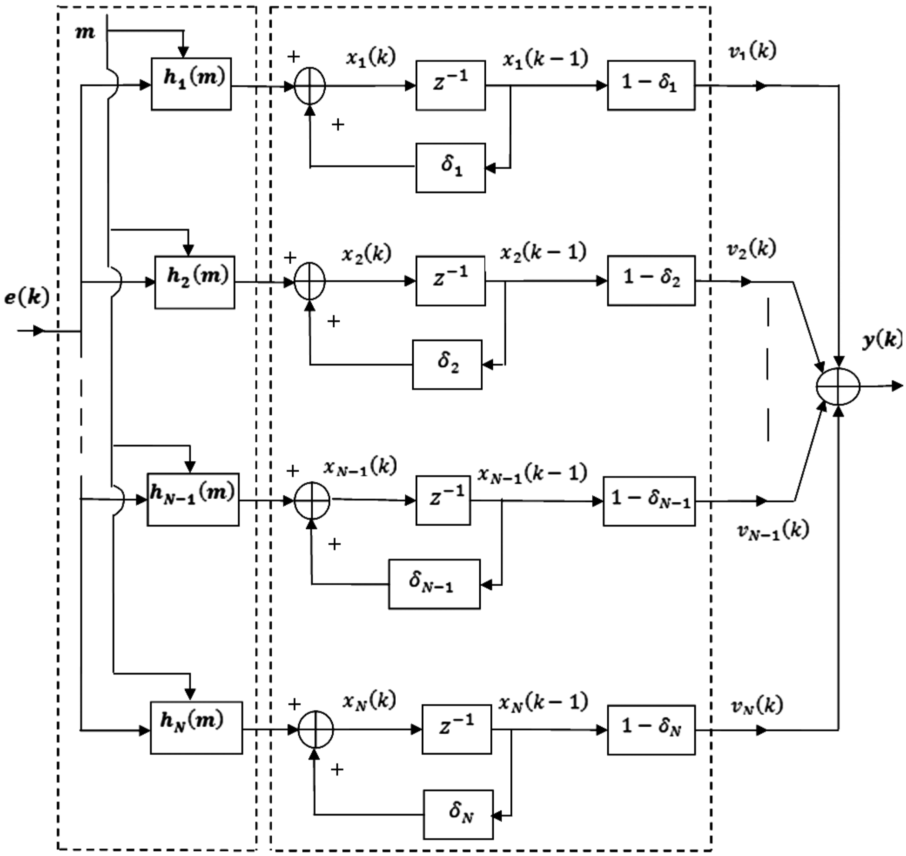

Figure 2: Proposed digital simulation of the fractional integrator s^{-m} $(m > 0)$

$$p_i = 10^{(0.5928i\ -6.4446)} \tag{25}$$

$$h_i(0.63) = (1.7550\,e-4)\left[\frac{\prod\limits_{j=1}^{19}\left(1-10^{0.5928(i\ -j\ -0.63)}\right)}{\prod\limits_{\substack{j=1\\ j\neq i}}^{20}\left(1-10^{0.5928(i\ -j)}\right)}\right] \tag{26}$$

$$h_i(1.74) = (1.5823e-10)\left[\frac{\prod\limits_{j=1}^{19}\left(1-10^{0.5928(i\ -j\ -1.74)}\right)}{\prod\limits_{\substack{j=1\\ j\neq i}}^{20}\left(1-10^{0.5928(i\ -j)}\right)}\right]. \tag{27}$$

We note that for both fractional order integrators $s^{-0.63}$ and $s^{-1.74}$, the poles of their rational function approximations are the same only the residues are different. In this example, we emphasize that for any fractional order integrator s^{-m} $(m > 0)$ the poles of its rational function approximation will be the ones of equation (25). Figs. 3 and 4 show the Bode plots of the ideal analog fractional order integrators $s^{-0.63}$ and $s^{-1.74}$ and of their rational function approximations of equations (23) and (24).

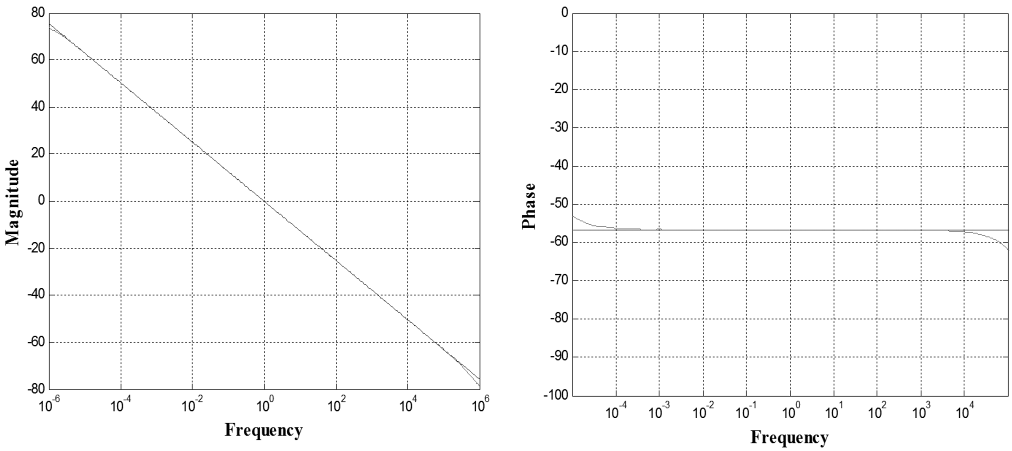

Figure 3: Bode plot of the fractional integrator $s^{-0.63}$ and its rational function approximation

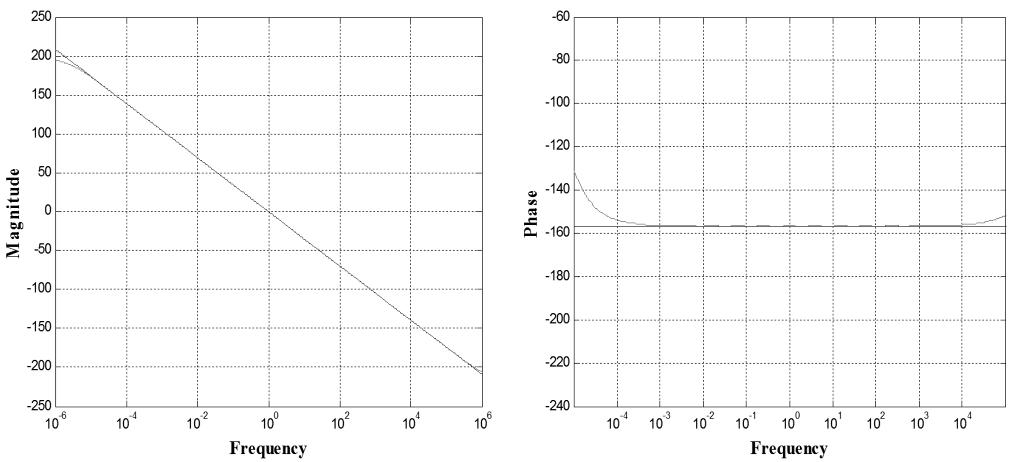

Figure 4: Bode plot of the fractional integrator $s^{-1.74}$ and its rational function approximation

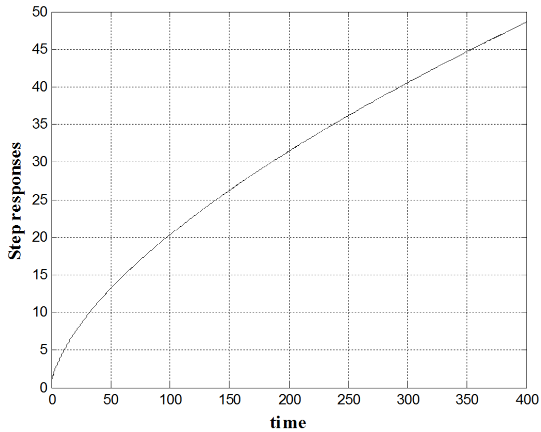

Figure 5: Step responses of the fractional order integrators $s^{-0.63}$ using MATLAB function `fode_sol()` and the proposed approximation structure

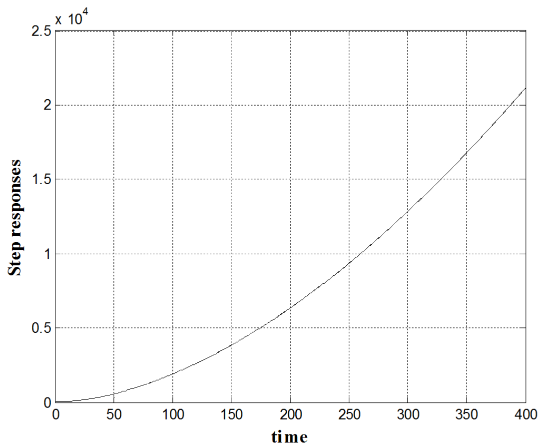

Figure 6: Step responses of the fractional order integrators $s^{-1.74}$ using MATLAB function `fode_sol()` and the proposed approximation structure

From Figs 3 and 4, we can easily see that the Bode plots of the ideal analog fractional order integrators $s^{-0.63}$ and $s^{-1.74}$ and their corresponding rational function approximations are quite overlapping in the frequency band of interest $[\omega_L, \omega_H] = [0.001\,\text{rad/s}, 100\,0\,\text{rad/s}]$. Figs 5 and 6 show the step responses of the fractional integrators $s^{-0.63}$ and $s^{-1.74}$ using the MATLAB function `fode_sol()` based on the Grunwald-Letnikov's fractional differentiation definition for the numerical solution of the linear fractional differential equation [24] and using the proposed approximation structure. The equations used for the step responses are given as:

Fractional order integrator $s^{-0.63}$

- using MATLAB function `fode_sol()` [24]:

  solve the fractional differential equation $\frac{d^{0.63}y(t)}{dt^{0.63}} = u(t)$ to get the step response of the fractional integrator $s^{-0.63}$ as:

  ```
  a = [1]; na = [0.63]; b = [1]; nb = [0]; t = 0 : 0.1 : 4001;
  u = ones(size(t)),
  y = fode_sol(a, na, b, nb, u, t)
  ```

- using the proposed approximation structure:

  For $i = 1, 2, \ldots, 20$, solve the 20 regular first order differential equations:

$$\begin{cases} \frac{dv_i(t)}{dt} & = & -10^{(0.5928i\ -\ 6.4446\ )}\ v_i(t) + \\ & + & 10^{(0.5928i\ -\ 10.2003\ )} \dfrac{\prod_{j=1}^{19}\left(1-10^{0.5928(i\ -j\ -0.63)}\right)}{\prod_{\substack{j=1\\ j\neq i}}^{20}\left(1-10^{0.5928(i\ -j)}\right)}\ e(t) \\ y(t) & = & \sum_{i=1}^{20} v_i(t) \end{cases}$$

Fractional order integrator $s^{-1.74}$

- using MATLAB function `fode_sol()` [24]:

  solve the fractional differential equation $\frac{d^{1.74}y(t)}{dt^{1.74}} = u(t)$ to get the step response of the fractional integrator $s^{-1.74}$ as:

  ```
  a = [1]; na = [1.74]; b = [1]; nb = [0]; t = 0 : 0.1 : 4001;
  u = ones(size(t)),
  y = fode_sol(a, na, b, nb, u, t)
  ```

- using the proposed approximation structure:

  For $i = 1, 2, \ldots, 20$, solve the 20 regular first order differential equations:

$$\begin{cases} \frac{dv_i(t)}{dt} & = & -10^{(0.5928i\ -\ 6.4446\ )}\ v_i(t) + \\ & + & 10^{(0.5928i\ -\ 16.2447\ )} \dfrac{\prod_{j=1}^{19}\left(1-10^{0.5928(i\ -j\ -1.74)}\right)}{\prod_{\substack{j=1\\ j\neq i}}^{20}\left(1-10^{0.5928(i\ -j)}\right)}\ e(t) \\ y(t) & = & \sum_{i=1}^{20} v_i(t) \end{cases}$$

From Figs. 5 and 6, we can easily see that the step responses of fractional integrators $s^{-0.63}$ and $s^{-1.74}$ using the proposed simulation structure and the MATLAB function `fode_sol()` are exactly the same.

3. Linear fractional order system: New structure

A linear single input single output (SISO) fractional order system is described by the following linear fractional order differential equation [24]:

$$\sum_{i=0}^{L} a_i D^{\alpha_i} y(t) = \sum_{j=0}^{M} b_j D^{\beta_j} e(t) \tag{28}$$

where $e(t)$ is the input, $y(t)$ is the output, the derivative orders α_i $(0 \leqslant i \leqslant L)$ and β_i $(0 \leqslant j \leqslant M-1)$ are constant real positive numbers such that $\alpha_{L-1} < \cdots < \alpha_1 < \alpha_0$, $\beta_{M-1} < \cdots < \beta_1 < \beta_0$, $\beta_0 \leqslant \alpha_0$, and $\alpha_L = \beta_M = 0$; the model parameters a_i $(1 \leqslant i \leqslant L)$ and b_i $(0 \leqslant j \leqslant M)$ are constant real numbers with $a_0 = 1$. With zero initial conditions, the fractional system transfer function is given as [24]:

$$G(s) = \frac{Y(s)}{E(s)} = \frac{\sum\limits_{j=0}^{M} b_j s^{\beta_j}}{\sum\limits_{i=0}^{L} a_i s^{\alpha_i}}. \tag{29}$$

From equation (29), we can write:

$$G(s) = \frac{Y(s)}{E(s)} = \frac{\sum\limits_{j=0}^{M} b_j s^{\beta_j}}{s^{\alpha_0} + \sum\limits_{i=1}^{L} a_i s^{\alpha_i}}. \tag{30}$$

So, we will have:

$$\left[s^{\alpha_0} + \sum_{i=1}^{L} a_i s^{\alpha_i} \right] Y(s) = \left[\sum_{j=0}^{M} b_j s^{\beta_j} \right] E(s) \tag{31}$$

$$s^{\alpha_0} Y(s) = -\left[\sum_{i=1}^{L} a_i s^{\alpha_i} \right] Y(s) + \left[\sum_{j=0}^{M} b_j s^{\beta_j} \right] E(s). \tag{32}$$

$Y(s)$ can then be obtained as:

$$Y(s) = -\left[\sum_{i=1}^{L} a_i \frac{1}{s^{\alpha_0 - \alpha_i}} \right] Y(s) + \left[\sum_{j=0}^{M} b_j \frac{1}{s^{\alpha_0 - \beta_j}} \right] E(s). \tag{33}$$

From section 2.1, in a given frequency band of interest $[\omega_L, \omega_H]$ and a given integer number N, the fractional order integrators $\frac{1}{s^{\alpha_0-\alpha_i}}$ and $\frac{1}{s^{\alpha_0-\beta_j}}$, for $i = 1,2,\dots,L$ and for $j = 0,2,\dots,M$, are approximated as:

$$\frac{1}{s^{\alpha_0-\alpha_i}} \cong \sum_{q=1}^{N} \frac{h_q(\alpha_0-\alpha_i)}{(1+s/p_q)} \tag{34}$$

$$\frac{1}{s^{\alpha_0-\beta_j}} \cong \sum_{q=1}^{N} \frac{h_q(\alpha_0-\beta_j)}{(1+s/p_q)} \tag{35}$$

The poles p_q and the residues $h_q(\sigma)$ (for $q = 1,2,\dots,N$ and $\sigma = (\alpha_0 - \alpha_i)$ or $\sigma = (\alpha_0 - \beta_j)$) are given as:

$$p_q = \omega_c 10^{(8q-6)\,\varepsilon}, \quad h_q(\sigma) = \frac{1}{\left[\omega_c 10^{(4\sigma-2)\,\varepsilon}\right]^{\sigma}} \frac{\prod\limits_{p=1}^{N-1}\left(1-10^{8(q-p-\sigma)\,\varepsilon}\right)}{\prod\limits_{\substack{p=1\\p\neq q}}^{N}\left(1-10^{8(q-p)\,\varepsilon}\right)} \tag{36}$$

where $\varepsilon = \frac{1}{(8N+2)}\left[\log_{10}(\omega_{\max}/\omega_c)\right]$, $\omega_c = \gamma\omega_L$, $(10^{-5} \leqslant \gamma \leqslant 1)$ and $\omega_{\max} = \theta\omega_H$, $(1 \leqslant \theta \leqslant 10^5)$.

Then equation (33) can be rewritten as:

$$Y(s) = -\left[\sum_{i=1}^{L} a_i \sum_{q=1}^{N} \frac{h_q(\alpha_0-\alpha_i)}{1+\frac{s}{p_q}}\right] Y(s) + \left[\sum_{j=0}^{M} b_j \sum_{q=1}^{N} \frac{h_q(\alpha_0-\beta_j)}{1+\frac{s}{p_q}}\right] E(s) \tag{37}$$

$$Y(s) = -\sum_{q=1}^{N}\left(\sum_{i=1}^{L} a_i h_q(\alpha_0 - \alpha_i)\right)\left(\frac{Y(s)}{1+\frac{s}{p_q}}\right) + \sum_{q=1}^{N}\left(\sum_{j=0}^{M} b_j h_q(\alpha_0 - \beta_j)\right)\left(\frac{E(s)}{1+\frac{s}{p_q}}\right) \tag{38}$$

$$Y(s) = \sum_{q=1}^{N} (A_q Y(s))\left(\frac{1}{1+\frac{s}{p_q}}\right) + \sum_{q=1}^{N} (B_q E(s))\left(\frac{1}{1+\frac{s}{p_q}}\right) \tag{39}$$

where the coefficients A_q and B_q, for $q = 1,2,\dots,N$, are given by the following expressions:

$$\begin{aligned} A_q &= -\sum_{i=1}^{L} a_i h_q(\alpha_0-\alpha_i) \\ B_q &= \sum_{j=0}^{M} b_j h_q(\alpha_0-\beta_j). \end{aligned} \tag{40}$$

3.1. Analog simulation

A linear SISO fractional order system is described by the linear fractional order differential equation of equation (28) as:

$$\sum_{i=0}^{L} a_i D^{\alpha_i} y(t) = \sum_{j=0}^{M} b_j D^{\beta_j} e(t). \tag{41}$$

From equation (39), its solution is given by the following expression:

$$Y(s) \;=\; \sum_{q=1}^{N} \left[A_q Y(s) + B_q E(s)\right] \left(\frac{1}{1+\frac{s}{p_q}}\right) = \sum_{q=1}^{N} V_q(s) \tag{42}$$

where the variables $V_q(s)$, for $q = 1, 2, \ldots, N$, are defined as follows:

$$V_q(s) \;=\; \left(A_q Y(s) + B_q E(s)\right) \left(\frac{1}{1+\frac{s}{p_q}}\right). \tag{43}$$

So, in the time domain, each variable $v_q(t)$ (for $q = 1, 2, \ldots, N$) is the solution of the following first order differential equation:

$$\frac{dv_q(t)}{dt} = -\,p_q v_q(t) + p_q\left(A_q y(t) + B_q e(t)\right). \tag{44}$$

Hence, from equations (42) and (44), the analog simulation of the linear SISO fractional order system described by the linear fractional order differential equation of equation (41) is given by:

$$\begin{cases} y(t) = \displaystyle\sum_{q=1}^{N} v_q(t) \\ \dfrac{dv_q(t)}{dt} = -p_q v_q(t) + p_q\left(A_q y(t) + B_q e(t)\right), \text{ for } \; q = 1,\ 2,\ \ldots,\ N \end{cases} \tag{45}$$

Fig. 7 shows the proposed analog simulation using equation (45) of the linear SISO fractional order system described by the linear fractional order differential equation of equation (41). The right part of Fig. 7 of the proposed simulation structure representing the second expression of equation (45) is a fixed structure made of first order sub-systems which are completely independent of the fractional orders α_i $(0 \leqslant i \leqslant L)$ and β_i $(0 \leqslant j \leqslant M)$ of the linear fractional order differential equation of equation (41). Then, this right part of the proposed analog simulation can be used for the simulation of any linear SISO fractional order system described by the linear fractional order differential equation of equation (41). The left part of Fig. 7 is an ensemble of functions depending only on the derivative orders α_i $(0 \leqslant i \leqslant L)$ and β_i $(0 \leqslant j \leqslant M)$ and the model coefficients a_i (for $0 \leqslant i \leqslant L$) and b_i $(0 \leqslant j \leqslant M)$ of equation (41).

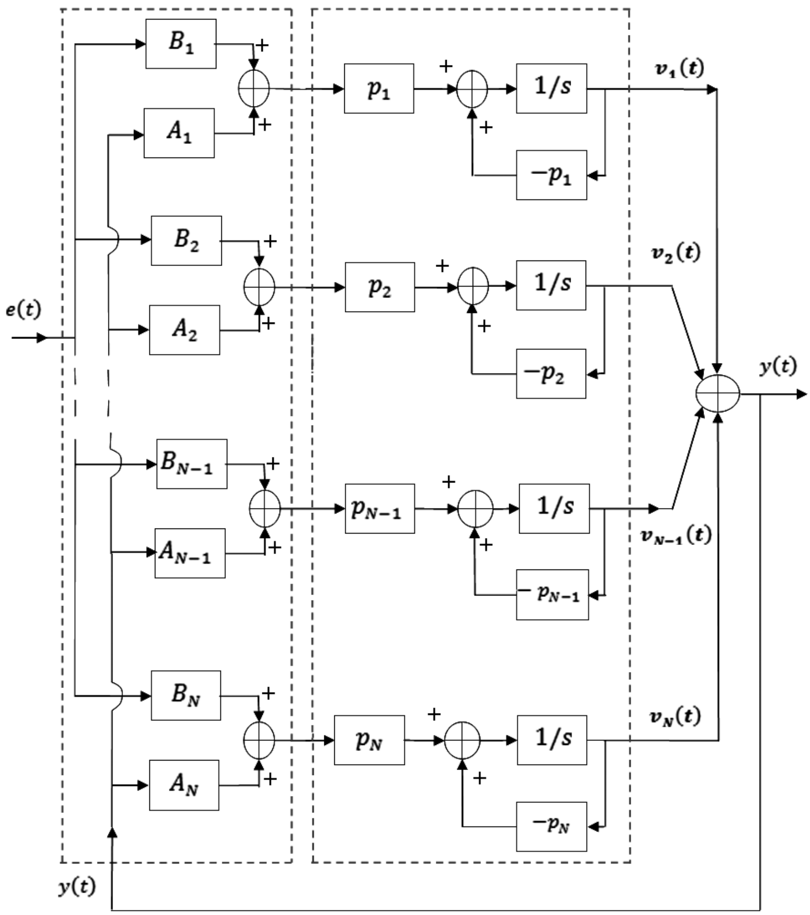

Figure 7: Analog simulation structure of the linear SISO fractional order system

3.2. Numerical resolution of the linear fractional differential equation

A linear SISO fractional system is described by the linear fractional differential equation of equation (28) as:

$$\sum_{i=0}^{L} a_i D^{\alpha_i} y(t) = \sum_{j=0}^{M} b_j D^{\beta_j} e(t). \tag{46}$$

The analog solution of the above differential equation is given by equation (42) as:

$$Y(s) \;=\; \sum_{q=1}^{N} V_q(s) \tag{47}$$

where the variables $V_q(s)$, for $q = 1, 2, \ldots, N$, are given from equation (43) by the expression:

$$V_q(s) \;=\; [\,A_q Y(s) + B_q E(s)]\;\frac{1}{1+\frac{s}{p_q}}. \tag{48}$$

The $\mathcal{Z}$ transform of the analog transfer function $\frac{1}{1+\frac{s}{p_q}}$ (for $q = 1, 2, \ldots, N$) of equation (48) with zero order hold (ZOH) is then obtained as follows [26]:

$$\mathcal{Z}\left\{(ZOH)\left(\frac{1}{1+\frac{s}{p_q}}\right)\right\} = (1-z^{-1})\mathcal{Z}\left\{\frac{1}{s\left(1+\frac{s}{p_q}\right)}\right\} = \frac{(1-\delta_q)z^{-1}}{1-\delta_q z^{-1}} \tag{49}$$

where $\delta_q = \exp(-Tp_q)$ (for $i = q, 2, \ldots, N$) and T is the sampling period. So, from equation (48) we can write that (for $q = 1, 2, \ldots, N$):

$$V_q(z) = (A_q Y(z) + B_q E(z))\left(\frac{(1-\delta_q)z^{-1}}{1-\delta_q z^{-1}}\right). \tag{50}$$

Rearranging equation (50), we will get (for $q = 1, 2, \ldots, N$):

$$V_q(z) = \delta_q z^{-1} V_q(z) + (1-\delta_q)\;\left(A_q z^{-1} Y(z) + B_q z^{-1} E(z)\right). \tag{51}$$

In the time domain, $v_q(k)$ (for $q = 1, 2, \ldots, N$) is given as:

$$V_q(z) = \delta_q z^{-1} V_q(z) + (1-\delta_q)\;\left(A_q z^{-1} Y(z) + B_q z^{-1} E(z)\right). \tag{52}$$

So, the numerical solution of the linear fractional order differential equation of equation (46) is obtained from equations (47) and (52) as follows:

$$\begin{cases} v_q(k) = \delta_q v_q(k-1) + (1-\delta_q)\;\left(A_q y(k-1) + B_q e(k-1)\right), \quad \text{for } q = 1,\ 2,\ \ldots,\ N \\ y(k) = \displaystyle\sum_{q=1}^{N} v_q(k) \end{cases} \tag{53}$$

where, for $q = 1, 2, \ldots, N$, $A_q = -\sum_{i=1}^{L} a_i h_q(\alpha_0 - \alpha_i)$, $B_q = \sum_{j=0}^{M} b_j h_q(\alpha_0 - \beta_j)$ and $\delta_q = \exp(-Tp_q)$. The parameters p_q and $h_q(\sigma)$ (for $q = 1, 2, \ldots, N$) and $\sigma = (\alpha_0 - \alpha_\mathrm{i})$ or $\sigma = (\alpha_0 - \beta_j)$ (for $i = 1, 2, \ldots, L$ and for $j = 0, 2, \ldots, M$) are obtained for a given frequency band of interest $[\omega_L, \omega_H]$ and a given integer number N as follows:

$$p_q = \omega_c 10^{(8q-6)\,\varepsilon}, \quad h_q(\sigma) = \frac{1}{\left[\omega_c 10^{(4\sigma-2)\,\varepsilon}\right]^{\sigma}}\;\frac{\displaystyle\prod_{p=1}^{N-1}\left(1-10^{8(q-p-\sigma)\,\varepsilon}\right)}{\displaystyle\prod_{\substack{p=1\\p\neq q}}^{N}\left(1-10^{8(q-p)\,\varepsilon}\right)} \tag{54}$$

where $\varepsilon = \frac{1}{(8N+2)}\left[\log_{10}\left(\frac{\omega_{\max}}{\omega_c}\right)\right]$, $\omega_c = \gamma\omega_L$ $(10^{-5} \leqslant \gamma \leqslant 1)$ and $\omega_{\max} = \theta\omega_H$ $(1 \leqslant \theta \leqslant 10^5)$.

3.3. Digital simulation

A linear SISO fractional order system is described by the linear fractional order differential equation of equation (46) as:

$$\sum_{i=0}^{L} a_i D^{\alpha_i} y(t) = \sum_{j=0}^{M} b_j D^{\beta_j} e(t) \tag{55}$$

The numerical solution of the above differential equation can be obtained from equation (47) as:

$$Y(z) \ = \ \sum_{q=1}^{N} V_q(z) \tag{56}$$

where the variables $V_q(z)$, for $q = 1, 2, \ldots, N$, are given from equation (50) by the expressions:

$$V_q(z) = (A_q Y(z) + B_q E(z)) \left(\frac{(1-\delta_q)z^{-1}}{1-\delta_q z^{-1}} \right). \tag{57}$$

Rearranging equation (57), we will get (for $i = 1, 2, \ldots, N$):

$$\frac{V_q(z)}{A_q Y(z) + B_q E(z)} = \frac{(1-\delta_q)\, z^{-1}}{1-\delta_q z^{-1}}. \tag{58}$$

The variables $X_q(z)$, for $q = 1, 2, \ldots, N$, are such that the above equation can be rewritten as :

$$\frac{V_q(z)}{X_q(z)} \cdot \frac{X_q(z)}{(A_q Y(z) + B_q E(z))} = \frac{(1-\delta_q)\, z^{-1}}{1-\delta_q z^{-1}}. \tag{59}$$

Let $\frac{V_q(z)}{X_q(z)} = (1-\delta_q)\, z^{-1}$ and $\frac{X_q(z)}{\left(A_q Y(z)+B_q E(z)\right)} = \frac{1}{1-\delta_q z^{-1}}$, we will then have:

$$V_q(z) = (1-\delta_q)\, z^{-1} X_q(z), \quad \left(1-\delta_q z^{-1}\right) X_q(z) = \left(A_q Y(z) + B_q E(z) \right). \tag{60}$$

So, in the time domain, (for $i = 1, 2, \ldots, N$), we will get:

$$v_q(k) \ = (1-\delta_q)\, x_q(k-1), \quad x_q(k) = \delta_q x_q(k-1) + \left(A_q y(k) + B_q e(q) \right). \tag{61}$$

Hence, from equations (56) and (60), the digital simulation of the linear SISO fractional order system described by the linear fractional order differential equation of equation (55) is given by:

$$\begin{cases} y(k) = \displaystyle\sum_{q=1}^{N} v_q(k) \\ \begin{cases} v_q(k) \ = (1-\delta_q)\, x_q(k-1) \\ x_q(k) = \delta_q x_q(k-1) + \left(A_q y(k) + B_q e(k) \right) \end{cases} \quad \text{for } \ q = 1,\ 2,\ \ldots,\ N \end{cases} \tag{62}$$

Fig. 8 shows the proposed digital simulation using equation (62) of the linear SISO fractional order system described by the differential equation of equation (55). This digital simulation structure is also made of two parts as the analog one. The right part, a structure of parallel first order sub-systems representing the two last expressions of equation (62), is completely independent of the fractional orders α_i $(0 \leqslant i \leqslant L)$ and β_i $(0 \leqslant j \leqslant M)$ of the linear fractional order differential equation of equation (55). Because it is fixed, this part can be used for the digital simulation of any linear SISO fractional system described by the linear fractional order differential equation of equation (55). The left part of Fig. 8 is the same structure of the analog simulation of Fig. 7.

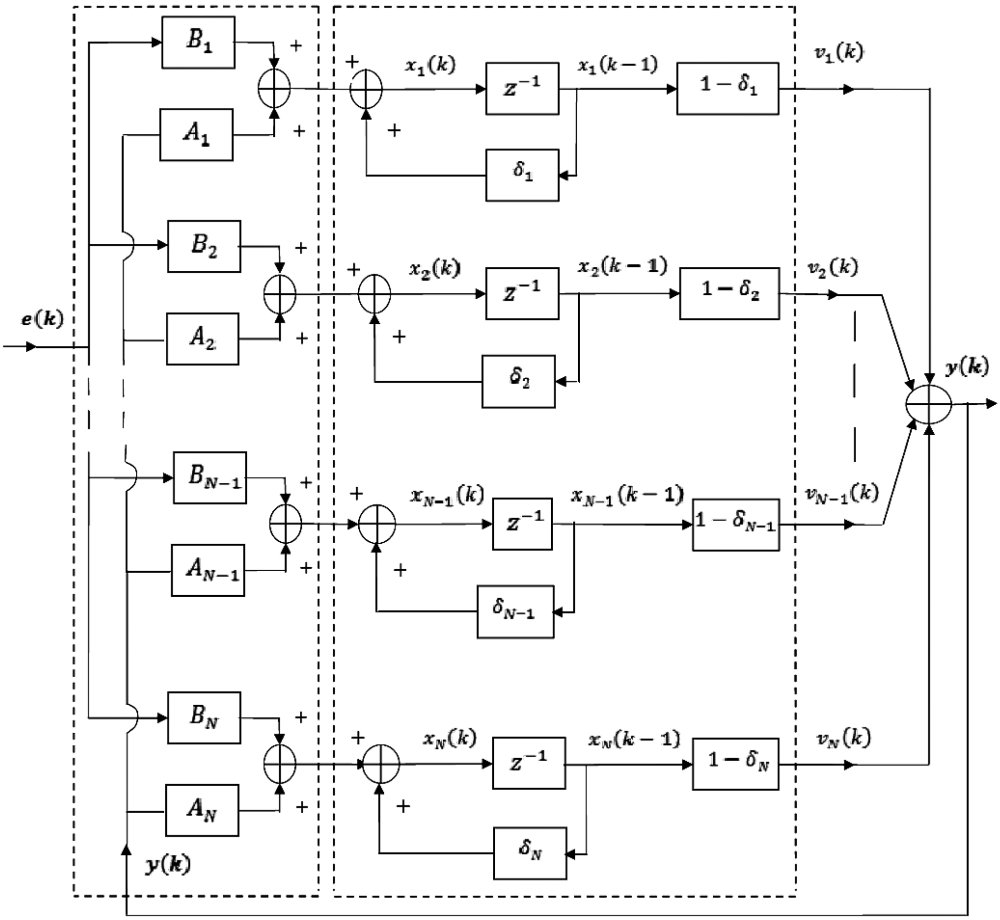

Figure 8: Digital simulation structure of the linear SISO fractional order system

3.4. Illustrative examples

In the first example we will consider a linear SISO fractional order system described by the following linear fractional order differential equation:

$$D^{\sqrt{5}}y(t)+20\,D^{\sqrt{3}}y(t)+3\,D^{0.85}y(t)+2y(t)=3\,D^{1.36}e(t)+8e(t). \tag{63}$$

Using Laplace transform of the above linear fractional order differential equation with zero initial conditions, we will get:

$$\left(s^{\sqrt{5}}+20s^{\sqrt{3}}+3s^{0.85}+2\right)Y(s)=\left(3\,s^{1.36}+8\right)E(s) \tag{64}$$

$$\begin{aligned} Y(s) \;&=\; -\left(20\frac{1}{s^{\left(\sqrt{5}-\sqrt{3}\right)}}+3\frac{1}{s^{\left(\sqrt{5}-0.85\right)}}+2\frac{1}{s^{\left(\sqrt{5}\right)}}\right)Y(s)\\ &+\;\left(3\frac{1}{s^{\left(\sqrt{5}-1.36\right)}}+8\frac{1}{s^{\left(\sqrt{5}\right)}}\right)E(s). \end{aligned} \tag{65}$$

In the frequency band $[\omega_{\mathrm{L}},\,\omega_{\mathrm{H}}]=[0.001\text{ rad/s},\,10000\text{ rad/s}]$ and for $N=22$. The rational function approximation of the fractional integrators $\frac{1}{s^{\left(\sqrt{5}-\sqrt{3}\right)}}$, $\frac{1}{s^{\left(\sqrt{5}-0.85\right)}}$, $\frac{1}{s^{\sqrt{5}}}$ and $\frac{1}{s^{\left(\sqrt{5}-1.36\right)}}$ are given as:

$$\begin{aligned} &\frac{1}{s^{\left(\sqrt{5}-\sqrt{3}\right)}}\cong\sum_{q=1}^{22}\frac{h_q\left(\sqrt{5}-\sqrt{3}\right)}{1+\frac{s}{p_q}}, && \frac{1}{s^{\left(\sqrt{5}-0.85\right)}}\cong\sum_{q=1}^{22}\frac{h_q\left(\sqrt{5}-0.85\right)}{1+\frac{s}{p_q}}\\ &\frac{1}{s^{\left(\sqrt{5}\right)}}\cong\sum_{q=1}^{22}\frac{h_q\left(\sqrt{5}\right)}{1+\frac{s}{p_q}}, && \frac{1}{s^{\left(\sqrt{5}-1.36\right)}}\cong\sum_{q=1}^{22}\frac{h_q\left(\sqrt{5}-1.36\right)}{1+\frac{s}{p_q}}. \end{aligned} \tag{66}$$

We note that all the poles of the rational function approximation of the above four analog fractional order integrators are the same.

For $\omega_c=0.0005\omega_L=5.0\cdot10^{-7}$ and $\omega_{\max}=100\omega_H=10^6$, $\varepsilon=0.0691$, the poles p_q and residues $h_q\left(\sqrt{5}-\sqrt{3}\right)$, $h_q\left(\sqrt{5}-0.85\right)$, $h_q\left(\sqrt{5}\right)$ and $h_q\left(\sqrt{5}-1.36\right)$ (for $1\leqslant q\leqslant 22$) are given as:

$$p_q=10^{(0.5529q\;-6.7156)}$$

$$h_q\left(\sqrt{5}-\sqrt{3}\right)=\left(1.4972\cdot10^4\right)\frac{\prod\limits_{p=1}^{21}\left(1-10^{0.5529\left(q-p-\sqrt{5}+\sqrt{3}\right)}\right)}{\prod\limits_{\substack{p=1\\p\neq q}}^{22}\left(1-10^{0.5529(q-p)}\right)}$$

$$h_q\left(\sqrt{5}-0.85\right) = \left(2.4783 \cdot 10^{8}\right) \frac{\prod\limits_{p=1}^{21}\left(1-10^{0.5529\left(q-p-\sqrt{5}+0.85\right)}\right)}{\prod\limits_{\substack{p=1\\ p\neq q}}^{22}\left(1-10^{0.5529(q-p)}\right)}$$

$$h_q\left(\sqrt{5}\right) = \left(1.0386 \cdot 10^{13}\right) \frac{\prod\limits_{p=1}^{21}\left(1-10^{0.5529\left(q-p-\sqrt{5}\right)}\right)}{\prod\limits_{\substack{p=1\\ p\neq q}}^{22}\left(1-10^{0.5529(q-p)}\right)}$$

$$h_q\left(\sqrt{5}-1.36\right) = \left(2.6857 \cdot 10^{5}\right) \frac{\prod\limits_{p=1}^{21}\left(1-10^{0.5529\left(q-p-\sqrt{5}+1.36\right)}\right)}{\prod\limits_{\substack{p=1\\ p\neq q}}^{22}\left(1-10^{0.5529(q-p)}\right)}$$

Hence, the analog simulation of the linear SISO fractional order system described by the linear fractional order differential equation of equation (63) is given by:

$$\begin{cases} y(t) = \sum\limits_{q=1}^{N} v_q(t) \\ \dfrac{dv_q(t)}{dt} = -p_q v_q(t) + p_q\left(A_q y(t) + B_q e(t)\right), \quad \text{for} \quad \mathrm{q} = 1, 2, \ldots, 22 \end{cases} \tag{67}$$

where, for $1 \leqslant q \leqslant 22$, p_q is as above; A_q and B_q are given as:

$$A_q = -\left\{\begin{array}{l} 20\left[\left(1.4972 \cdot 10^{4}\right) \dfrac{\prod\limits_{p=1}^{21}\left(1-10^{0.5529\left(q-p-\sqrt{5}+\sqrt{3}\right)}\right)}{\prod\limits_{\substack{p=1\\ p\neq q}}^{22}\left(1-10^{0.5529(q-p)}\right)}\right] + \\ 3\left[\left(2.4783 \cdot 10^{8}\right) \dfrac{\prod\limits_{p=1}^{21}\left(1-10^{0.5529\left(q-p-\sqrt{5}+0.85\right)}\right)}{\prod\limits_{\substack{p=1\\ p\neq q}}^{22}\left(1-10^{0.5529(q-p)}\right)}\right] + \\ 2\left[\left(1.0386 \cdot 10^{13}\right) \dfrac{\prod\limits_{p=1}^{21}\left(1-10^{0.5529\left(q-p-\sqrt{5}\right)}\right)}{\prod\limits_{\substack{p=1\\ p\neq q}}^{22}\left(1-10^{0.5529(q-p)}\right)}\right] \end{array}\right\} =$$

$$= \frac{\left\{\begin{array}{l}\left[\left(2.9944\cdot 10^{5}\right)\prod\limits_{p=1}^{21}\left(1-10^{0.5529\left(q-p-\sqrt{5}+\sqrt{3}\right)}\right)\right]+\\ \left[\left(4.9944\cdot 10^{8}\right)\prod\limits_{p=1}^{21}\left(1-10^{0.5529\left(q-p-\sqrt{5}+0.85\right)}\right)\right]+\\ \left[\left(2.0772\cdot 10^{13}\right)\prod\limits_{p=1}^{21}\left(1-10^{0.5529\left(q-p-\sqrt{5}\right)}\right)\right]\end{array}\right\}}{\prod\limits_{\substack{p=1\\ p\neq q}}^{22}\left(1-10^{0.5529(q-p)}\right)}$$

$$B_q = \left\{\begin{array}{l} 3\left[\left(2.6857\cdot 10^{5}\right)\dfrac{\prod\limits_{p=1}^{21}\left(1-10^{0.5529\left(q-p-\sqrt{5}+1.36\right)}\right)}{\prod\limits_{\substack{p=1\\ p\neq q}}^{22}\left(1-10^{0.5529(q-p)}\right)}\right]+\\ 8\left[\left(1.0386\cdot 10^{13}\right)\dfrac{\prod\limits_{p=1}^{21}\left(1-10^{0.5529\left(q-p-\sqrt{5}\right)}\right)}{\prod\limits_{\substack{p=1\\ p\neq q}}^{22}\left(1-10^{0.5529(q-p)}\right)}\right]\end{array}\right\} =$$

$$= \frac{\left\{\begin{array}{l}\left[\left(4.9944\cdot 10^{8}\right)\prod\limits_{p=1}^{21}\left(1-10^{0.5529\left(q-p-\sqrt{5}+1.36\right)}\right)\right]+\\ \left[\left(8.0571\cdot 10^{9}\right)\prod\limits_{p=1}^{21}\left(1-10^{0.5529\left(q-p-\sqrt{5}\right)}\right)\right]\end{array}\right\}}{\prod\limits_{\substack{p=1\\ p\neq q}}^{22}\left(1-10^{0.5529(q-p)}\right)}$$

The numerical solution of the differential equation of equation (63) is given as follows:

$$\left\{\begin{array}{l} y(k) = \sum\limits_{q=1}^{N} v_q(k) \\ v_q(k) = -\delta_q v_q(k-1) + (1-\delta_q)\,\left(A_q y(k-1) + B_q e(k-1)\right), \quad \text{for } q = 1,\ 2,\ \ldots, 22 \end{array}\right. \tag{68}$$

where, for a sampling period $T = 0.002$ s $\delta_q = \exp\left(-T p_q\right) = \exp\left(-10^{(0.5529q-9.4146)}\right)$ (for $1 \leqslant q \leqslant 22$). Fig. 9 shows the step responses of the linear SISO fractional order system described by the linear fractional order differential equation of equation (63) using the MATLAB function `fode_sol()` [4] and using the proposed approximation structure of equation (68).

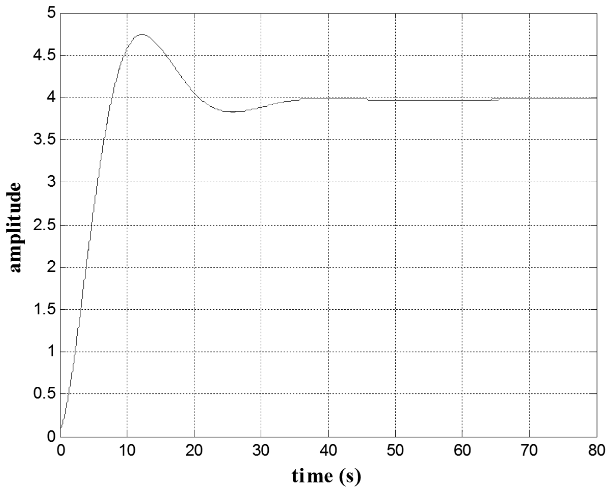

Figure 9: Step responses of the fractional order system of eqn. (63) using the proposed structure and the MATLAB function `fode_sol()`

- using MATLAB function `fode_sol()` [24]:

  for $e(t) = u(t)$, the step response of the linear fractional order differential equation of equation (63) is obtained as:

```
a=[1 20 3 2];    na=[sqrt(5) sqrt(3) 0.85 0];    b=[3 8];
nb=[1.36 0];t=0:0.002:80;u=ones (size(t))

y = fode_sol(a,na,b,nb,u,t)
```

  The digital simulation of the linear SISO fractional order system described by the linear fractional order differential equation of equation (63) is given by:

$$\begin{cases} \begin{cases} v_q(k) = (1-\delta_q)x_q(k-1) \\ x_q(k) = -\delta_q x_q(k-1) + (\,A_q y(k) + B_q e(k)) \end{cases}, \quad \text{for} \quad q = 1,\ 2,\ \ldots, 22 \\ y(k) = \sum_{q=1}^{N} v_q(k) \end{cases} \tag{69}$$

  where, for $1 \leqslant q \leqslant 22$, δ_q, A_q and B_q are as above; and the sampling period $T = 0.002$ s.
  In the second example a more oscillatory linear SISO fractional order system

is considered. It is described by the following linear fractional order differential equation:

$$D^{2.45}y(t)+10\,D^{1.87}y(t)+D^{0.58}y(t)+10\,y(t)=10\,e(t) \tag{70}$$

whose transfer function is given as:

$$H(s)=\frac{Y(s)}{E(s)}=\frac{10}{s^{2.45}+10\,s^{1.87}+s^{0.58}+10}. \tag{71}$$

For $N=22$ and for $[\omega_L,\omega_H]=[0.01\text{rad/s } 1000\text{rad/s}]$ the parameters ω_c, $\omega_{\max}$ and ε are:

$$\omega_c=0.005\omega_L=5\cdot 10^{-5},\quad \omega_{\max}=100\omega_H=10^6,\quad \varepsilon=0.0579$$

Then, for a sampling period $T=0.002$ s, the numerical solution of the linear fractional order differential equation of equation (70) is given as follows:

$$\begin{cases} v_q(k)=-\delta_q v_q(k-1)+(1-\delta_q)\left(A_q y(k-1)+B_q e(k-1)\right), \text{ for } q=1,\ 2,\ \ldots,\ 22 \\ y(k)=\sum\limits_{q=1}^{N} v_q(k) \end{cases} \tag{72}$$

where, for $1\leqslant q\leqslant 22$, δ_q, A_q and B_q are given as:

$$\delta_q=\exp(-Tp_q),\ \ A_q=-\left\{h_q(0.58)+h_q(1.87)+10h_q(2.45)\right\},\ \ B_q=10h_q(2.45)$$

with

$$p_q=10^{(0.4630q-4.6482)}$$

$$h_q(0.58)=(3.0472\cdot 10^2)\frac{\prod\limits_{p=1}^{21}\left(1-10^{0.4630(q-p-0.58)}\right)}{\prod\limits_{\substack{p=1\\p\neq q}}^{22}\left(1-10^{0.4630(q-p)}\right)}$$

$$h_q(1.87)=(2.8177\cdot 10^7)\frac{\prod\limits_{p=1}^{21}\left(1-10^{0.4630(q-p-1.87)}\right)}{\prod\limits_{\substack{p=1\\p\neq q}}^{22}\left(1-10^{0.4630(q-p)}\right)}$$

$$h_q(2.45)=(2.7008\cdot 10^9)\frac{\prod\limits_{p=1}^{21}\left(1-10^{0.4630(q-p-2.45)}\right)}{\prod\limits_{\substack{p=1\\p\neq q}}^{22}\left(1-10^{0.4630(q-p)}\right)}$$

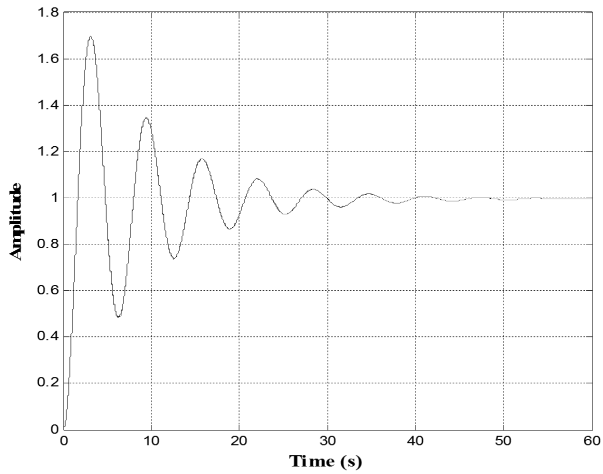

Figure 10: Step responses of the fractional order system of eqn. (70) using the proposed structure and the MATLAB function `fode_sol()`

Fig. 10 shows the step responses of the linear SISO fractional order system of equation (70) using the MATLAB function `fode_sol()` [24] and using the proposed approximation structure of equation (72).

- using MATLAB function `fode_sol()` [24]:

for $e(t) = u(t)$, the step response of the linear fractional order differential equation of equation (70) is obtained as:

```
a=[1 10 1 10]; na=[2.45 1.87 0.58 0]; b=[1 0]; nb=[0];
t=0:0.002:60;u=ones (size(t))

y = fode_sol(a,na,b,nb,u,t)
```

4. Conclusion

In this paper, an original structure of the fractional order integrator has been presented to facilitate the analog and the digital simulations of the fractional order integrators and systems as well as the numerical resolution of the linear fractional order differential equations. The proposed simulation structure of the fractional integrator s^{-m} is composed of two parts. The right part is a fixed structure made of parallel first order regular systems which are completely independent of the fractional order m designed only once for $m = 0.5$. So, this part can be used for the simulation of the fractional integrator of any fractional order $m > 0$. The left part is a structure composed of an ensemble of functions depending on the fractional order m only. Then, the proposed fractional order integrator structure has been extended to the analog and digital simulations as well as the resolution of the linear fractional order systems described by the linear fractional order differential equation $\sum_{i=0}^{L} a_i D^{\alpha_i} y(t) = \sum_{j=0}^{M} b_j D^{\beta_j} e(t)$. The analog or digital simulation structures obtained are also composed of two connected parts. The right part is exactly the right part of the fractional order integrator. In this case it is also completely independent of the fractional orders α_i $(0 \leqslant i \leqslant L)$ and β_i $(0 \leqslant j \leqslant M)$ of the above differential equation; so it can be used for the simulation of any linear SISO fractional order system described by the linear fractional order differential equation. The left part is an ensemble of functions depending on the derivative orders α_i $(0 \leqslant i \leqslant L)$ and β_i $(0 \leqslant j \leqslant M)$ and the model coefficients a_i (for $1 \leqslant i \leqslant L$) and b_i $(0 \leqslant j \leqslant M)$ of the above differential equation.

Some illustrative examples have been presented to show the efficiency and the effectiveness of the proposed simulations and resolution techniques. The step responses of the fractional integrator and the fractional order system using the proposed method are compared to those obtained using the Grunwald-Letnikov's fractional derivative definition. The comparison results were very satisfactory.

It is also worth mentioning that the proposed structures have practical significance to circuit designers who would be interested in the hardware implementation of the linear fractional order operators and systems in the fields of control system, signal processing and identification. In the future, the use of the proposed fractional order integrator structure for the simulation of variable order integrators and systems will be investigated.

References

[1] M. Aoun, R. Malti, F. Levron and A. Oustaloup: Numerical simulations of fractional systems: An overview of existing methods and improvements. *Nonlinear Dynamics*, **38** (2004), 117-131.

[2] D. Baleanu, J.A.T Machado and A.C.J. Luo (Eds.): Fractional Dynamics and Control. Springer-Verlag, New York, 2012.

[3] D. Boucherma, A. Charef, H. Nezzari: The solution of state space linear fractional system of commensurate order with complex eigenvalues using regular exponential and trigonometric functions. *Int. J. of Dynamics and Control*, **5**(1), (2017), 79-94.

[4] A. Charef: Modeling and analog realization of the fundamental linear fractional order differential equation. *Nonlinear Dynamics*, **46** (2006), 195-210.

[5] A. Charef and H. Nezzari: On the fundamental linear fractional order differential Eequation. *Nonlinear Dynamics*, **65** (2011), 335-348.

[6] A. CHAREF: Analogue realization of fractional order integrator, differentiator and fractional $PI^{\lambda}D^{\mu}$ controller. *IEE Proc. on Control Theory and Applications*, **153** (2006), 714-720.

[7] A. CHAREF and D. IDIOU: Design of analog variable fractional order differentiator and integrator. *Nonlinear Dynamics*, **69** (2012), 1577-1588.

[8] A. CHAREF, H.H. SUN, Y.Y. TSAO and B. ONARAL: Fractal system as represented by singularity function. *IEEE Trans. on Automatic Control*, **37** (1992), 1465-1470.

[9] Y.Q. CHEN and B.M. VINAGRE: A new IIR-type digital fractional order differentiator. *Signal Processing*, **83** (2003), 2359-2365.

[10] M. DALIR and M. BASHOUR: Applications of fractional calculus. *Applied Mathematical Sciences*, **4** (2010), 1021-1032.

[11] S.K. DAMARLA and M. KUNDU: Numerical solution of multi order fractional differential equations using generalized triangular function operational matrices. *Applied Mathematics and Computation*, **263** (2015), 189-203.

[12] S. DAS and I. PAN (EDS.): Fractional Order Signal Processing: Introductory Concepts and Applications. Springer, New York, 2012.

[13] A. DJOUAMBI, A. CHAREF and T. BOUKTIR: Fractional order robust control and $PI^{\lambda}D^{\mu}$ controllers. *WSEAS Trans. on Circuits and Systems*, **8** (2005), 850-857.

[14] R. GARRA and F. POLITO: Analytic solutions of fractional differential equations by operational methods. *Applied Mathematics and Computation*, **218** (2012), 10642-10646.

[15] K. HAMDAOUI and A. CHAREF: A new discretization method for fractional order differentiators via bilinear transformation. *15th Int. Conf. on Digital Signal Processing*, (2007), 280-283.

[16] Y. HU, Y. LUO and Z. LU: Analytical solution of the linear fractional differential equation by Adomian decomposition method. *J. of Computational and Applied Mathematics*, **215** (2008), 220-229.

[17] C.X. JIANG, J.E. CARLETTA, T.T HARTLEY and R.J. VEILLETTE: A systematic approach for implementing fractional-order operators and systems. *IEEE J. on Emerging and Selected Topics in Circuits and Systems*, **3** (2013), 301-312.

[18] T. KACZOREK: Realization problem for fractional continuous time systems. *Archives of Control Sciences*, **18**(1), (2008), 43-58.

[19] M.M. KHADER: A new fractional Chebyshev FDM: an application for solving the fractional differential equations generated by optimization problem. *Int. J. of Systems Science*, **46** (2015), 2598-2606.

[20] S. KUMAR, K. SINGH and R. SAXENA: Closed-form analytical expression of fractional order differentiation in fractional Fourier transform domain. *Circuits, Systems, and Signal Processing*, **32** (2012), 1875-1889.

[21] C. LI, Y. LI, A. CHEN and J. YE: Numerical approaches to fractional calculus and fractional ordinary differential equation. *J. of Computational Physics*, **230** (2011), 3352-3368.

[22] X. LI: Numerical solution of fractional differential equations using cubic B-spline wavelet collocation method. *Communications in Nonlinear Science and Numerical Simulation*, **17** (2012), 3934-3946.

[23] R.L. MAGIN: Fractional calculus in bioengineering. Begell House, Redding, 2006.

[24] A. MONJE, Y.Q. CHEN, B.M. VINAGRE, D. XUE and V. FELLIN: Fractional-order Systems and Controls Fundamentals and Applications. Springer, London, 2010.

[25] Z.M. OBIDAT: Analytic study on linear systems of fractional differential equations. *Computers and Mathematics with Applications*, **59** (2010), 1171-1183.

[26] K. OGATA: Discrete-time control systems. Prentice Hall. Englewood Cliffs, 1987.

[27] K. OPRZEDKIEWICZ: Approximation method for a fractional order transfer function with zero and pole. *Archives of Control Sciences*, **24**(4), (2014), 447-463.

[28] G. OTURANC, A. KURNAZ and Y. KESKIN: A new analytical approximate method for the solution of fractional differential equations. *Int. J. of Computer Mathematics*, **85** (2008), 131-142.

[29] A. OUSTALOUP: La Commande CRONE, Editions Hermés, Paris, 1991.

[30] F. PADULA and A. VASIOLI: Advances in Robust Fractional Control. Springer, New York, 2015.

[31] I. PETRAS: Fractional-Order Nonlinear Systems: Modeling, Analysis and Simulation. Springer-Verlag, Berlin, 2011.

[32] A. SAADATMANDIA and M. DEHGHANB: A new operational matrix for solving fractional order differential equations. *Computers and Mathematics with Applications*, **59** (2010), 1326-1336.

[33] J. SABATIER, O.P. AGRAWAL and J.A. TENREIRO MACHADO(EDS.): Advances in Fractional Calculus: Theoretical Development and Applications in Physics and Engineering. Springer, Dordrecht, 2007.

[34] H. SHENG, Y.Q. CHEN and T.S QIU: Fractional Processes and Fractional-Order Signal Processing: Techniques and Applications. Springer-Verlag, Berlin, 2012.

[35] M.P. TRIPATHI, V.K. BARANWAL, R.K. PANDEY and O.P. SINGH: A new numerical algorithm to solve fractional differential equations based on operational matrix of generalized hat functions. *Communications in Nonlinear Science and Numerical Simulation*, **18** (2013), 1327-1340.

[36] C.C. TSENG: Design of FIR and IIR fractional order Simpson digital integrators. *Signal Processing*, **87** (2007), 1045-1057.

Archives of Control Sciences
Volume 27(LXIII), 2017
No. 1*, pages 119–128*

Eigenvalue assignment in fractional descriptor discrete-time linear systems

TADEUSZ KACZOREK and KAMIL BORAWSKI

The problem of eigenvalue assignment in fractional descriptor discrete-time linear systems is considered. Necessary and sufficient conditions for the existence of a solution to the problem are established. A procedure for computation of the gain matrices is given and illustrated by a numerical example.

Key words: eigenvalue assignment, fractional, descriptor, discrete-time linear system, gain matrix.

1. Introduction

A dynamical system is called a fractional-order system if its state equations are given by fractional-order derivative of state vector. Mathematical fundamentals of the fractional calculus are given in the [23, 25, 26]. The standard and positive fractional linear systems have been investigated in [18, 24] and the positive fractional linear electrical circuits in [20]. Some recent interesting results in the fractional systems theory and its applications can be found in [8, 27, 28, 30].

Descriptor (singular) linear systems were considered in many papers and books [1-7, 9-11, 17, 18, 22, 29, 31]. The positive standard and descriptor systems and their stability have been analyzed in [13-16, 28]. Descriptor positive discrete-time and continuous-time nonlinear systems have been analyzed in [10] and the positivity and linearization of nonlinear discrete-time systems by state-feedbacks in [14]. New stability tests of positive standard and fractional linear systems have been investigated in [12]. The controllability of dynamical systems has been investigated in [21].

In this paper the eigenvalue assignment problem for fractional descriptor discrete-time linear systems will be investigated and procedure for computation of the state-feedback gain matrices will be presented.

The paper is organized as follows. In section 2 the problem of eigenvalue assignment in fractional descriptor discrete-time linear systems is formulated. In section 3 the

The authors is with Bialystok University of Technology, Faculty of Electrical Engineering, Wiejska 45D, 15-351 Bialystok, Poland. E-mail: kaczorek@ee.pw.edu.pl

This work was supported by National Science Centre in Poland under work No. 2014/13/B/ST7/03467.
Received 18.08.2016.

problem is solved and procedure for computation of the state-feedback gain matrices is presented. Concluding remarks are given in section 4.

The following notation will be used: $\Re$ — the set of real numbers, $\Re^{n\times m}$ — the set of $n\times m$ real matrices and $\Re^n = \Re^{n\times 1}$, I_n — the $n\times n$ identity matrix, Z_+ — the set of nonnegative integers.

2. Problem formulation

Consider the descriptor discrete-time linear system

$$E\Delta^{\alpha}x_{k+1} = Ax_k + Bu_k, \quad k\in Z_+ = \{0,1,\dots\} \tag{1}$$

where $x_k\in\Re^n$, $u_k\in\Re^m$ are the state and input vectors and $E,A\in\Re^{n\times n}$, $B\in\Re^{n\times m}$. The fractional difference of the order α is defined by

$$\Delta^{\alpha}x_k = \sum_{i=0}^{k}(-1)^k\begin{pmatrix}\alpha\\ i\end{pmatrix}x_{k-i}, \quad \begin{pmatrix}\alpha\\ i\end{pmatrix} = \begin{cases} 1 & \text{for} \quad i=0,\\ \frac{\alpha(\alpha-1)\dots(\alpha-i+1)}{i!} & \text{for} \quad i=1,2,\dots\end{cases} \tag{2}$$

Substituting (2) into (1) yields

$$Ex_{k+1} = A_{\alpha}x_k + \sum_{i=1}^{k+1}c_iEx_{k-i+1} + Bu_k \tag{3}$$

where

$$A_{\alpha} = A + \alpha E, \quad c_i = (-1)^i\begin{pmatrix}\alpha\\ i+1\end{pmatrix}, \quad i=1,2,\dots\,. \tag{4}$$

It is assumed that $\operatorname{rank}E = r < n$ and $\operatorname{rank}B = m$. In practical problems it is also assumed that i is bounded by natural number $h = k+1 > n$. We may write the equation (3) in the form

$$\bar{E}\bar{x}_{k+1} = \bar{A}\bar{x}_k + \bar{B}u_k, \tag{5}$$

where

$$\bar{A} = \begin{bmatrix} A_\alpha & c_1E & c_2E & \cdots & c_{h-1}E & c_hE \\ I_n & 0 & 0 & \cdots & 0 & 0 \\ 0 & I_n & 0 & \cdots & 0 & 0 \\ \vdots & \vdots & \vdots & \ddots & \vdots & \vdots \\ 0 & 0 & 0 & \cdots & I_n & 0 \end{bmatrix} \in \Re^{\bar{n}\times\bar{n}}, \quad \bar{B} = \begin{bmatrix} B \\ 0 \\ 0 \\ \vdots \\ 0 \end{bmatrix} \in \Re^{\bar{n}\times m},$$

$$\bar{E} = \begin{bmatrix} E & 0 & 0 & \cdots & 0 \\ 0 & I_n & 0 & \cdots & 0 \\ 0 & 0 & I_n & \cdots & 0 \\ \vdots & \vdots & \vdots & \ddots & \vdots \\ 0 & 0 & 0 & \cdots & I_n \end{bmatrix} \in \Re^{\bar{n}\times\bar{n}}, \quad \bar{x}_k = \begin{bmatrix} x_k \\ x_{k-1} \\ x_{k-2} \\ \vdots \\ x_{k-h} \end{bmatrix} \in \Re^{\bar{n}}, \quad k \in Z_+, \ \bar{n} = n(h+1). \tag{6}$$

Let us consider the system (1) with the state-feedback

$$\bar{u}_k = K_1\bar{x}_{k+1} + K_2\bar{x}_k \tag{7}$$

where $\bar{u}_k \in \Re^m$ is a new input vector and $K_1, K_2 \in \Re^{m\times\bar{n}}$ are gain matrices. Substitution of (7) into (5) yields

$$(\bar{E} - \bar{B}K_1)\bar{x}_{k+1} = (\bar{A} + \bar{B}K_2)\bar{x}_k. \tag{8}$$

The problem can be stated as follows. Given E, A, B, $\alpha \in (0,1)$ find K_1, K_2 such that the closed-loop system has desired eigenvalues $z_1, z_2, \ldots, z_n$, $|z_k| < 1$, $k = 1, \ldots n$.

3. Problem solution

The problem will be solved by the use of the following two steps procedure.

Step 1. (Subproblem 1) Find K_1 such that $\bar{E} - \bar{B}K_1 = I_{\bar{n}}$.

Step 2. (Subproblem 2) Find K_2 such that $\bar{A} + \bar{B}K_2$ has desired eigenvalues.

The first subproblem has a solution if and only if [3]

$$\operatorname{rank}[\ \bar{E} \quad \bar{B}\ ] = \bar{n}, \quad \operatorname{rank}\bar{B} = m. \tag{9}$$

Theorem 8 *If the conditions* (9) *are satisfied then the equation*

$$\bar{E} - \bar{B}K_1 = I_{\bar{n}} \tag{10}$$

has the solution

$$K_1 = \{[\bar{B}^T\bar{B}]^{-1}\bar{B}^T + K[I_{\bar{n}} - \bar{B}[\bar{B}^T\bar{B}]^{-1}\bar{B}^T]\}(\bar{E} - I_{\bar{n}}), \tag{11}$$

where K is an arbitrary matrix.

Proof From (10) we have

$$\bar{B}K_1 = \bar{E} - I_{\bar{n}}. \tag{12}$$

If conditions (9) are met then there exists the left pseudoinverse of the matrix $\bar{B}$ given by the formula [19]

$$\bar{B}_L = [\bar{B}^T\bar{B}]^{-1}\bar{B}^T + K[I_{\bar{n}} - \bar{B}[\bar{B}^T\bar{B}]^{-1}\bar{B}^T] \tag{13}$$

and

$$K_1 = \bar{B}_L(\bar{E} - I_{\bar{n}}) = \{[\bar{B}^T\bar{B}]^{-1}\bar{B}^T + K[I_{\bar{n}} - \bar{B}[\bar{B}^T\bar{B}]^{-1}\bar{B}^T]\}(\bar{E} - I_{\bar{n}}), \tag{14}$$

which is equivalent to (11). □

Remark 1 In particular case when $K = 0$ we have

$$K_1 = [\bar{B}^T\bar{B}]^{-1}\bar{B}^T(\bar{E} - I_{\bar{n}}) = \begin{bmatrix} [B^TB]^{-1}B^T(E - I_n) & 0 & \cdots & 0 \end{bmatrix} \tag{15}$$

and then

$$K_1\bar{x}_{k+1} = [B^TB]^{-1}B^T(E - I_n)x_{k+1}. \tag{16}$$

The second subproblem will be solved substituting (10) into (8). Thus we have

$$\bar{x}_{k+1} = (\bar{A} + \bar{B}K_2)\bar{x}_k. \tag{17}$$

Theorem 9 *There exists a matrix K_2 such that the matrix $\bar{A} + \bar{B}K_2$ has the desired eigenvalues λ_k, $k = 1, \ldots, \bar{n}$ if and only if the pair $(\bar{A}, \bar{B})$ is controllable.*

Proof The proof is given in [11].

To solve the problem one of the well-known methods [11] can be applied. To simplify the notation we consider the single-input system (17) with a controllable pair $(\bar{A}, \bar{B})$. Following [11] there exists a matrix

$$P = \begin{bmatrix} p_1 \\ p_1\bar{A} \\ \vdots \\ p_1\bar{A}^{\bar{n}-1} \end{bmatrix} \tag{18}$$

that transforms every controllable pair $(\bar{A}, \bar{B})$ to the canonical form

$$\widetilde{A} = P\bar{A}P^{-1} = \begin{bmatrix} 0 & 1 & 0 & \cdots & 0 \\ 0 & 0 & 1 & \cdots & 0 \\ \vdots & \vdots & \vdots & \ddots & \vdots \\ 0 & 0 & 0 & \cdots & 1 \\ -\widetilde{a}_0 & -\widetilde{a}_1 & -\widetilde{a}_2 & \cdots & -\widetilde{a}_{\bar{n}-1} \end{bmatrix}, \quad \widetilde{B} = P\bar{B} = \begin{bmatrix} 0 \\ 0 \\ \vdots \\ 0 \\ 1 \end{bmatrix}. \tag{19}$$

The vector p_1 in (18) is the $\bar{n}$-th row of the matrix

$$[\, \bar{B} \quad \bar{A}\bar{B} \quad \cdots \quad \bar{A}^{\bar{n}-1}\bar{B}]^{-1}. \tag{20}$$

The characteristic polynomial of the matrix $\widetilde{A}$ has the form

$$\det[I_{\bar{n}}z - \widetilde{A}] = z^{\bar{n}} + \widetilde{a}_{\bar{n}-1}z^{\bar{n}-1} + \ldots + \widetilde{a}_1 z + \widetilde{a}_0 \tag{21}$$

and the characteristic polynomial of the closed-loop system matrix $\widetilde{A} + \widetilde{B}K_2$ has the form

$$\det[I_{\bar{n}}z - \widetilde{A} - \widetilde{B}K_2] = z^{\bar{n}} + \widetilde{d}_{\bar{n}-1}z^{\bar{n}-1} + \ldots + \widetilde{d}_1 z + \widetilde{d}_0. \tag{22}$$

The matrix satisfying (22) is given by

$$K_2 = [\ \widetilde{d}_0 - \widetilde{a}_0 \quad \widetilde{d}_1 - \widetilde{a}_1 \quad \cdots \quad \widetilde{d}_{\bar{n}-1} - \widetilde{a}_{\bar{n}-1}\ ]. \tag{23}$$

The considerations can be easily extended to multi-input systems [11].

From the above we have the following procedure.

Procedure 1.

Step 1. Knowing A, B, E, α choose $h > n$ and compute the matrices $\bar{A}$, $\bar{B}$, $\bar{E}$ defined by (6).

Step 2. Check the conditions (9), then using $\bar{E}$ and $\bar{B}$ compute K_1 defined by (11). In particular case when $K = 0$ we can use matrices E and B (see (15)).

Step 3. Applying one of the well-known methods [11] and using $\bar{A}$, $\bar{B}$ compute K_2 such that the matrix $\bar{A} + \bar{B}K_2$ has the desired eigenvalues λ_k, $k = 1, \ldots, \bar{n}$, $\mathrm{Re}\,\lambda_k < 0$. The method for single-input systems presented above can be used.

Example 1 Consider the fractional descriptor discrete-time linear system (1) with the matrices

$$E = \begin{bmatrix} 1 & 0 & 0 \\ 0 & 1 & 0 \\ 0 & 0 & 0 \end{bmatrix}, \quad A = \begin{bmatrix} 0 & 1 & 0 \\ 0 & 0 & 1 \\ 1 & 0 & 0 \end{bmatrix}, \quad B = \begin{bmatrix} 0 \\ 0 \\ 1 \end{bmatrix} \tag{24}$$

and $\alpha = 0.5$. Find K_1 and K_2 such that the closed-loop system has the eigenvalues $\lambda_k = 0$, $k = 1,\dots,9$. Using the Procedure 1 we obtain the following.

Step 1. Step 1. We choose $h = 2$. From (6) we have

$$\bar{A} = \begin{bmatrix} 0.5 & 1 & 0 & 0.125 & 0 & 0 & 0.0625 & 0 & 0 \\ 0 & 0.5 & 1 & 0 & 0.125 & 0 & 0 & 0.0625 & 0 \\ 1 & 0 & 0.5 & 0 & 0 & 0 & 0 & 0 & 0 \\ 1 & 0 & 0 & 0 & 0 & 0 & 0 & 0 & 0 \\ 0 & 1 & 0 & 0 & 0 & 0 & 0 & 0 & 0 \\ 0 & 0 & 1 & 0 & 0 & 0 & 0 & 0 & 0 \\ 0 & 0 & 0 & 1 & 0 & 0 & 0 & 0 & 0 \\ 0 & 0 & 0 & 0 & 1 & 0 & 0 & 0 & 0 \\ 0 & 0 & 0 & 0 & 0 & 1 & 0 & 0 & 0 \end{bmatrix},$$
$$\bar{E} = \begin{bmatrix} 1 & 0 & 0 & 0 & 0 & 0 & 0 & 0 & 0 \\ 0 & 1 & 0 & 0 & 0 & 0 & 0 & 0 & 0 \\ 0 & 0 & 0 & 0 & 0 & 0 & 0 & 0 & 0 \\ 0 & 0 & 0 & 1 & 0 & 0 & 0 & 0 & 0 \\ 0 & 0 & 0 & 0 & 1 & 0 & 0 & 0 & 0 \\ 0 & 0 & 0 & 0 & 0 & 1 & 0 & 0 & 0 \\ 0 & 0 & 0 & 0 & 0 & 0 & 1 & 0 & 0 \\ 0 & 0 & 0 & 0 & 0 & 0 & 0 & 1 & 0 \\ 0 & 0 & 0 & 0 & 0 & 0 & 0 & 0 & 1 \end{bmatrix}, \ \bar{B} = \begin{bmatrix} 0 \\ 0 \\ 1 \\ 0 \\ 0 \\ 0 \\ 0 \\ 0 \\ 0 \end{bmatrix}. \tag{25}$$

Step 2. The conditions (9) are satisfied. Using (25) with (11) for $K = [\ 1 \ \ 0 \ \ 0 \ \ 0 \ \ 0 \ \ 0 \ \ 0 \ \ 0 \ \ 0]$ we obtain the first gain matrix

$$K_1 = [\ 0 \ \ 0 \ \ -1 \ \ 0 \ \ 0 \ \ 0 \ \ 0 \ \ 0 \ \ 0\ ]. \tag{26}$$

It is easy to check that $\bar{E} - \bar{B}K_1 = I_9$.

Step 3. Step 3. Using the presented algorithm for single-input systems we compute the matrix

$$[\ \bar{B}\quad \bar{A}\bar{B}\quad \cdots\quad \bar{A}^{\bar{n}-1}\bar{B}]^{-1} = \tag{27}$$

$$= \begin{bmatrix} 0 & 0 & 1 & -1 & 0 & -0.5 & 0 & 0 & 0 \\ 0 & 0 & 0 & 0 & 0 & -1 & -1 & 0 & -0.5 \\ -13.5 & 0.5 & 0 & 5.5 & 10.5 & -0.5 & 2.4 & 3.1 & 5.4 \\ 54 & 52 & 0 & -48 & -96 & -52 & 3.3 & 22.7 & 9.2 \\ 82 & 370 & 0 & -2 & -248 & -370 & -49.3 & -104.8 & -29.2 \\ -688 & -1656 & 0 & 376 & 1776 & 1656 & 114 & 84 & -174 \\ 384 & 1056 & 0 & -160 & -984 & -1056 & -104 & -156 & 24 \\ -1024 & -2368 & 0 & 576 & 2560 & 2368 & 160 & 112 & 224 \\ 640 & 1408 & 0 & -384 & -1600 & -1408 & -80 & -16 & 176 \end{bmatrix}$$

The vector has the form

$$p_1 = [\ 640 \quad 1408 \quad 0 \quad -384 \quad -1600 \quad -1408 \quad -80 \quad -16 \quad 176\ ]. \tag{28}$$

Using (18) we compute the matrix

$$P = \begin{bmatrix} 640 & 1408 & 0 & -384 & -1600 & -1408 & -80 & -16 & 176 \\ -64 & -256 & 0 & 0 & 160 & 256 & 40 & -88 & 40 \\ -32 & -32 & 0 & 32 & 56 & 32 & -4 & -16 & -4 \\ 16 & 8 & 0 & -8 & -20 & -8 & -2 & -2 & -2 \\ 0 & 0 & 0 & 0 & -1 & 0 & 1 & 0.5 & 1 \\ 0 & -1 & 0 & 1 & 0.5 & 1 & 0 & 0 & 0 \\ 1 & 0 & 0 & 0 & -0.1 & 0 & 0 & -0.1 & 0 \\ 0.5 & 0.9 & 0 & 0.1 & -0.1 & 0.1 & 0.1 & 0 & 0.1 \\ 0.4 & 0.9 & 1 & 0.1 & 0.1 & 0.1 & 0 & 0.1 & 0 \end{bmatrix} \tag{29}$$

which transforms the pair $(\bar{A}, \bar{B})$ to the canonical form (see (19))

$$\widetilde{A} = \begin{bmatrix} 0 & 1 & 0 & 0 & 0 & 0 & 0 & 0 & 0 \\ 0 & 0 & 1 & 0 & 0 & 0 & 0 & 0 & 0 \\ 0 & 0 & 0 & 1 & 0 & 0 & 0 & 0 & 0 \\ 0 & 0 & 0 & 0 & 1 & 0 & 0 & 0 & 0 \\ 0 & 0 & 0 & 0 & 0 & 1 & 0 & 0 & 0 \\ 0 & 0 & 0 & 0 & 0 & 0 & 1 & 0 & 0 \\ 0 & 0 & 0 & 0 & 0 & 0 & 0 & 1 & 0 \\ 0 & 0 & 0 & 0 & 0 & 0 & 0 & 0 & 1 \\ 0 & 0 & -0.002 & -0.0117 & -0.0234 & -0.0781 & 1.125 & -0.5 & 1.5 \end{bmatrix},$$

$$\widetilde{B} = [0\ 0\ 0\ 0\ 0\ 0\ 0\ 0\ 1]^T. \tag{30}$$

Using (23) we have the second gain matrix

$$K_2 = [\ 0 \quad 0 \quad -0.002 \quad -0.0117 \quad -0.0234 \quad -0.0781 \quad 1.125 \quad -0.5 \quad 1.5\ ]. \tag{31}$$

The closed-loop system matrix is given by

$$\widetilde{A} + \widetilde{B}K_2 = \begin{bmatrix} 0 & 1 & 0 & 0 & 0 & 0 & 0 & 0 & 0 \\ 0 & 0 & 1 & 0 & 0 & 0 & 0 & 0 & 0 \\ 0 & 0 & 0 & 1 & 0 & 0 & 0 & 0 & 0 \\ 0 & 0 & 0 & 0 & 1 & 0 & 0 & 0 & 0 \\ 0 & 0 & 0 & 0 & 0 & 1 & 0 & 0 & 0 \\ 0 & 0 & 0 & 0 & 0 & 0 & 1 & 0 & 0 \\ 0 & 0 & 0 & 0 & 0 & 0 & 0 & 1 & 0 \\ 0 & 0 & 0 & 0 & 0 & 0 & 0 & 0 & 1 \\ 0 & 0 & 0 & 0 & 0 & 0 & 0 & 0 & 0 \end{bmatrix} \tag{32}$$

and has desired eigenvalues $\lambda_k = 0$, $k = 1, \ldots, 9$.

4. Concluding remarks

The problem of eigenvalue assignment in fractional descriptor discrete-time linear systems has been considered. Necessary and sufficient conditions for the existence of a solution to the problem have been established. A procedure for computation of the gain matrices has been given and illustrated by a numerical example.

The considerations can be extended to fractional descriptor continuous-time linear systems.

References

[1] R. Bru, C. Coll and E. Sanchez: About positively discrete-time singular systems. In Mastorakis M.E. (Ed.), System and Control: Theory and Applications, World Scientific and Engineering Society, Athens, 2000, 44-48.

[2] R. Bru, C. Coll, S. Romero-Vivo and E. Sanchez: Some problems about structural properties of positive descriptor systems. In Benvenuti A., de Santis A. and Farina L. (Eds.), Positive Systems, Lecture Notes in Control and Information Sciences, **294** (2003), Springer, Berlin, 233-240.

[3] A. BUNSE-GERSTNER , N. NICHOLS and V. MEHRMANN: Regularization of descriptor systems by derivative and proportional state feedback. *SIAM J. on Matrix Analysis and Applications*, **13**(1), (1992), 46-67.

[4] S.L. CAMPBELL, C.D. MEYER AND N.J. ROSE: Applications of the Drazin inverse to linear systems of differential equations with singular constant coefficients. *SIAM J. on Applied Mathematics*, **31**(3), (1976), 411-425.

[5] L. DAI: Singular Control Systems. Lecture Notes in Control and Information Sciences, Springer-Verlag, Berlin, 1989.

[6] M. DODIG and M. STOSIC: Singular systems state feedbacks problems. *Linear Algebra and its Applications*, **431**(8), (2009), 1267-1292.

[7] G.R. DUAN: Analysis and Design of Descriptor Linear Systems. Springer, New York, 2010.

[8] A. DZIELIŃSKI, D. SIEROCIUK and G. SARWAS: Ultracapacitor parameters identification based on fractional order model. *Proc. 10th European Control Conference ECC'09*, Budapest, (2009).

[9] M.M. FAHMY and J. O'REILL: Matrix pencil of closed-loop descriptor systems: Infinite-eigenvalues assignment. *Int. J. of Control*, **49**(4), (1989), 1421-1431.

[10] T. KACZOREK: Descriptor positive discrete-time and continuous-time nonlinear systems. *Proc. of SPIE*, **9290**(2014), 1-11.

[11] T. KACZOREK: Linear Control Systems vol. 1, Research Studies Press, J. Wiley, New York, 1992.

[12] T. KACZOREK: New stability tests of positive standard and fractional linear systems. *Circuits and Systems*, **2**(4), (2011), 261-268.

[13] T. KACZOREK: Positive 1D and 2D Systems, Springer-Verlag, London, 2001.

[14] T. KACZOREK: Positivity and linearization of a class of nonlinear discrete-time systems by state feedbacks. *Logistyka*, **6** (2014), 5078-5083.

[15] T. KACZOREK: Positive descriptor discrete-time linear systems. *Problems of Nonlinear Analysis in Engineering Systems*, **1**(7), (1998), 38-54.

[16] T. KACZOREK: Positivity and stability of discrete-time nonlinear systems. *Proc. of 2nd IEEE Intern. Conf. on Cybernetics CYBCONF*, (2015), Gdynia, Poland.

[17] T. KACZOREK: Positive singular discrete time linear systems. *Bull. Pol. Acad. Techn. Sci.*, **45**(4), (1997), 619-631.

[18] T. KACZOREK: Selected Problems of Fractional Systems Theory, Springer-Verlag, Berlin 2012.

[19] T. KACZOREK: Vectors and Matrices in Automation and Electrotechnics, WNT, Warszawa, 1998 (in Polish).

[20] T. KACZOREK and K. ROGOWSKI: Fractional Linear Systems and Electrical Circuits. Studies in Systems, Decision and Control, **13** Springer, 2015.

[21] J. KLAMKA: Controllability of dynamical systems. A survey. *Bull. Pol. Acad. Techn. Sci.*, **61**(2), (2013), 221-229.

[22] KUCERA and P. ZAGALAK: Fundamental theorem of state feedback for singular systems. *Automatica*, **24**(5), (1988), 653-658.

[23] K.B. OLDHAM and J. SPANIER: The Fractional Calculus. Academic Press, New York 1974.

[24] P. OSTALCZYK: Discrete Fractional Calculus. World Scientific Publ. Co., New Jersey 2016.

[25] P. OSTALCZYK: Epitome of the fractional calculus: Theory and its Applications in Automatics. Wydawnictwo Politechniki Łódzkiej, Łódź, 2008 (in Polish).

[26] I. PODLUBNY: Fractional Differential Equations. Academic Press, San Diego 1999.

[27] A.G. RADWAN, A.M. SOLIMAN, A.S. ELWAKIL and A. SEDEEK: On the stability of linear systems with fractional-order elements. *Chaos, Solitons and Fractals*, **40**(5), (2009), 2317-2328.

[28] E.J. SOLTEIRO PIRES, J.A. TENREIRO MACHADO and P.B. MOURA OLIVEIRA: Fractional dynamics in genetic algorithms. *Workshop on Fractional Differentiation and its Application*, **2** (2006), 414-419.

[29] P. VAN DOOREN: The computation of Kronecker's canonical form of a singular pencil. *Linear Algebra and its Applications*, **27** (1979), 103-140.

[30] B.M. VINAGRE, C.A. MONJE and A.J. CALDERON: Fractional order systems and fractional order control actions. Lecture 3 IEEE CDC'02 TW#2: Fractional calculus Applications in Automatic Control and Robotics, (2002).

[31] E. VIRNIK: Stability analysis of positive descriptor systems. *Linear Algebra and its Applications*, **429**(10), (2008), 2640-2659.